

**EFFECT OF CLAY SURFACE MODIFICATION ON
PHYSICAL PROPERTIES OF NATURAL RUBBER
NANOCOMPOSITES**

Chalermpan Keawkumay

**A Thesis Submitted in Partial Fulfillment of Requirements for the
Degree of Master of Engineering in Polymer Engineering
Suranaree University of Technology**

Academic year 2009

ผลของการปรับเปลี่ยนพื้นผิวเคลือบต่อสมบัติทางกายภาพ
ของนาโนคอมโพสิตจากยางธรรมชาติ

นายเฉลิมพันธ์ เขียวคำอ้าย

วิทยานิพนธ์นี้เป็นส่วนหนึ่งของการศึกษาตามหลักสูตรปริญญาวิศวกรรมศาสตรมหาบัณฑิต
สาขาวิชาวิศวกรรมพอลิเมอร์
มหาวิทยาลัยเทคโนโลยีสุรนารี
ปีการศึกษา 2552

EFFECT OF CLAY SURFACE MODIFICATION ON PHYSICAL PROPERTIES OF NATURAL RUBBER NANOCOMPOSITES

Suranaree University of Technology has approved this thesis submitted in partial fulfillments of the requirement for a Master's Degree.

Thesis Examining Committee

(Asst. Prof. Dr. Wimonlak Sutapun)

Chairperson

(Asst. Prof. Dr. Nitinat Suppakarn)

Member (Thesis Advisor)

(Asst. Prof. Dr. Kasama Jarukumjorn)

Member

(Asst. Prof. Dr. Yupaporn Ruksakulpiwat)

Member

(Asst. Prof. Dr. Visit Vao-soongnern)

Member

(Prof. Dr. Sukit Limpijumnong)

Vice Rector for Academic Affairs

(Assoc. Prof. Dr. Vorapot Khompis)

Dean of Institute of Engineering

เฉลิมพันธ์ เขียวคำอ้าย : ผลของการปรับเปลี่ยนผิวหน้าเคลย์ต่อสมบัติทางกายภาพของ
นาโนคอมโพสิตจากยางธรรมชาติ (EFFECT OF CLAY SURFACE MODIFICATION
ON PHYSICAL PROPERTIES OF NATURAL RUBBER NANOCOMPOSITES)
อาจารย์ที่ปรึกษา : ผู้ช่วยศาสตราจารย์ ดร.นิธินาถ สุภกาญจน์, 100 หน้า.

วิทยานิพนธ์นี้มอนด์โมริลโลไนท์ถูกใช้เป็นตัวเติมสำหรับยางธรรมชาติ ผิวหน้าของ
มอนด์โมริลโลไนท์ที่ถูกปรับเปลี่ยนโดยใช้สารปรับเปลี่ยนผิวหน้าที่แตกต่างกัน 3 ชนิดได้แก่
ออกตะเดซิลเอมีน ออกตะเดซิลไตรเมทิลแอมโมเนียมโบรไมด์ และเตตระเดซิลไตรเมทิล
แอมโมเนียมโบรไมด์ ในปริมาณของสารปรับเปลี่ยนผิวหน้าที่แตกต่างกัน ได้แก่ 0.5 1 และ 2 เท่า
ของความจุในการแลกเปลี่ยนประจุบวก สเปกตรัมจากการเลี้ยวเบนของรังสีเอกซ์ สเปกตรัมจาก
อินฟราเรดสเปกโตรสโคปี และเทอร์โมแกรมจากเครื่องเทอร์โมการวิเมตริแสดงให้เห็นว่าสาร
ปรับเปลี่ยนผิวหน้าได้แทรกตัวเข้าไปในชั้นของมอนด์โมริลโลไนท์

นาโนคอมโพสิตของยางธรรมชาติที่มีออร์กาโนเคลย์ในปริมาณ 5 ส่วนต่อหนึ่งร้อยละ
ของยางธรรมชาติถูกเตรียมขึ้นโดยเครื่องผสมแบบสองลูกกลิ้ง ในนาโนคอมโพสิตของยาง
ธรรมชาติกับออร์กาโนเคลย์ทั้งหมด พบว่า นาโนคอมโพสิตของยางธรรมชาติกับมอนด์โมริลโล
ไนท์ที่ปรับเปลี่ยนผิวหน้าด้วยเตตระเดซิลไตรเมทิลแอมโมเนียมโบรไมด์ในปริมาณ 2 เท่าของความ
จุในการแลกเปลี่ยนประจุบวกมีค่าการทนทานต่อแรงดึงสูงสุด มีเวลาสกอรัชและเวลาการคงรูปที่
เหมาะสมที่สุด

ดังนั้น มอนด์โมริลโลไนท์ที่ปรับเปลี่ยนผิวหน้าด้วยเตตระเดซิลไตรเมทิลแอมโมเนียม
โบรไมด์ในปริมาณ 2 เท่าของความจุในการแลกเปลี่ยนประจุบวกถูกเลือก เพื่อนำไปเตรียม
นาโนคอมโพสิตระหว่างยางธรรมชาติกับออร์กาโนเคลย์ที่มีปริมาณของออร์กาโนเคลย์
แตกต่างกัน ได้แก่ 1 3 5 และ 10 ส่วนต่อหนึ่งร้อยละของยางธรรมชาติ เมื่อเพิ่มปริมาณของ
มอนด์โมริลโลไนท์ที่ปรับเปลี่ยนผิวหน้าด้วยเตตระเดซิลไตรเมทิลแอมโมเนียมโบรไมด์ใน
ปริมาณ 2 เท่าของความจุในการแลกเปลี่ยนประจุบวกในนาโนคอมโพสิตของยางธรรมชาติขึ้น
ไปถึง 5 ส่วนต่อหนึ่งร้อยละของยางธรรมชาติ เวลาสกอรัชและเวลาการคงรูปลดลง ในขณะที่
ค่าการทนทานต่อแรงดึงเพิ่มขึ้น

นอกจากนี้ ยางธรรมชาติอีพ็อกซีไคซ์ถูกผสมกับยางธรรมชาติเพื่อปรับปรุงความเป็นขี้
ของเมทริกซ์ อัตราส่วนผสมของยางธรรมชาติกับยางธรรมชาติอีพ็อกซีไคซ์ คือ 60 ต่อ 40 และ
40 ต่อ 60 ร้อยละโดยน้ำหนัก ปริมาณของมอนด์โมริลโลไนท์ที่ปรับเปลี่ยนผิวหน้าด้วยเตตระ
เดซิลไตรเมทิลแอมโมเนียมโบรไมด์ในปริมาณ 2 เท่าของความจุในการแลกเปลี่ยนประจุบวก

ถูกกำหนดให้คงที่ ที่ 5 ส่วนต่อหนึ่งร้อยส่วนของยางธรรมชาติ การผสมยางธรรมชาติอีพ็อกซีได้ซ์
กับยางธรรมชาติปรับปรุงสมบัติทางกลของนาโนคอมโพสิตของยางธรรมชาติได้เล็กน้อย

สาขาวิชา วิศวกรรมพอลิเมอร์

ปีการศึกษา 2552

ลายมือชื่อนักศึกษา _____

ลายมือชื่ออาจารย์ที่ปรึกษา _____

ลายมือชื่ออาจารย์ที่ปรึกษาร่วม _____

ACKNOWLEDGEMENTS

I wish to acknowledge the financial supports from Suranaree University of Technology and National Center of Excellence for Petroleum, Petrochemical and Advance Materials.

I am deeply indebted to my thesis advisor, Asst. Prof. Dr. Nitinat Suppakarn, who always gives me a kind suggestions and supports me throughout the period of the study. Furthermore, the grateful thank and appreciation is given to the thesis co-advisor, Asst. Prof. Dr. Kasama Jarukumjorn for her valuable suggestions.

My thanks go to Asst. Prof. Dr. Wimonlak Sutapun, Asst. Prof. Dr. Yupaporn Ruksakulpiwat and Asst. Prof. Dr. Visit Vao-soongnern for their valuable suggestions and guidance given as committee.

I would like to express my appreciation to the faculty and staff of School of Polymer Engineering and Center for Scientific and Technological Equipment of Suranaree University of Technology. Special thanks are extended to Mr. Suriyan Rakmae and all friends for their helps, supports and encouragement.

Last but not least, I would like to thank my parents, Mr. Jaras and Mrs. Boonmee Keawkumay, and my younger brother, Mr. Rachane Keawkumay, who give me a valuable life and protect my mind from an evil with their unconditional loves.

Chalermpan Keawkumay

TABLE OF CONTENTS

	Page
ABSTRACT (THAI).....	I
ABSTRACT (ENGLISH)	III
ACKNOWLEDGEMENTS	V
TABLE OF CONTENTS.....	VI
LIST OF TABLES	X
LIST OF FIGURES.....	XI
SYMBOLS AND ABBREVIATIONS	XVI
CHAPTER	
I INTRODUCTION.....	1
1.1 Background	1
1.2 Research objectives.....	3
1.3 Scope and limitation of the study.....	4
II LITERATURE REVIEW	5
2.1 Clay (Montmorillonite).....	5
2.2 Nanocomposite structure	7
2.3 Organically modified clay.....	10
2.4 Polymer/clay nanocomposites.....	15
2.5 Rubber/clay nanocomposites	17

TABLE OF CONTENTS (Continued)

	Page
2.5.1 Synthetic rubber	17
2.5.2 Natural rubber	21
III EXPERIMENTAL	25
3.1 Materials	25
3.2 Experimental	26
3.2.1 Preparation of organoclays.....	26
3.2.2 Preparation of NR nanocomposites	27
3.3 Material characterization.....	29
3.3.1 Characterization of clay and organoclays	29
3.3.1.1 Structure of clay and organoclays	29
3.3.1.2 Functional groups and chain conformation	29
3.3.1.3 Thermal properties	29
3.3.2 Characterization of NR nanocomposites	30
3.3.2.1 Structure of clay and organoclays	30
3.3.2.2 Cure characteristics	30
3.3.2.3 Mechanical properties	30
3.3.2.4 Crosslink density.....	31
IV RESULTS AND DISCUSSION	32
4.1 Characterization of clay and organoclays	32

TABLE OF CONTENTS (Continued)

	Page
4.1.1	Structure of clay and organoclays 32
4.1.2	Functional groups and chain conformations 36
4.1.3	Decomposition temperature 41
4.2	Effect of surfactant on properties of NR nanocomposites 46
4.2.1	Dispersion and structures of clay and organoclays 46
4.2.2	Cure characteristics 51
4.2.3	Mechanical properties 58
4.3	Effect of organoclay content on properties of NR nanocomposites 67
4.3.1	Dispersion and structures of organoclays 67
4.3.2	Cure characteristics 68
4.3.3	Mechanical properties 71
4.4	Effect of matrix polarity on properties of NR nanocomposites 76
4.4.1	Dispersion and structures of organoclay 77
4.4.2	Cure characteristics 79
4.4.3	Mechanical properties 82

TABLE OF CONTENTS (Continued)

	Page
V CONCLUSIONS	86
REFERENCES	88
APPENDIX A Publications	93
BIOGRAPHY	100

LIST OF TABLES

Table	Page
2.1 Clay mineral used for polymer nanocomposites.....	6
3.1 Formulations of NR nanocomposites.....	28
3.2 Formulations of NR/ENR blend nanocomposites.....	28
4.1 2 Theta (2θ) and interlayer spacing of MMT and modified MMT	35
4.2 FTIR wavenumber of asymmetric CH_2 ($\nu_{\text{as}}(\text{CH}_2)$) and symmetric CH_2 ($\nu_{\text{s}}(\text{CH}_2)$) stretching vibrations of modified MMT.....	39
4.3 The onset decomposition temperature of MMT and modified MMT	44
4.4 Cure characteristics of NR nanocomposites at various surfactant types and surfactant contents.....	52
4.5 Mechanical properties and crosslink density of NR nanocomposites at various surfactant types and surfactant contents.....	64
4.6 Cure characteristics of NR nanocomposites at various contents of MMT-TDMA2.....	69
4.7 Mechanical properties and crosslink density of NR nanocomposites at various contents of MMT-TDMA2.....	75
4.8 Cure characteristics of nanocomposites containing 5 phr of MMT-TDMA2.....	81
4.9 Mechanical properties and crosslink density of nanocomposites containing 5 phr of MMT-TDMA2	85

LIST OF FIGURES

Figure	Page
2.1 Structure of clay minerals represented by montmorillonite. They are built up from combinations of tetrahedral and octahedral sheets whose basic units are usually Si–O tetrahedron and Al–O octahedron, respectively	8
2.2 Scheme of different structures of polymer/clay nanocomposites: a) conventional microcomposite, b) intercalated nanocomposite and c) exfoliated nanocomposite	9
2.3 A reaction to prepare an organoclay.....	10
2.4 Arrangements of alkylammonium ions in layered silicates with different layer charges. a) lateral monolayer, b) lateral bilayer, c) paraffin-type monolayer and d) paraffin-type bilayer	11
2.5 Different chain arrangements leading to the same interlayer spacing: (a) tilted, <i>all-trans</i> chains and (b) chains with numerous <i>gauche</i> conformers. Open circles (o) represent CH ₂ segments while cationic head groups are represented by filled circles (●)	12
3.1 Chemical structures of (a) ODA (b) TDMA-Br, and (c) ODTMA-Br.....	25
4.1 XRD spectra of MMT and modified MMT with (a) ODA, (b) ODTMA-Br and (c) TDMA-Br at 0.5, 1 and 2 times clay CEC	34

LIST OF FIGURES (Continued)

Figure	Page
4.2	FTIR spectra of MMT and modified MMT with (a) ODA, (b) ODTMA-Br and (c) TDMA-Br at 0.5, 1 and 2 times clay CEC37
4.3	TGA thermograms of MMT and modified MMT with (a) ODA, (b) ODTMA-Br and (c) TDMA-Br at 0.5, 1 and 2 times clay CEC42
4.4	DTG thermograms of MMT and modified MMT with (a) ODA, (b) ODTMA-Br and (c) TDMA-Br at 0.5, 1 and 2 times clay CEC43
4.5	XRD spectra of NR nanocomposites containing 5 phr of (a) MMT-ODA, (b) MMT-ODTMA and (c) MMT-TDMA at 0.5, 1 and 2 times clay CEC47
4.6	TEM micrographs of NR nanocomposites containing 5 phr of (a) MMT, (b) MMT-ODA0.5, (c) MMT-ODA1 and (d) MMT-ODA248
4.7	TEM micrographs of NR nanocomposites containing 5 phr of (a) MMT-ODTMA0.5, (b) MMT-OTMDA1, (c) MMT-OTMDA2 (d) MMT-TDMA0.5, (e) MMT-TDMA1 and (f) MMT-TDMA249
4.8	Scorch time of NR nanocomposites at various surfactant types and surfactant contents53
4.9	Cure time of NR nanocomposites at various surfactant types and surfactant contents.53
4.10	Maximum torque of NR nanocomposites at various surfactant types and surfactant contents.55

LIST OF FIGURES (Continued)

Figure	Page
4.11 Torque difference of NR nanocomposites at various surfactant types and surfactant contents.....	56
4.12 Minimum torque of NR nanocomposites at various surfactant types and surfactant contents.....	56
4.13 Tensile strength of NR nanocomposites at various surfactant types and surfactant contents.....	59
4.14 Elongation at break of NR nanocomposites at various surfactant types and surfactant contents.....	60
4.15 Modulus at 100% elongation of NR nanocomposites at various surfactant types and surfactant contents.....	61
4.16 Modulus at 300% elongation of NR nanocomposites at various surfactant types and surfactant contents.....	61
4.17 Hardness of NR nanocomposites at various surfactant types and surfactant contents.....	62
4.18 Crosslink density of NR nanocomposites at various surfactant types and surfactant contents.....	63
4.19 XRD spectra of NR nanocomposites at various contents of MMT-TDMA2: (a) 1 phr, (b) 3 phr, (c) 5 phr, (d)10 phr, and (e) MMT-TDMA2.....	68

LIST OF FIGURES (Continued)

Figure	Page
4.20	Scorch time and cure time of NR nanocomposites at various contents of MMT-TDMA2.....69
4.21	Minimum torque, maximum torque and torque difference of NR nanocomposites at various contents of MMT-TDMA2.....71
4.22	Tensile strength and elongation at break of NR nanocomposites at various contents of MMT-TDMA2.....72
4.23	Modulus at 100% elongation and modulus at 300% elongation of NR nanocomposites at various contents of MMT-TDMA273
4.24	Hardness and crosslink density NR nanocomposites at various contents of MMT-TDMA274
4.25	XRD spectra of (a) NR, (b) NR/ENR (60/40), (c) NR/ENR (40/60) and (d) ENR nanocomposites with 5 phr of MMT-TDMA278
4.26	TEM micrographs of (a) NR, (b) NR/ENR (60/40), (c) NR/ENR (40/60) and (d) ENR nanocomposites with 5 phr of MMT-TDMA279
4.27	Scorch time and cure time of nanocomposites containing 5 phr of MMT-TDMA280
4.28	Minimum torque, maximum torque and torque difference of nanocomposites containing 5 phr of MMT-TDMA2.....80
4.29	Tensile strength and elongation at break of nanocomposites containing 5 phr of MMT-TDMA2.....83

LIST OF FIGURES (Continued)

Figure		Page
4.30	Modulus at 100% elongation and modulus at 300% elongation of nanocomposites containing 5 phr of MMT-TDMA2.....	83
4.31	Hardness and crosslink density of nanocomposites containing 5 phr of MMT-TDMA2	84

SYMBOLS AND ABBREVIATIONS

%	=	Percent
°	=	Degree
°C	=	Degree Celsius
μm	=	Micrometer
NR	=	Natural rubber
ENR	=	Epoxidized natural rubber
CEC	=	Cation exchange capacity
XRD	=	X-Ray diffractometer
TGA	=	Thermogravimetric analyzer
IRHD	=	International rubber hardness degrees tester
FTIR	=	Fourier transform infrared spectrometer
TEM	=	Transmission electron microscope
MDR	=	Moving die rheometer
ODA	=	Octadecylamine
ODTMA-Br	=	Octadecyltrimethyl ammonium bromide
TDMA-Br	=	Tetradecyltrimethyl ammonium bromide
MPa	=	Mega Pascal
MMT	=	Montmorillonite
kV	=	Kilo volt
m ²	=	Square meter

SYMBOLS AND ABBREVIATIONS (Continued)

m^3	=	Cubic meter
μS	=	Microsiemens
\AA	=	Angstrom
g	=	Gram
min	=	Minute
mm	=	Millimeter
nm	=	Nanometer
cm^3	=	Cubic centimeter
cm^{-1}	=	Reciprocal centimeter
ml	=	Milliliter
meq	=	Milliequivalent
mol	=	Mole
wt%	=	Percent by weight
mol%	=	Percent by mole
phr	=	Part per hundred of rubber
dNm	=	Deci newton meter
conc	=	Concentrated
CBS	=	N-Cyclohexyl-2-benzothiazolesulfenamide
V_0	=	Molar volume of the solvent
Φ_r	=	Volume fraction of polymer
χ	=	Flory-Huggins polymer-solvent interaction
ca	=	Circa

CHAPTER I

INTRODUCTION

1.1 Background

Thailand is one of the largest producer of natural rubber (NR). However, most of the produced natural rubber is exported (90%) as raw rubber while the rest is used to produce rubber products for exporting and use within the country. NR has many attractive properties including low cost, low hysteresis, high resilience, excellent dynamic properties, *etc.* (Teh, Mohd Ishak, Hashim, Karger-Kocsis, and Ishiaku, 2004). The major use of NR product is in tire industry. To increase the value added products of natural rubber, the manufacturers need to improved performance of rubber products.

Typically, performance of a NR product depends on the right combination of rubbers with rubber chemicals and a reinforcing filler system. Reinforcing fillers are used in rubber compounding mainly to improve mechanical properties of the final product.

A typical reinforcing filler for rubber compound is carbon black which causes pollution and gives a rubber a black color. A light color filler commonly used in some rubber applications is silica. In addition, clay layered silicate is another type of filler that is increasingly used in rubber applications.

Clay minerals consist of layers made up of two tetrahedrally coordinated silicon atoms fused to an edge-shared octahedral sheet of either aluminum or magnesium hydroxide. The layer thickness is around 1 nm, the lateral dimensions of

these layers are varied from 30 nm to several microns or larger, and surface area is around 700–800 m²/g depending on the particular layered silicate (Alexandre and Dubois, 2000; Zeng, Yu, Lu, and Paul, 2005).

In general, dispersion of clay particles in a plastic or a rubber matrix could possibly form three types of composites: conventional composites, intercalated nanocomposites and exfoliated nanocomposites depending on types of clay and preparation conditions. Both intercalated and exfoliated nanocomposites offer some special physical and mechanical properties with low loading of clay compared with the conventional composites due to the large surface area and the high aspect ratio of clay (Alexandre and Dubois, 2000).

One of the drawbacks of using the clay mineral as a filler for a rubber is the incompatibility between hydrophilic clay and hydrophobic polymer, which often causes agglomeration of the clay in the polymer matrix. Therefore, surface modification of the clay is an important parameter to achieve polymer nanocomposite. Such modified clays are commonly called organoclays (Zeng *et al.*, 2005).

Normally, the modification of clay surface can be done via ion exchange of the interlayer cations of clay with those of organic surfactants. Ion exchange reactions depend on types of organic surfactant and the cation exchange capacity (CEC) of the clay. The CEC of clay is very important factor for producing nanocomposite because it determines the amount of surfactants, which can be intercalated between the silicate layers (Ray and Okamoto, 2003). Organic surfactants normally used to modify clay are alkyl amine surfactants. The length of alkyl chain and the number of alkyl tails on the surfactant molecules directly affect ion exchange reaction.

Another way to improve interaction between clay and NR is to adjust matrix polarity since clay and organoclay can be more easily dispersed in polar matrix phase than in non-polar matrix phase. NR with the substitution of epoxide groups along the NR backbone, *i.e.* epoxidized natural rubber (ENR), has higher polarity compared to NR. Blending NR with ENR should be beneficial when compounding the modified NR matrix with polar fillers, such as layered silicates. In addition, ENR shows excellent oil resistance, less air permeability, good damping and wet grip performance. Therefore, blending NR with ENR could adjust the polarity of matrix phase leading to the improvement of clay dispersion in the nanocomposite and the enhancement of mechanical properties of the nanocomposite.

1.2 Research objectives

The aims of this research are as follows:

- (i) To determine effect of surfactant type on mechanical properties and cure characteristics of NR nanocomposites.
- (ii) To determine effect of surfactant content on mechanical properties and cure characteristics of NR nanocomposites.
- (iii) To determine effect of matrix polarity on mechanical properties and cure characteristics of NR nanocomposites.

1.3 Scope and limitation of the study

Sodium-montmorillonite (Na^+ -MMT) was surface treated with either octadecylamine (ODA) or tetradecyltrimethyl ammonium bromide (TDMA-Br) or octadecyltrimethyl ammonium bromide (ODTMA-Br) surfactants. The amounts of added surfactants correspond to surfactant to CEC ratio of 0.5, 1 and 2.

The natural rubber used was STR5L. The epoxidized natural rubber with 50 mol% of epoxide groups (ENR50) was blended with NR to adjust polarity of NR matrix. The blends ratios of NR/ENR was 100/0, 60/40, 40/60 and 0/100 by weight.

NR/organoclay nanocomposites were prepared using a two-roll mill and a compression molding machine, respectively. A conventional sulfur vulcanization system was used in this study.

The structures of clay, organoclay and clay in NR/clay nanocomposites were analyzed by an X-ray diffraction spectrometer (XRD). The dispersion of clay in NR/clay nanocomposites were determined by a transmission electron microscope (TEM). Functional groups of the surfactant on organoclay surface were identified by a Fourier transform infrared spectrometer (FTIR). The thermal decomposition temperature and weight loss of clay and organoclay were determined by a thermogravimetric analyzer (TGA). Cure characteristics of NR/clay nanocomposites were determined using a moving die rheometer (MDR). The mechanical properties of NR/clay nanocomposites were investigated by a universal testing machine. Hardness was measured by using an international rubber hardness degrees tester (IRHD). Crosslink density of NR/organoclay nanocomposites was determined on the basis of rapid solvent-swelling measurements.

CHAPTER II

LITERATURE REVIEW

Polymer/clay nanocomposites have become an important area of studies in academic, government and industrial laboratories. These types of materials were firstly reported as early as 1950. However, attentions on these nanocomposites were widespread after Toyota researchers have introduced intercalated ϵ -caprolactam/clay nanocomposites (Wang Shaohui, Zhang Yong, Peng Zonglin, and Zhang Yinxi, 2005). Numerous other researchers later used this concept for nanocomposites based on unsaturated polyester, poly (ϵ -caprolactone), poly (ethylene oxide), polystyrene, polyimide, rubber, *etc.*

2.1 Clay (Montmorillonite)

Clay minerals are hydrous aluminum silicates and are generally classified as layered silicates. The layered silicates of clay are generated by a combination of silicon tetrahedral sheet and aluminium octahedral sheets. Such minerals include both natural clays and synthetic clays (Tjong, 2006; Zeng *et al.*, 2005).

The layer silicates can be classified using several aspects as shown in Table 2.1. The commonly used layered silicates for the preparation of nanocomposites belong to the smectite family with the structure consisting of aluminium octahedral sheet sandwiched in between two silicon tetrahedral sheets as called 2:1 layered silicates (Zeng *et al.*, 2005).

Table 2.1 Clay mineral used for polymer nanocomposites (Zeng *et al.*, 2005)

Type of clay	Group	Formula	Origin	Substitution	Layer charge
2 : 1 type	MMT	$M_x(Al_{2-x}Mg_x)Si_4O_{10}(OH)_2.nH_2O$	N	Octahedral	Negative
	Hectorite	$M_x(Mg_{3-x}Li_x)Si_4O_{10}(OH)_2.nH_2O$	N	Octahedral	Negative
	Saponite	$M_xMg_3(Si_{4-x}Al_x)O_{10}(OH)_2.nH_2O$	N	Tetrahedral	Negative
	Fluorohectorite	$M_x(Mg_{3-x}Li_x)Si_4O_{10}F_2.nH_2O$	S	Octahedral	Negative
	Laponite	$M_x(Mg_{3-x}Li_x)Si_4O_{10}(OH)_2.nH_2O$	S	Octahedral	Negative
	Fluromica (Somasif)	$NaMg_{2.5}Si_4O_{10}F_2$	S	Octahedral	Negative
1 : 1 type	Kaolinite	$Al_2Si_2O_5(OH)_4$	N	-	Neutral
	Halloysite	$Al_2Si_2O_5(OH)_4.2H_2O$	N	-	Neutral
Layered silicic acid	Kanemite	$Na_2Si_4O_9.5H_2O$	N/S	Tetrahedral	Negative
	Makatite	$NaHSi_2O_5.7H_2O$	N/S	Tetrahedral	Negative
	Octasilicate	$Na_2Si_8O_{17}.9H_2O$	S	Tetrahedral	Negative
	Magadiite	$Na_2Si_{14}O_{29}.10H_2O$	N/S	Tetrahedral	Negative
	Kenvaite	$Na_2Si_{20}O_{44}.10H_2O$	S	Tetrahedral	Negative

M indicates exchangeable ions represented by monovalent ions. Symbols : N(nature) and S(synthetic)

The most commonly used 2:1 layered silicates for preparation of polymer/clay nanocomposites is montmorillonite (MMT). As shown in Figure 2.1, montmorillonite clay (MMT) consists of layers made up of two tetrahedrally coordinated silicon atoms fused to an edge-shared octahedral sheet of either aluminum or magnesium hydroxide. The layer thickness is around 1 nm, and the lateral dimensions of these layers may vary from 30 nm to several microns or larger, depending on types of layered silicate.

Characteristics of layered clays which can be applied in nanocomposite preparation are: 1) the ability of layered clays to disperse as separated layers with a thickness of about 1 nm and 2) the ability of the clay surface to be modified with organic and inorganic cations.

2.2 Nanocomposite structure

In recent year, researchers have been working on a new scale of reinforcement by incorporating a fine dispersion of clay silicate layers in the polymer matrix to obtain polymer nanocomposites. Nanoscale layered clays, due to their high aspect ratio and high strength, can play an important role in forming effective polymer nanocomposites.

In general, dispersion of clay particles in a polymer matrix could possibly form three types of composites depending on types of clay and preparation conditions: (a) conventional composites (b) intercalated nanocomposites and (c) exfoliated nanocomposites, as shown in Figure 2.2.

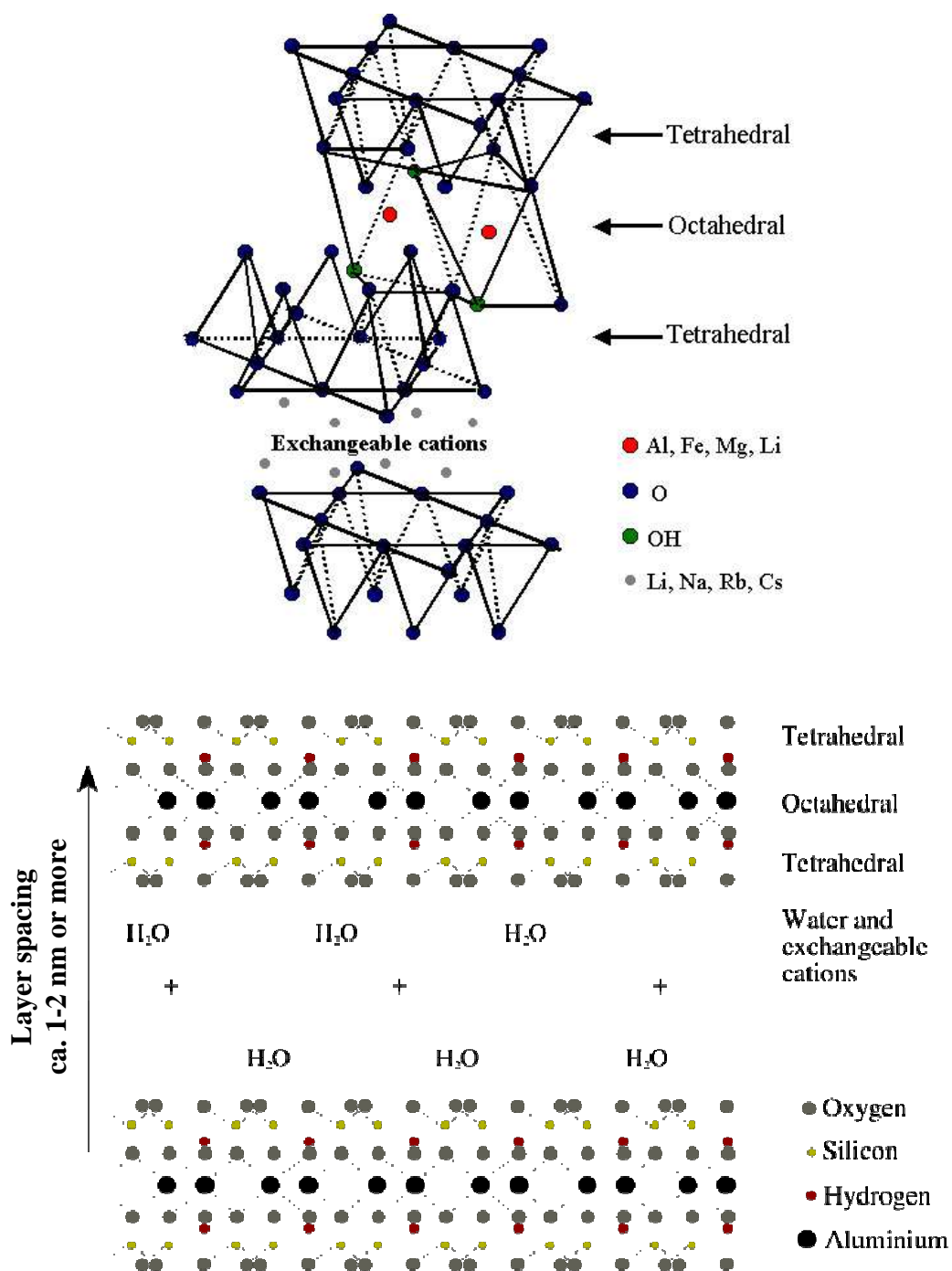


Figure 2.1 Structure of clay minerals represented by montmorillonite. They are built up from combinations of tetrahedral and octahedral sheets whose basic units are usually Si–O tetrahedron and Al–O octahedron, respectively (Alexandre and Dubois, 2000).

In a conventional composite (Figure 2.2 (a)), there is no intercalation of polymer into the intergallery of nanoparticles when clay nanolayers are mixed with the polymer. Intercalated nanocomposites (Figure 2.2 (b)) are formed when a single (and sometimes more than one) extended polymer chain is intercalated between the clay galleries resulting in a well ordered multi-layer morphology built up with alternating polymeric and inorganic layers. When the silicate layers are completely and uniformly dispersed in a continuous polymer matrix, exfoliated nanocomposites (Figure 2.2 (c)) are obtained. Exfoliated nanocomposites show greater phase homogeneity than intercalated nanocomposites. Each nanolayer in an exfoliated nanocomposite contributes fully to interfacial interactions with the matrix. Both intercalated and exfoliated nanocomposites offer some special physical and mechanical properties compared to the conventional composites (Alexandre and Dubois, 2000).

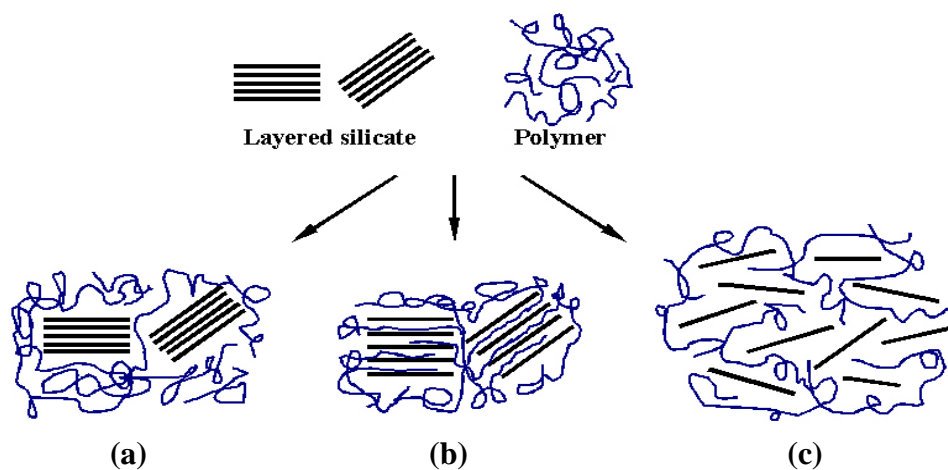


Figure 2.2 Scheme of different structures of polymer/clay nanocomposites: (a) conventional microcomposite, (b) intercalated nanocomposite and (c) exfoliated nanocomposite (Alexandre and Dubois, 2000).

2.3 Organically modified clay

One of the drawbacks of using clays as a filler for a polymer is the incompatibility between hydrophilic clay and hydrophobic polymer, which often causes agglomeration of clay mineral in the polymer matrix. Therefore, surface modification of clay mineral is an important parameter needed to be considered to achieve polymer nanocomposite. Such modified clays are commonly called organoclays. Normally, the modification of clay surface can be done via ion exchange of the inorganic cations with those of organic surfactants. The methods frequently used to modify clay is exchanging the interlayer inorganic cation (Na^+ or Ca^{2+}) with organic ammonium cations as shown in Figure 2.3.

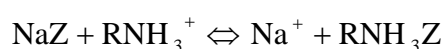


Figure 2.3 A reaction to prepare an organoclay (Vansant and Peeters, 1978).

From the Figure 2.3, NaZ is montmorillonite with Na^+ as interlayer cations and R is the alkyl chain of the acidified primary amine surfactant. After modification, the surface of the clay becomes organophilic.

Ion exchange reactions depend on the cation exchange capacity (CEC) of the clay. The CEC of clay is very important factor for producing nanocomposite because it determines the amount of surfactants, which can be intercalated between the silicate layers.

Organic surfactants normally used to modify clay including primary, secondary, tertiary and quaternary alkylammonium cations are water soluble. So, most cation exchange reactions are performed in aqueous suspensions.

Alkylammonium cations in the organosilicates lower the surface energy of the inorganic host and improve the wetting ability between the organoclay and the polymer matrix, resulting in a larger interlayer spacing of the organoclays. The length of alkyl chain and the number of alkyl tails on the surfactant molecules directly affect ion exchange reaction (Tjong, 2006).

Under most conditions, a wide range of the molecular arrangement of the surfactant used depends on the cation exchange capacity (CEC) of the layer silicate (packing density of the chains), and the chain length of organic tail. Increasing the CEC of clay or chain length of the surfactant improves the ordering of the chains. The arrangement of alkylammonium ions in layered silicates are shown in Figure 2.4.

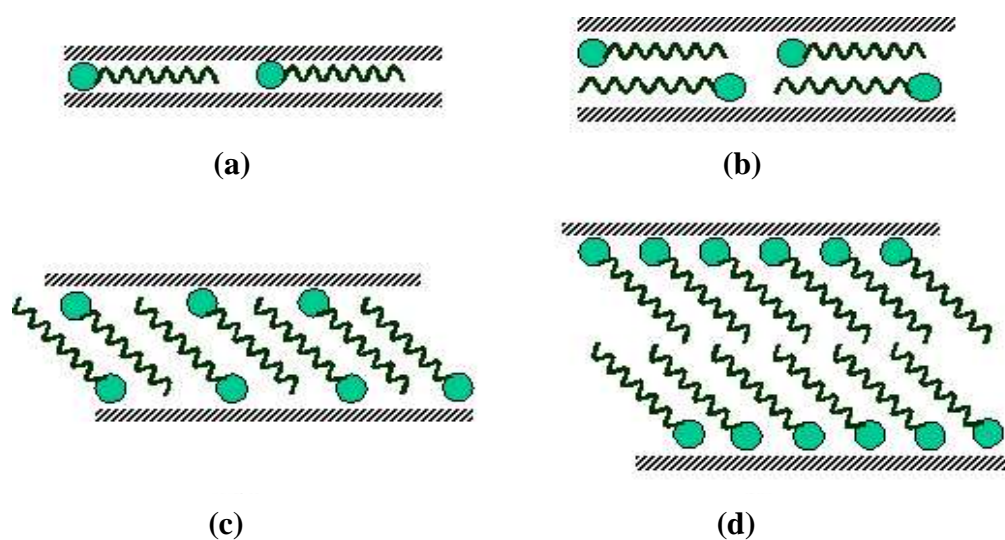


Figure 2.4 Arrangements of alkylammonium ions in layered silicates with different layer charges. (a) lateral monolayer, (b) lateral bilayer, (c) paraffin-type monolayer and (d) paraffin-type bilayer (Tjong, 2006).

Based on XRD analysis, Lagaly (1981) had proposed various arrangements of alkyl chains in organoclays which detected by the interlayer spacing of organoclay. Depending on the alkyl ammonium packing density and the chain length, the carbon chain can be arranged in the MMT layers and formed either monolayers or bilayers or pseudotrimolecular layers or paraffin complexes.

Vaia *et al.* (1994) studied primary amine and quaternary ammonium cations inside the interlayer space by using FTIR spectroscopy. They had proposed conformations of alkyl chains as a function of CEC, ammonium head group and chain length by monitoring frequency shifted of the CH₂ stretching ($\approx 2920\text{ cm}^{-1}$) and scissoring ($\approx 2850\text{ cm}^{-1}$) vibrations. Band of CH₂ stretching shifted from lower frequencies, characteristic of ordered *all-trans* conformations, to higher frequencies, characteristic of highly disordered *gauche* conformations, as shown in Figure 2.5.

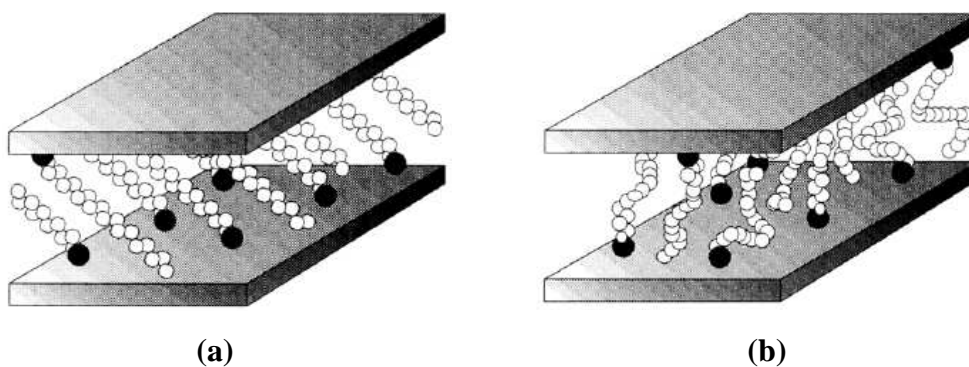


Figure 2.5 Different chain arrangements leading to the same interlayer spacing: (a) tilted, *all-trans* chains and (b) chains with numerous *gauche* conformers. Open circles (o) represent CH₂ segments while cationic head groups are represented by filled circles (●) (Vaia *et al.*, 1994).

Arroyo, Lopez-Manchado, and Herrero (2003) modified MMT clay with octadecylamine (ODA). The result showed that interlayer spacing of modified MMT was higher than that of unmodified MMT. To confirm the appearance of adsorbed surfactant in clay layer, FTIR was used to investigate the intercalated surfactant. The organoclay presented a peak at 2918 and 2850 cm^{-1} attributed to the C-H asymmetric and symmetric stretching vibrations of ODA surfactant, respectively.

Magaraphan R., Thaijaroen W., and Lim-ochakun R. (2003) modified surface of MMT clay using primary amine (dodecylamine, tetradecylamine, hexadecylamine, octadecylamine) and quaternary ammonium surfactants (hexadecyltrimethyl ammonium bormide, octadecyltrimethyl ammonium chloride). Octadecylamine modified clay showed the highest interlayer spacing. The result indicated that the long alkyl chain of amine surfactants played an important role in the expansion of clay layers. The interlayer spacing of quaternary amine modified MMT was lower than that of primary amine modified MMT. This suggested that the bulkiness of the modifying agent retarded the ion exchange process.

Wibulswas R. (2004) modified MMT clay using quaternary ammonium cation (QACs), *i.e.* hexadecyltrimethyl ammonium (HDTMA), tetradecyltrimethyl ammonium (TDMA), benzyldimethylhexadecyl ammonium (BDHDMA) and tetramethyl ammonium (TMA). The contents of QACs were varied and equivalent to 0.5, 1 and 2 times CEC of MMT. BDHDMA modified MMT showed the highest interlayer spacing. With increasing QACs content from 1 CEC to 2 CEC, an insignificant increase in interlayer spacing of clays was observed. This suggested that the cation exchange mechanism may be dominant for the intercalation of the QACs between the interlayer of the clays.

Xi, Ding, He, and Forst (2004) studied the structure of organoclay which has been intercalated with a long-chain organic surfactant (octadecyltrimethylammonium bromide (ODTMA)). The contents of ODTMA were varied and equivalent to 0.2, 0.4, 0.6, 0.8, 1.0, 1.5, 2.0, 3.0 and 4.0 times clay CEC. The result showed that the content of ODTMA at 4.0 times clay CEC gave the highest interlayer spacing of the organoclay. The researcher had proposed that structural arrangement of ODTMA within the layer of modified MMT was dependent on ODTMA content. At ODTMA content of 0.2 to 0.4 times clay CEC, the arrangement of ODTMA molecules was a lateral monolayer. With increasing ODTMA content from 0.6 to 0.8 times clay CEC, the arrangement of ODTMA molecules became a lateral bilayer. Additionally, the arrangement of ODTMA molecules was pseudotrimolecular when the added ODTMA content was between 1.5 to 4.0 times clay CEC. At ODTMA-Br content of 1.0 times clay CEC, the arrangement of ODTMA was between bilayer and pseudotrimolecular layer structure. Nevertheless, they studied the thermal decomposition of the organoclays by using thermogravimetric analysis (TGA). The thermal decomposition of the organoclays took place in four steps. The first mass loss step, due to water evaporation was observed at room temperature. The second mass loss step was observed over the temperature range 87.0 to 135.5°C and attributed to a loss of surfactant. The third mass loss step occurred from 178.9 to 384.5°C assigned to a loss of surfactant. The fourth mass loss step was ascribed to the loss of OH units through dehydroxylation over the temperature range 556-636.4°C.

Marras, Tsimpliaraki, Zuburtikudis, and Panayiotou (2007) studied clay surface by modifying with hexadecylammonium cation (HDA). The contents of HDA were varied between to 0.15 to 3.0 times clay CEC. They found that the interlayer

spacing was gradually increased with increasing amount of HDA. The decomposition of HDA took place at temperature between 200-500°C. As the content of HDA increase, new peak was observed at lower temperature and attributed to the decomposition of the adsorbed surfactant at the external surfaces of clay.

Heinz, Vaia, Krishnamoorti, and Farmer (2007) studied the structure and dynamics of alkylammonium surfactant of different ammonium head groups and different chain length on clay surface using molecular dynamic simulation and compared to the experimental data. They found that primary amine head group (NH_2) can form hydrogen bonds ($\text{N-H}\cdots\text{O-Si}$) to the clay surface while quaternary ammonium head group ($\text{N}(\text{CH}_3)_3$) form flexibly hydrogen bonded ($\text{H}\cdots\text{O}$) with clay surface. The interlayer spacing increased with increasing alkyl chain length. The monolayer was observed when clay was modified with primary amine of 10 carbon atoms or less or quaternary amine of 8 carbon atoms. In addition, the surfactant alignment was changed to bilayer structure with increasing alkyl chain length to 22 carbon atoms for primary amine or to 20 carbon atoms for quaternary amine.

2.4 Polymer/clay nanocomposites

Zhang and Loo (2008) studied amorphous polyamide (aPA)/organoclay nanocomposites at various organoclay content preparing by melt intercalation. Clay surface was prepared by using quaternary ammonium surfactants with phenyl (dimethyl benzyl hydrogenated tallow ammonium chloride, 10AMMT) and hydroxyl (methyl tallow bis-2-hydroxyethyl ammonium chloride, 30BMMT) groups. The result showed that organoclays containing phenyl or hydroxyl groups were compatible with the chemical groups in aPA resulted in a well-exfoliated clay morphology and strong

interfacial adhesion between the clay surface and matrix. Tensile tests showed that the addition of organoclay caused a dramatic increase in Young's modulus and yield strength of the nanocomposites compared with the homopolymer. The aPA nanocomposites exhibited ductile behavior up to 5 wt% of organoclay. Nevertheless, the mechanical properties (*e.g.*, Young's modulus and yield stress) of nanocomposites from 10AMMT were slightly better than those from 30BMMT. Since 10AMMT contained hydrophobic phenyl ring, the interfacial adhesion between 10AMMT and matrix was better than that of 30BMMT and matrix. Although the hydroxyl groups in 30BMMT help to improve polymer–surfactant interactions through hydrogen-bond formation, they can also serve to weaken polymer–clay interactions.

Marras, Tsimpliaraki, Zuburtikudis, and Panayiotou (2009) studied effect of the modification degree of MMT on structure, thermal and mechanical properties of poly (L-lactic acid) (PLLA)/organoclay nanocomposites. Clay surface was modified by hexadecylammonium cation (HDA) with a concentration ranging from 0.3 to 3 times clay CEC. XRD analysis showed that proper separation of the clay layers was achieved and the inorganic cations in the interlayer spacing were completely exchanged by alkylammonium cations. However, high amount of surfactant molecule may restrict penetration of polymer chains into clay layer. The optimal interactions between the organoclay and the PLLA matrix can be achieved at surfactant loading of 1.5 times clay CEC. This led to the best compromise between thermal and mechanical properties of the PLLA/organoclay nanocomposites. The tensile properties of the nanocomposites increased with increasing surfactant contents. In addition, an increase in HDA content improved the miscibility between matrix and the organoclay leading to an enhancement the ductility and stiffness of the nanocomposites. At high

surfactant content, some of the excess surfactant leached from the organoclay to the polymer and acted as stress concentrators resulting in a dramatic deterioration of the mechanical properties of the material. Moreover, TGA results revealed that the low content of surfactant improved thermal stability and increased the initial decomposition temperature of the polymer.

2.5 Rubber/clay nanocomposites

A rubber has been considered an ideal matrix for nanocomposites. The high molecular weight of rubber is beneficial with respect to shearing, which facilitates the peeling apart of the clay layers. Numerous other researchers later used this concept for nanocomposites based on polybutadiene rubber (BR), styrene-butadiene rubber (SBR), isobutylene-isoprene rubber (IIR), ethylene-propylene-diene rubber (EPDM), epoxydized natural rubber (ENR) and natural rubber (NR).

2.5.1 Synthetic rubber

Wang *et al.* (2005) prepared BR/clay nanocomposites by melt mixing. Clay surface was modified by dimethyldi hydrogenate tallow ammonium chloride (DDAC). The results showed that the organoclay decreased the cure time and scorch time of BR nanocomposites. The tensile strength, elongation at break, and tear strength of the BR/organoclay were greatly improved in comparison with those of gum BR and BR/clay nanocomposites. Kim M-S., Kim D-W., Chowdhury S. R., and Kim G-H. (2006) prepared BR nanocomposites containing two types of organoclay, *i.e.* cloisite 15A and Cloisite 20A. Both organoclay were prepared by modifying clay surface with different contents of dimethyldi hydrogenated tallow quaternary ammonium; *i.e.* 125 and 95 meq/100g clay. The result showed the good

dispersion of organoclay in BR. The tensile and tear strengths of the BR/Cloisite 20A were 4.4 times and 2 times higher than those of the gum BR, respectively. The rebound resilience, compression set, and abrasion resistance of the BR nanocomposites were also improved by the addition of organoclay. This was due to the good dispersion of organoclay in BR matrix. The BR nanocomposite with 3 phr organoclay showed higher torque values and torque difference than gum BR. Scorch time and cure time of the BR nanocomposites were reduced drastically when organoclays were incorporated into BR. This indicated that the organoclay acted as accelerators of BR vulcanization. Wan Chaoying, Dong Wei, Zhang Yinxi, and Zhang Yong (2008) prepared BR/clay composites by melt mixing method. Clay surface were modified by two different types of surfactants, *i.e.* octadecylamine (primary ammonium cation (P-OMMT)) and dimethyl dihydrogenated tallow ammonium chloride (quaternary ammonium cation (Q-OMMT)). Both BR/P-OMMT and BR/Q-OMMT nanocomposites showed intercalated structure. This indicated homogeneous swelling of organoclays with no reaggregation of the layers. The tensile strength and elongation at break of BR/Q-OMMT nanocomposites were enhanced compared with those of the gum BR. This was due to the well-ordered intercalated clay layers oriented under the tensile stress and the alignment of BR chains absorbed on the clay layers. The tear strength, modulus at 100% elongation and hardness of BR/Q-OMMT was the highest among those of the nanocomposites.

Zhang Liqun, Wang Yizhong, Wang Yiqing, Sui Yuan, and Yu Dingsheng (2000) studied SBR/clay nanocomposites. SBR nanocomposites were prepared by mixing the SBR latex with clay/water dispersion and coagulated the mixture. Carbon black and silica were used as fillers in SBR matrix, in order to

compare to the properties of SBR/clay nanocomposites. The SBR/clay nanocomposites showed aggregated structure. The tensile strength of SBR/clay nanocomposites was the highest among those of the SBR composites. All the mechanical properties of the nanocomposites with lower content of clay reached the level of the SBR/carbon black composite. Wang, Zhang, Tang, and Yu (2000) prepared SBR/clay nanocomposites using two different methods, *i.e.* latex and solution methods. The tensile strength and tear strength of SBR/clay nanocomposites prepared from latex method were better than those of SBR/clay nanocomposites prepared from solution method. Compared with the solution methods, the latex method was more convenient and became widely used to prepare rubber/clay nanocomposites. Sadhu and Bhowmick (2003) prepared nanoclays with different alkyl chain lengths of surfactants base on Na^+ -MMT in SBR nanocomposites by solution method. Clay surface modification was done using organic amines of various alkyl chain lengths, *i.e.* decylamine (DA), dodecylamine (DD), hexadecylamine (HD) and octadecylamine (OC). The interlayer spacing of Na^+ -MMT/DD was the highest among all organoclays. The SBR/organoclay nanocomposites showed the exfoliated structure. The tensile strength of SBR/ Na^+ -MMT/OC nanocomposite was the highest among all of SBR/organoclay nanocomposites. This indicated the better interaction between SBR and Na^+ -MMT/OC.

Liang Y., Wang Y., Wu Y., Lu Y., Zhang H., and Zhang L. (2005) prepared IIR/clay nanocomposites using solution and melt intercalation methods. IIR/clay nanocomposites prepared from both methods showed exfoliated and intercalated structures. The aspect ratio of clay layers in the IIR/organoclay nanocomposite prepared from solution method was larger than that in the

IIR/organoclay nanocomposite. In addition, the nanocomposites prepared from solution method gave better tensile strength and gas barrier properties than those prepared from melt intercalation.

Gatos and Karger-Kocsis (2005) studied effect of primary and quaternary amine surfactants on dispersion of modified MMT in EPDM matrix of various polarities. The EPDM nanocomposites with 10 phr of organoclay were prepared using melt compounding method. Clay surface was modified using octadecylamine (MMT-PRIM) and octadecyltrimethylamine (MMT-QUAT). In order to adjust the polarity of EPDM, EPDM-g-MA was added to the EPDM at a weight ratio of 50/50. In EPDM/MMT-PRIM nanocomposite, intercalated, deintercalated and exfoliated structures were generated. On the contrary, only exfoliated and deintercalated structures were obtained in EPDM-MA/MMT-PRIM nanocomposites. Both EPDM and EPDM-MA filled MMT-QUAT nanocomposites showed intercalated structures. The tensile strength of EPDM-MA/MMT-PRIM was increased with increasing organoclay content, whereas a deterioration of tensile strength of the EPDM-MA/MMT-QUAT occurred at high organoclay content. The 10 phr of organoclay loading appeared to be an optimum content for enhancing tensile strength of the EPDM-MA nanocomposites. Increasing the polarity of the EPDM supported the intercalation/exfoliation of organoclay irrespective to the type of surfactant (PRIM, QUAT).

Rajasekar R., Pal K., Heinrich G., Das A., and Das C. K. (2009) studied the incorporation of ENR/organoclay nanocomposites (EC) as compatibilizer in NBR matrix in order to improve the properties of NBR/organoclay composites. The morphology, cure characteristics and mechanical properties of NBR nanocomposites

were investigated. They found an intercalated structure of organoclay in ENR. Incorporation of 5 phr of EC in NBR matrix, exfoliated structure of organoclay in NBR matrix was observed. However, upon increasing EC content to 10 phr led to intercalated/exfoliated dispersion of organoclay in NBR. NBR/5EC and NBR/10EC showed faster scorch time, cure time and increase in maximum torque compared to gum NBR. The mechanical properties of NBR/EC were enhanced due to the better dispersion of organoclay in the NBR matrix and the rubber-filler interaction. In addition, SEM micrograph showed the increase in roughness of EC filled NBR matrix compared to gum NBR. This may be due to the increase in effective network chains from the high reinforcing efficiency of the organoclay in the NBR matrix.

2.5.2 Natural rubber

Arroyo, Lopez-Manchado, and Herrero (2003) prepared NR/clay nanocomposite by melt compounding method. Properties of NR filled with 10 phr of clay or organoclay (octadecylamine modified montmorillonite; MMT-ODA) were compared with those of NR filled with 10 phr and 40 phr of carbon black. NR/MMT-ODA nanocomposite showed exfoliated structure. The interlayer spacing of NR/MMT-ODA was higher than that of NR composites. The vulcanization rate and torque value of NR nanocomposites were sensibly higher than those of NR filled with 40 phr of carbon black. The mechanical properties of NR nanocomposites with 10 phr of MMT-ODA were comparable to those of NR composite with 40 phr of carbon black. Moreover, addition of organoclay drastically improved the strength of NR nanocomposites while reduced the elasticity of the material.

Magaraphan R., *et al.* (2003) prepared organoclay by using primary amine and quaternary amine. The NR nanocomposites were prepared by dissolving in toluene at various contents of organoclay. The dispersion of the organoclay in the NR nanocomposites showed exfoliated structure when organoclay content was below 10 phr. However, partially exfoliated structure was observed with adding more than 10 phr of organoclay. Moreover, addition of long alkyl chain of primary amine modified clays helped improved mechanical properties of the NR nanocomposites more than addition of quaternary ammonium modified clays. The curing properties of NR nanocomposites were also improved. NR nanocomposites with 7 phr of organoclay showed the highest mechanical properties compared with NR/silica and NR/carbon black composites of equal content of the filler.

Varghese and Karger-Kocsis (2004) prepared NR/clay composites by melt compounding with sulfur curing. Clay surfaces were modified using primary amine (MMT-ODA) and quaternary amine (MMT-TMDA). The organoclay content was 10 phr. The dispersions of clay in NR nanocomposites were partly exfoliated, partly intercalated and partly reaggregated structures. The interlayer spacing of NR/MMT-ODA nanocomposite was higher than that of NR/MMT-TMDA nanocomposite. Adding MMT-ODA and MMT-TMDA gave NR nanocomposites with better mechanical properties and faster curing compared to those NR composites prepared from pristine layered silicates and silica.

Teh *et al.* (2004) prepared NR/organoclay nanocomposites by melt compounding method. ENR25 (25 mol% epoxidation) and ENR50 (50 mol% epoxidation) were used as compatibilizers. Clay surface was modified using octadecyltrimethylamine (MMT-ODTMA). The organoclay content was fixed at 2 phr

while ENR content was varied, *i.e.* 5 or 10 phr. NR/MMT-ODTMA showed mostly intercalated structure of the organoclay. The best dispersion of organoclay in NR nanocomposites was achieved by adding ENR50. This was due to the incorporation of ENR50 in NR facilitates the penetration of both molecules in between the silicate layers. The tensile strength and tear strength of the ENR50 compatibilized NR/organoclay nanocomposites were better than those of ENR25 compatibilized and uncompatibilized NR/organoclay nanocomposites. This was because the epoxy groups of ENR50 promoted the interaction between the organoclay and NR matrix leading to strong interfacial adhesion between matrix and organoclay.

Arroyo, Lopez-Manchado, Valentin, and Carretero (2007) prepared NR nanocomposites by melt mixing. The nanocomposites were prepared by blending NR with ENR25 (25 mol% epoxidation) and ENR50 (50 mol% epoxidation). Clay surfaces were modified using dimethyldi hydrogenated tallow (MMT-2M2HT) and methyl tallow bis-2-hydroxyl quaternary ammonium (MMT-MT2EtOH). NR/organoclay nanocomposite blended with ENR showed exfoliated structure. This was due to the polarity of ENR, which favoured the intercalation of rubber molecules into the clay layers, and the dispersion of the organoclay in the matrix. The interaction between NR and organoclay was improved due to the good dispersion of organoclay in the NR matrix. NR/ENR50 blends filled with MMT-2M2HT gave the highest mechanical properties among all of NR nanocomposites.

Varghese, Karger-Kocsis, and Gatos (2003) prepared ENR/clay nanocomposites by melt compounding method. The 10 phr of clay (sodium bentonite and sodium fluorohectorite) and organoclays (MMT-base) were used. Octadecylamine (MMT-ODA) and quaternary amine (MMT-MTH) were used to modify clay surface.

Both ENR/MMT-ODA and ENR/MMT-MTH nanocomposites showed an intercalated structure. Among ENR composites, ENR/MMT-ODA nanocomposite showed the fastest scorch time and cure time. The tensile strength and tear strength of ENR/MMT-ODA were higher than those of ENR/MMT-MTH, ENR/sodium bentonite and ENR/sodium flourohectorite composites. This was due to the good dispersion of MMT-ODA in ENR nanocomposite.

CHAPTER III

EXPERIMENTAL

3.1 Materials

Natural rubber (STR 5L) was purchased from Thai Hoa Rubber Public Co., Ltd. Epoxidized natural rubber (ENR50) was purchased from Muang Mai Guthrie Public Co., Ltd. Sodium montmorillonite clay (Na⁺-MMT) with cation exchange capacity (CEC) value of 80 meq/100g was supplied by Thai Nippon Co., Ltd. Octadecylamine (ODA: CH₃(CH₂)₁₇NH₂) was purchased from Acros. Tetradecyl trimethyl ammonium bromide (TDMA-Br: [CH₃(CH₂)₁₃](CH₃)₃NBr) and octadecyl trimethyl ammonium bromide (ODTMA-Br: [CH₃(CH₂)₁₇](CH₃)₃NBr) surfactants were purchased from Fluka and Aldrich, respectively. Chemical structures of these surfactants are shown in Figure 3.1.

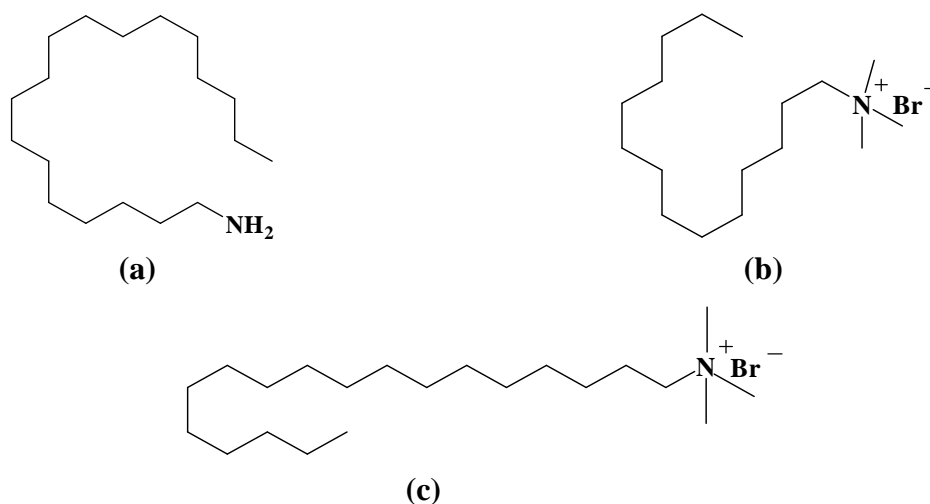


Figure 3.1 Chemical structures of (a) ODA (b) TDMA-Br and (c) ODTMA-Br.

3.2 Experimental

3.2.1 Preparation of organoclays

100 g of MMT was dispersed in 2000 ml of hot water (70°C) with continuous stirring. Added surfactant content was varied and calculated using equation (3.1) based on CEC of MMT (Umpush J. and Wibulswas R., 2006).

$$\text{Weight of surfactant (g)} = n \times \text{CEC} \left(\frac{\text{meq}}{\text{g}} \right) \times A \text{ (g)} \times B \left(\frac{\text{g}}{\text{mol}} \right) \quad (3.1)$$

where A is weight of clay (g), B is molecular weight of surfactant (g/mol).

ODA and conc. hydrochloric acid were dissolved in 1000 ml of hot deionized water, with vigorous stirring. Then the ODA solution was poured into the hot clay-water dispersion and vigorously stirred for 2 hours. After that, the suspension was washed several times with hot deionized water (70°C) until water conductivity was below 10 μS . The modified clay, called organoclay, was vacuum-filtrated, dried at 70°C in an oven and ground for further uses. The contents of ODA added were equivalent to 0.5, 1 and 2 times CEC of the MMT. So, the ODA modified clays were called MMT-ODA0.5, MMT-ODA1 and MMT-ODA2, respectively.

TDMA-Br was dissolved into 3000 ml of hot water with continuous stirring. Then, 100 g of MMT was added to the TDMA-Br solution. The suspension was stirred vigorously for 2 hours. After that the suspension was washed several times with deionized water until water conductivity was below 10 μS . The modified clay was vacuum-filtrated, dried at 70°C in an oven and ground for further uses. The contents of TDMA-Br added were equivalent to 0.5, 1 and 2 times CEC of the MMT. So, the TDMA-Br modified clays were called MMT-TDMA0.5, MMT-TDMA1 and

MMT-TDMA2, respectively. In addition, ODTMA-Br modified clays was prepared using the same method as that of TDMA-Br modified clays. Then, the ODTMA-Br modified clays were called MMT-ODTMA0.5, MMT-ODTMA1 and MMT-ODTMA2, depending on the content of the added ODTMA-Br.

3.2.2 Preparation of NR nanocomposites

NR/organoclay nanocomposites were prepared on a two-roll mill (CHAICHAROEN) at room temperature. Mixing time was 15 min. The rotors were operated at a speed ratio of 1:1.4. Firstly, NR was milled. Then 5 phr of clay (MMT) or organoclays (MMT-ODA0.5, MMT-ODA1, MMT-ODA2, MMT-TDMA0.5, MMT-TDMA1, MMT-TDMA2, MMT-ODTMA0.5, MMT-ODTMA1 and MMT-ODTMA2) were added. The vulcanization ingredients were added to the compound after the incorporation of clay and, lastly, sulfur was added. The formulations of the rubber compounds are given in Table 3.1.

One of the organoclays was chosen according to the mechanical properties of the obtained NR nanocomposites. The selected organoclay was mixed with NR at various contents of organoclay (1, 3, 5 and 10 phr) in order to observe effect of organoclay content on the mechanical of NR nanocomposites. The types and the amounts of added vulcanization ingredients were all the same to the previous experiment.

Table 3.1 Formulations of NR nanocomposites

Material	Content (phr)				
NR	100	100	100	100	100
Zinc oxide	5	5	5	5	5
Stearic acid	2	2	2	2	2
CBS ^a	1	1	1	1	1
Sulfur	2.5	2.5	2.5	2.5	2.5
MMT	-	5	-	-	-
MMT-ODA ^b	-	-	5	-	-
MMT-TDMA ^c	-	-	-	5	-
MMT-ODTMA ^d	-	-	-	-	5

^a N-Cyclohexyl-2-benzothiazolesulfenamide

^b MMT-ODA 0.5CEC, 1CEC, 2CEC

^c MMT-TDMA 0.5CEC, 1CEC, 2CEC

^d MMT-TDMA 0.5CEC, 1CEC, 2CEC

Table 3.2 Formulations of NR/ENR blend nanocomposites

Material	Content (phr)			
NR	100	60	40	0
ENR	0	40	60	100
Zinc oxide	5	5	5	5
Stearic acid	2	2	2	2
CBS	1	1	1	1
Sulfur	2.5	2.5	2.5	2.5
Organoclay ^a	Δ	Δ	Δ	Δ

^a The selected organoclay

Δ The selected organoclay content

ENR was blended with NR on a two-roll mill in order to adjust polarity of matrix. The NR/ENR blend ratios were 100/0, 60/40, 40/60 and 0/100 by weight. The fixed content of the selected organoclay was added. The vulcanization ingredients were added to the compound after the incorporation of clay and, lastly, sulfur was added. Each vulcanization ingredient was added with the same amount as in the previous experiment. The formulations of NR/ENR blended with organoclay were shown in Table 3.2.

3.3 Material characterization

3.3.1 Characterization of clay and organoclays

3.3.1.1 Structure of clay and organoclays

Structures of clay and organoclay were analyzed by an X-ray diffraction spectrometer (XRD) (OXFORD/D5005) with a Cu-K α as a radiation source ($\lambda = 1.5418 \text{ \AA}$). The instrument was operated at a voltage of 35 kV with a step size of 0.02° and a scan speed of $1.0^\circ/\text{min}$.

3.3.1.2 Functional groups and chain conformation

Functional groups of the surfactant on organoclay surface were identified by a Fourier transform infrared spectrometer (FTIR) (BIO-RAD/FTS175C, KBr pellet technique). The spectrum was recorded in the $4000\text{-}400 \text{ cm}^{-1}$ region with 2 cm^{-1} resolution.

3.3.1.3 Thermal properties

Thermal decomposition temperature and weight loss of clay and organoclay were determined by a thermogravimetric analyzer (TGA)

(TA INSTRUMENT/SDT2960). Sample was heated under a nitrogen atmosphere from room temperature to 500°C at a rate of 20°C/min.

3.3.2 Characterization of NR nanocomposites

3.3.2.1 Structure of clay and organoclays

Structures of clay/organoclay in NR nanocomposites were analyzed using XRD.

Dispersion of clay/organoclay in NR nanocomposites were determined by a transmission electron microscope (TEM) (OXFORD/JOEL JEM-2010) at an accelerator voltage of 120 kV. Thin sections (ca.100 nm) of the cured samples were cut using a diamond knife at -120°C.

3.3.2.2 Cure characteristics

Cure characteristics of NR nanocomposites were determined using a moving die rheometer (MDR) (GOTECH/GT-M200F) at a temperature of 150°C. Scorch time (T_{s1}), cure time (T_{c90}), maximum torque (S_{max}), minimum torque (S_{min}) and torque difference ($S_{max} - S_{min}$) of the nanocomposites were determined.

3.3.2.3 Mechanical properties

NR nanocomposite was vulcanized at 150°C for the time corresponding to cure time using a compression molding machine. Compression molded NR nanocomposites samples were cut into dumbbell shape with a die cutter (type C). Tensile properties of NR/clay nanocomposites were tested according to ASTM D412–98a. The specimens were performed on a universal testing machine (INSTRON/model 5569), with a cross-head speed of 500 mm/min. Tensile strength, elongation at break and modulus at 100% and 300% elongation of the NR nanocomposites were determined.

Hardness was measured according to ASTM D2240 by an international rubber hardness degrees (IRHD) tester (BAI EISS/digi test).

3.3.2.4 Crosslink density

Crosslink density (n) of NR/organoclay nanocomposites was determined on the basis of rapid solvent-swelling measurements. The samples were swollen in toluene at 27°C for 72 hours until equilibrium swelling was reached.

The crosslink density of NR/organoclay nanocomposites was calculated by application of Flory-Rhener equation (Flory, 1953):

$$n = \frac{-[\ln(1 - \Phi_r) + \Phi_r + \chi\Phi_r^2]}{V_0[\Phi_r^{1/3} - (\Phi_r / 2)]} \quad (3.2)$$

where Φ_r is the volume fraction of polymer in the swollen mass, V_0 is the molar volume of the solvent (106.2 for toluene), and χ is the Flory-Huggins polymer-solvent interaction term (the value of χ is 0.393 for toluene). The volume fraction of polymer, Φ_r , is calculated by the following expression (Avalos, Ortiz, Zitzumbo, Lopez-Manchado, Verdejo, and Arroyo, 2008):

$$\Phi_r = \frac{(W_r / \rho_r)}{\left(\frac{W_r}{\rho_r}\right) + \left(\frac{W_s}{\rho_s}\right)} \quad (3.3)$$

where W_r and W_s are weight of the rubber samples and weight of swollen rubber, respectively. ρ_r and ρ_s are density of the rubber samples and density of the solvent, respectively.

CHAPTER IV

RESULTS AND DISCUSSION

4.1 Characterization of clay and organoclays

4.1.1 Structures of clay and organoclays

X-ray diffraction (XRD) spectroscopy is a common technique used in investigating surfactant intercalation and expansion of MMT. As MMT interlayer spacing can expand or contract, the peak position in the XRD spectrum of MMT shifts proportionally. Then, the interlayer spacing of MMT can be calculated from the XRD peak position using Bragg's law:

$$d = \lambda / (2 \sin\theta) \quad (4.1)$$

where d is the interlayer spacing of clay, λ is the X-ray wavelength of CuK_α equal to 1.5418 Å, and θ is the incident angle of X-ray.

Figure 4.1 presents XRD spectra of MMT and modified MMT at various surfactant types, *i.e.* ODA, ODTMA-Br, TDMA-Br, and surfactant contents, *i.e.* 0.5, 1, 2 times clay CEC. From the figure, MMT showed a diffraction peak at $2\theta = 6.4^\circ$ with an interlayer spacing of 1.38 nm. After treating MMT with all types of surfactant, the diffraction peaks of modified MMT shifted to a lower 2θ values compared with that of MMT. This implied that the MMT interlayer spacing was expanded due to the intercalation of alkylammonium surfactants. As shown in Figure 4.1 (a)-4.1 (c), the interlayer spacing of the modified MMT increased with increasing

surfactant contents up to 2 times clay CEC, suggesting a coexistence of intercalated surfactant molecules within the interlayer spacing of MMT. From Figure 4.1, it can be concluded that all types of surfactant used in the study effectively expanded the interlayer spacing of MMT.

The values of interlayer spacing of clay and organoclay are summarized in Table 4.1. Among three surfactant contents, *i.e.* 0.5, 1, 2 times clay CEC, the interlayer spacing of ODA treated MMT and that of ODTMA-Br treated MMT increased with increasing the corresponding surfactant content up to 2 times clay CEC. However, the interlayer spacing of TDMA treated MMT increased with increasing TDMA-Br content up to 1 times clay CEC. Then its value was level off at TDMA-Br content of 2 times clay CEC. These results indicated that the content of surfactant used to treat MMT affected the expansion of the MMT interlayer spacing in various ways depending on types of surfactant used.

In comparison between a primary amine (ODA) and a quaternary amine (ODTMA-Br), which have 18 carbon atoms in their alkyl chains, MMT-ODTMA1 had higher interlayer spacing than MMT-ODA1. This may be because ODTMA-Br had bigger head group than ODA. Furthermore, both MMT-ODTMA2 and MMT-ODA2 showed two diffraction peaks. The first peak at lower 2θ value was the peak of high ordered surfactant arrangement in clay layers. The second peak at higher 2θ value belonged to the peak of incomplete alkyl chain arrangement or the loss of coherence from well ordered arrangement of the surfactants in the clay layers. This was due to the arrangement of long alkyl chain of surfactant molecules during modification.

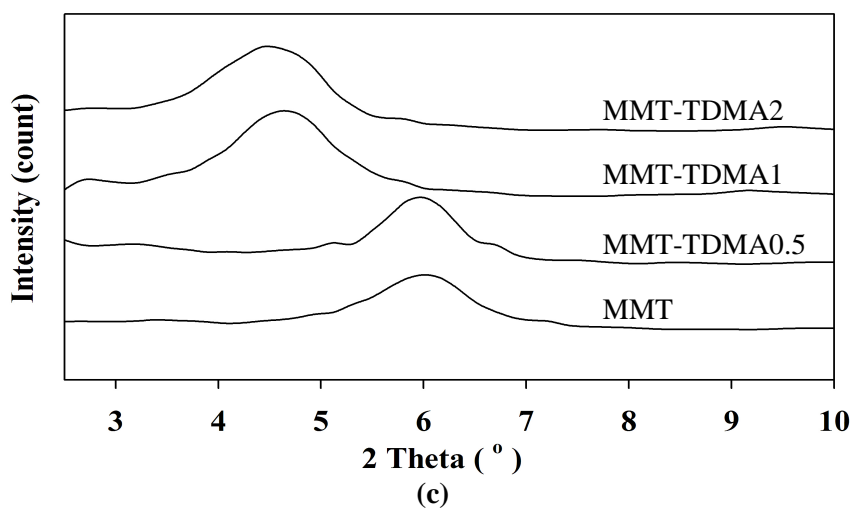
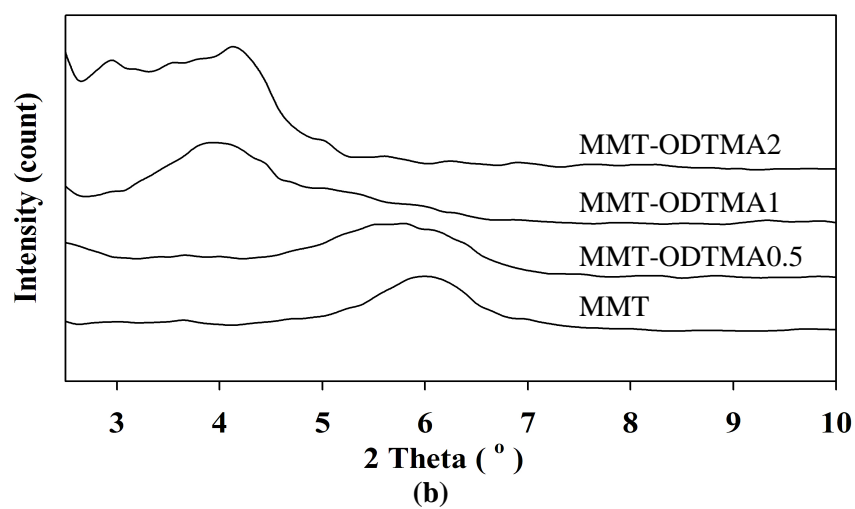
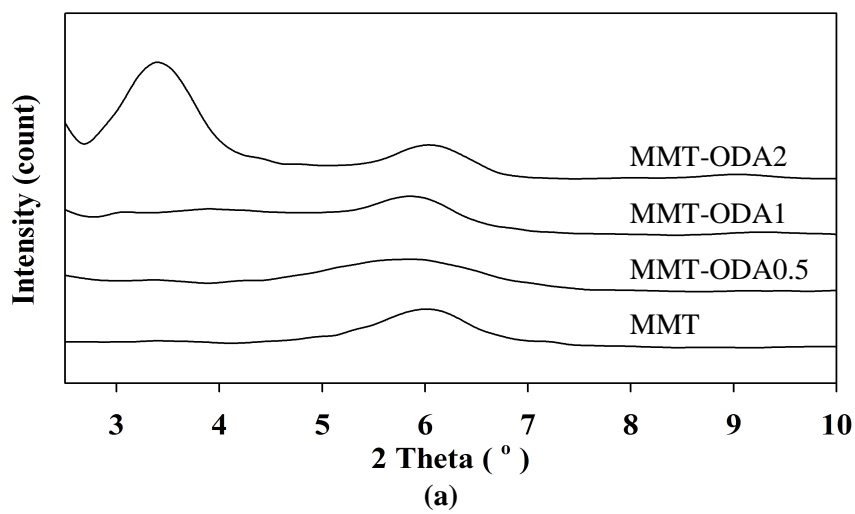


Figure 4.1 XRD spectra of MMT and modified MMT with (a) ODA, (b) ODTMA-Br and (c) TDMA-Br at 0.5, 1 and 2 times clay CEC.

Table 4.1 2 Theta (2θ) and interlayer spacing of MMT and modified MMT

Clay/Organoclay	2 Theta ($^{\circ}$)	Interlayer spacing (nm)
MMT	6.40	1.38
MMT-ODA0.5	5.94	1.48
MMT-ODA1	5.44	1.62
MMT-ODA2	2.92, 5.68	3.02, 1.55
MMT-ODTMA0.5	5.52	1.60
MMT-ODTMA1	3.98	2.22
MMT-ODTMA2	2.90, 4.14	3.04, 2.13
MMT-TDMA0.5	6.02	1.47
MMT-TDMA1	4.68	1.89
MMT-TDMA2	4.66	1.90

In comparison between two types of quaternary ammonium cation surfactant, *i.e.* TDMA-Br with 14 carbon atoms in its alkyl chain and ODTMA-Br with 18 carbon atoms in its alkyl chain, MMT-ODTMA had higher interlayer spacing than MMT-TDMA of an equal surfactant content. This indicated that the surfactant with longer alkyl chain length in its molecule was beneficial to expand the interlayer spacing of MMT. The similar result was reported by Lagaly *et al.* (1976) for their investigation on interlayer spacing of organoclays modified with alkyl ammonium compounds of different alkyl chain length ($n= 6, 7, 8...16, 17, 18$).

From the results, the modified MMT had larger interlayer spacing than MMT which should be beneficial to produce the NR nanocomposite.

4.1.2 Functional groups and chain conformations

Fourier transform infrared spectroscopy (FTIR) was used to identify functional groups of MMT and modified MMT. Figure 4.2 (a)-4.2 (c) show FTIR spectra of MMT and modified MMT. The spectrum of MMT showed a broad band between 3644-3324 cm^{-1} corresponding to the OH stretching vibration of water, and a band at 1638 cm^{-1} corresponding to the OH bending vibration of the interlayer water of the MMT. In addition, a sharp band corresponding to the Si-O stretching vibration of the layered silicate was observed at 1038 cm^{-1} . Furthermore, the Si-O and Al-O bending vibration bands were observed at 600-400 cm^{-1} . FTIR spectra of organoclays (ODA, TDMA-Br and ODTMA-Br modified MMT with surfactant content of 0.5, 1 and 2 times clay CEC) showed four additional peaks compared with that of MMT. Bands around 2920 cm^{-1} and 2850 cm^{-1} attributed to the C-H asymmetric, $\nu_{\text{as}}(\text{CH}_2)$ and C-H symmetric $\nu_{\text{s}}(\text{CH}_2)$, stretching vibration of alkyl chains, respectively. Bands around 1470 cm^{-1} and 1380 cm^{-1} corresponded to the C-H asymmetric and symmetric bending vibration of alkyl chains, respectively. These results indicated that the surfactants may intercalate into MMT galleries or adsorb on the surface of MMT.

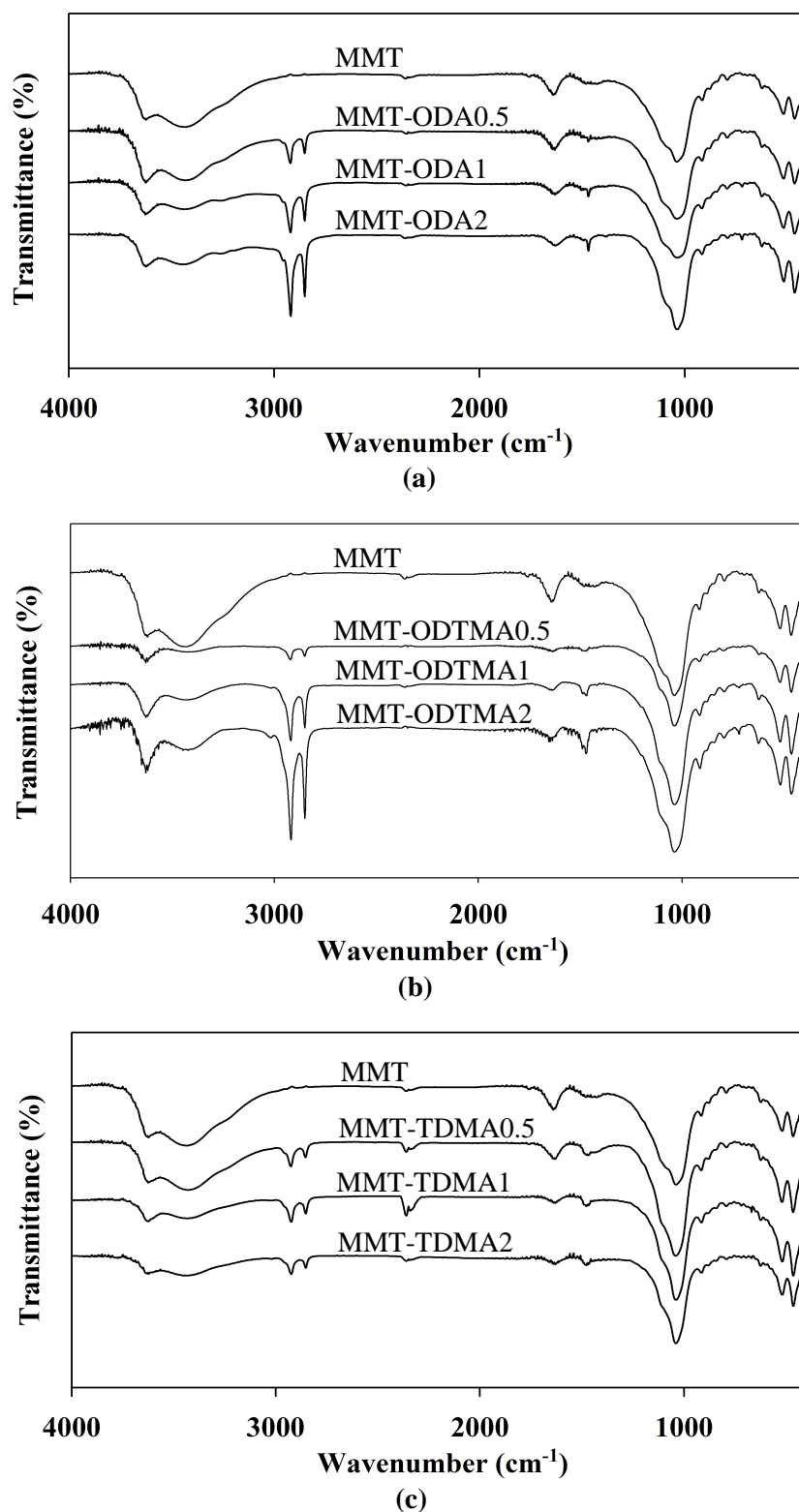


Figure 4.2 FTIR spectra of MMT and modified MMT with (a) ODA, (b) ODTMA-Br and (c) TDMA-Br at 0.5, 1 and 2 times clay CEC.

In addition, FTIR was used to monitor conformations of surfactant as functions of surfactant content, surfactant type (ammonium head group) and alkyl chain length. Vaia *et al.* (1994) found that the shift in wavelength (frequency) of the CH₂ stretching bands largely reflected the change in chain conformation of the surfactants located in interlayer spacing of MMT. As the surfactant content or the surfactant chain length increased, the intercalated surfactant molecules became highly ordered (solidlike structures, *i.e.* *trans* conformations) and their CH₂ stretching band shifted to lower frequencies (Figure 2.5 in Chapter 2). Increases in *trans* conformations led to increases in interchain contacts resulting in lower mobility of alkyl chains. In contrast, increases in *gauche* conformations (liquidlike character) led to a flexible orientation resulting in greater mobility of alkyl chains (Vaia *et al.*, 1994).

Table 4.2 shows the wavenumber of the CH₂ stretching band of MMT-ODA, MMT-ODTMA and MMT-TDMA at various contents of surfactant, *i.e.* 0.5, 1 and 2 times clay CEC. With increasing the surfactant content from 0.5 to 2 times clay CEC, $\nu_{\text{as}}(\text{CH}_2)$ of MMT-ODA and MMT-ODTMA shifted from 2921 cm⁻¹ to 2919 cm⁻¹ and their $\nu_{\text{s}}(\text{CH}_2)$ shifted from 2851 cm⁻¹ to 2850 cm⁻¹. Meanwhile, $\nu_{\text{as}}(\text{CH}_2)$ of MMT-TDMA shifted from 2927 cm⁻¹ to 2925 cm⁻¹ and its $\nu_{\text{s}}(\text{CH}_2)$ shifted from 2853 cm⁻¹ to 2851 cm⁻¹. This reflected that, with increasing surfactant content, the liquidlike state of the intercalated surfactants may probably change to a solidlike state (Vaia *et al.*, 1994; Zhu *et al.*, 2005).

Table 4.2 FTIR wavenumber of asymmetric CH₂ ($\nu_{as}(\text{CH}_2)$) and symmetric CH₂ ($\nu_s(\text{CH}_2)$) stretching vibrations of modified MMT

Organoclay	Wavenumber (cm ⁻¹)	
	$\nu_{as}(\text{CH}_2)$	$\nu_s(\text{CH}_2)$
MMT-ODA0.5	2921	2851
MMT-ODA1	2919	2850
MMT-ODA2	2919	2850
MMT-ODTMA0.5	2921	2851
MMT-ODTMA1	2919	2850
MMT-ODTMA2	2919	2850
MMT-TDMA0.5	2927	2853
MMT-TDMA1	2925	2951
MMT-TDMA2	2923	2851
pure ODA	2918	2849
pure TDMA-Br	2918	2849
pure ODTMA-Br	2918	2849

Among three surfactant contents (0.5, 1, 2 times clay CEC) of MMT-ODA, MMT-ODTMA and MMT-TDMA, the $\nu_s(\text{CH}_2)$ and $\nu_{as}(\text{CH}_2)$ stretching vibrations of the intercalated surfactant molecules shifted to lower frequency with increasing surfactant content from 0.5 to 2 times clay CEC. This indicated that the coexistence of high amounts of surfactant molecules in the MMT layers may be decrease the mobility of alkyl chains.

In comparison between a primary amine, ODA (R-NH_3^+), and a quaternary amine, ODTMA-Br (R-NMe_3^+), with increasing surfactant content from 0.5 to 2 times clay CEC, the $\nu_{\text{as}}(\text{CH}_2)$ stretching vibration values of MMT-ODA were similar to those of MMT-ODTMA at corresponding surfactant content. This implied that the difference in ammonium head group had no effect on the shift of $\nu_{\text{as}}(\text{CH}_2)$ stretching vibration.

In comparison between two types of a quaternary ammonium surfactant, *i.e.* TDMA-Br with 14 carbon atoms in its alkyl chain and ODTMA-Br with 18 carbon atoms in its alkyl chain, the $\nu_{\text{as}}(\text{CH}_2)$ stretching vibrations of MMT-TDMA was higher than that of MMT-ODTMA at corresponding surfactant content. This was because TDMA-Br had larger available surface area per surfactant molecule than ODTMA-Br since TDMA-Br has shorter alkyl chain length than ODTMA-Br. So, the molecules of TDMA-Br are more flexible and have greater mobility within MMT-TDMA layer than those of ODTMA-Br. These results were similar to the research work investigated by Vaia *et al.* (1994). They found that the frequency shift in $\nu_{\text{as}}(\text{CH}_2)$ stretching of primary alkyl amine ($\text{C}_n\text{H}_{2n+1}\text{NH}_2$, $n = 6, 9, 10, 11, 12, 13, 14, 16$ and 18) surfactants increased with decreasing an alkyl chain length.

From the FTIR results, TDMA-Br with a shorter alkyl chain presented the liquidlike state and gave a greater mobility of alkyl chain on the organoclay surface as compared with other surfactants used in this study. Therefore, MMT-TDMA should be more beneficial to produce NR nanocomposite than MMT-ODA and MMT-ODTMA.

4.1.3 Decomposition temperatures

Thermogravimetric analysis (TGA) was used to study the thermal stability of organoclay and the intercalated surfactant molecules.

Figure 4.3-4.4 show TGA and DTG thermograms of MMT and MMT modified with ODA, ODTMA-Br or TDMA-Br at 0.5, 1 and 2 times clay CEC. Onset thermal decomposition temperatures and weight loss of MMT and modified MMT are summarized in Table 4.3. MMT and modified MMT showed weight loss at temperatures which were lower than 100°C indicating evaporation of the absorbed water. Nonetheless, the modified MMT had lower amounts of absorbed water than MMT. As observed from Figure 4.3 and 4.4, the thermal decomposition behaviors of modified MMT were varied with surfactant types and contents.

At the surfactant content of 0.5 times clay CEC, all modified MMT showed one decomposition step at the temperature which was higher than decomposition temperature of the corresponding surfactant. This implied the good interaction between the surfactant molecules and the MMT surface. With increasing surfactant content to 1 or 2 times clay CEC, the thermal decomposition patterns of modified MMT were changed to two decomposition steps. The new decomposition step was observed at a lower temperature as compared with the ones reported at the surfactant content of 0.5 times clay CEC. Additionally, the lower decomposition temperature of the modified MMT was close to the decomposition temperature of the pure surfactant. This indicated that the excess surfactant molecules had lower interaction with MMT surface and decomposed at lower temperature than the intercalated surfactant.

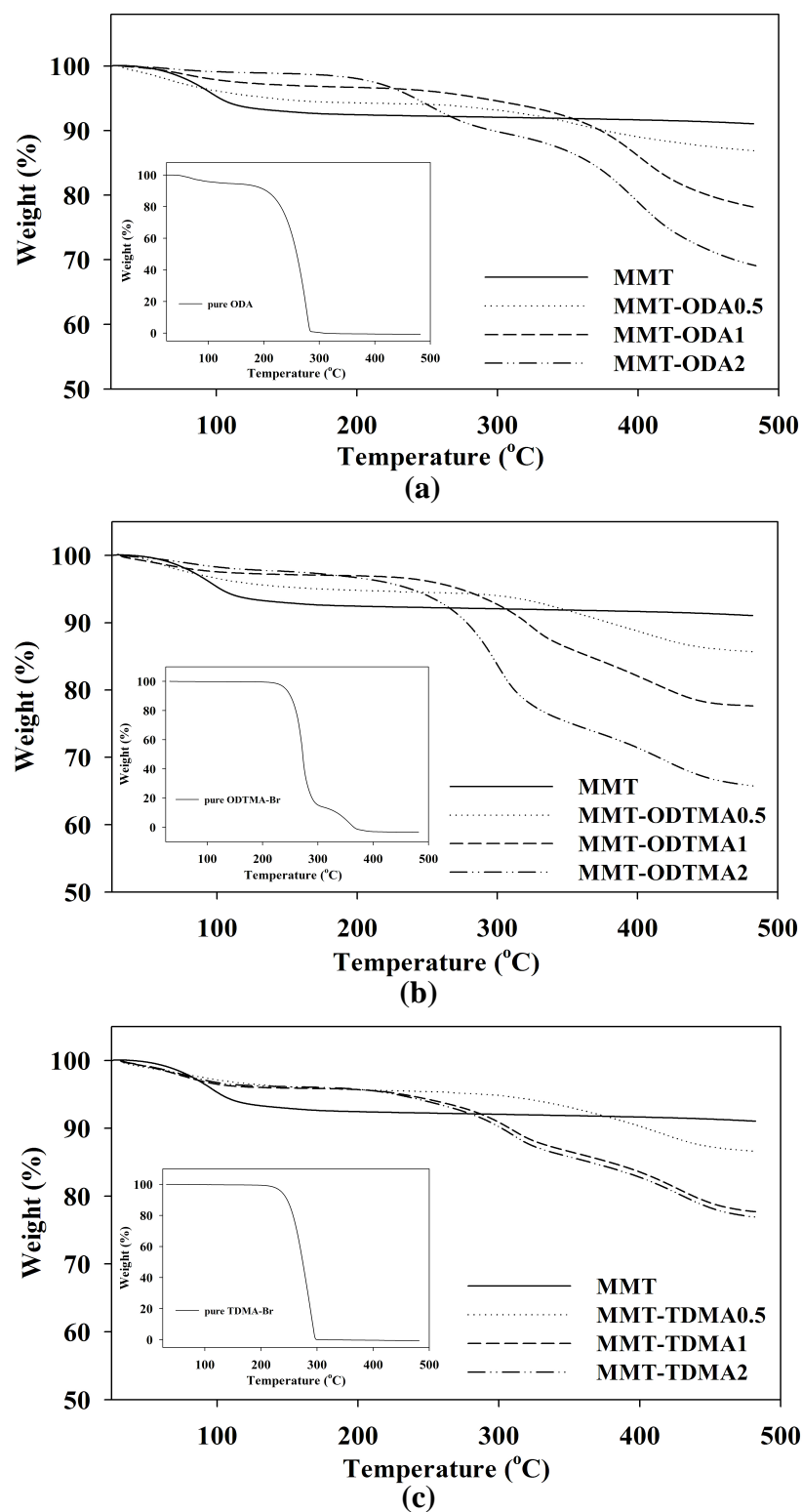


Figure 4.3 TGA thermograms of MMT and modified MMT with (a) ODA, (b) ODTMA-Br and (c) TDMA-Br at 0.5, 1 and 2 times clay CEC.

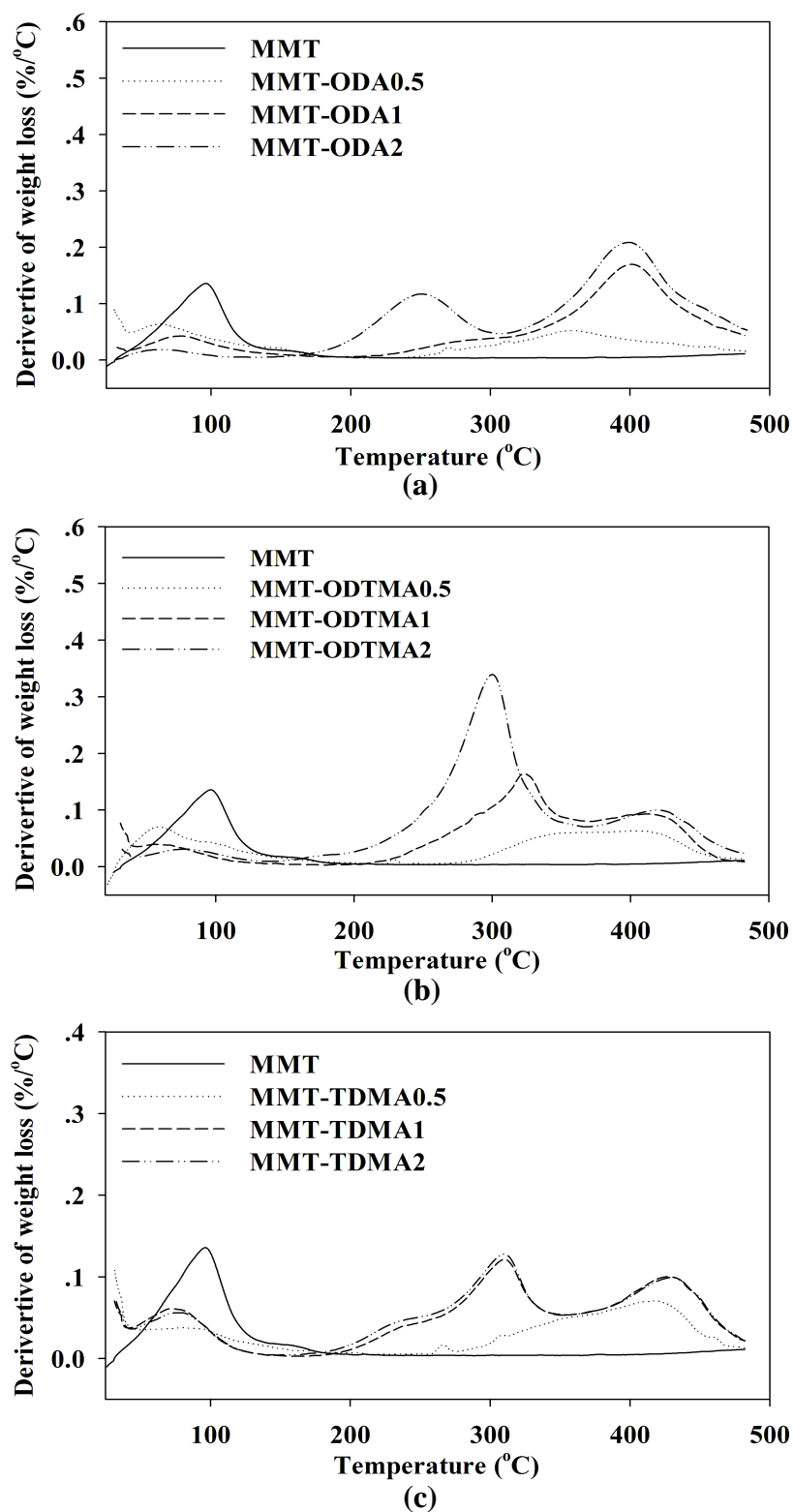


Figure 4.4 DTG thermograms of MMT and modified MMT with (a) ODA, (b) ODTMA-Br and (c) TDMA-Br at 0.5, 1 and 2 times clay CEC.

Table 4.3 The onset decomposition temperature of MMT and modified MMT

Clay/Organoclay	Water evaporation		1 st step		2 nd step	
	Wt. loss (%)	T _d (°C)	Wt. loss (%)	T _d (°C)	Wt. loss (%)	T _d (°C)
MMT	6.0	75.3	-	-	-	-
pure ODA	6.0	80.0	94.0	230.0	-	-
MMT-ODA0.5	5.0	64.0	-	-	8.0	300.0
MMT-ODA1	3.0	78.4	-	-	18.0	330.0
MMT-ODA2	1.0	66.6	10.0	230.3	19.0	358.5
pure ODTMA-Br	-	-	83.0	260.8	17.0	320.8
MMT-ODTMA0.5	4.0	58.6	-	-	10.5	323.3
MMT-ODTMA1	2.5	56.0	8.0	262.5	7.5	359.2
MMT-ODTMA2	2.0	78.3	19.5	262.7	12.0	365.4
pure TDMA-Br	-	-	100.0	250.0	-	-
MMT-TDMA0.5	3.0	80.7	-	-	8.5	335.2
MMT-TDMA1	3.0	72.7	8.5	252.2	10.0	365.0
MMT-TDMA2	3.0	77.8	8.5	252.5	10.0	365.1

Among three surfactant types *i.e.* ODA, ODTMA-Br and TDMA-Br, with increasing surfactant content from 1 to 2 times clay CEC, the weight loss and the decomposition temperature in both steps of MMT-TDMA did not significantly change. This indicated that the amounts of surfactant in the interlayer spacing of MMT-TDMA1 were similar to those in the interlayer spacing of MMT-TDMA2. This TGA result also supported XRD result that the interlayer expansion of MMT-TDMA1 was similar to that of MMT-TDMA2. On the other hand, the weight loss of MMT-

ODTMA increased with increasing surfactant content from 1 to 2 times clay CEC while the decomposition temperature was decreased. This may be because the excess ODTMA-Br molecules on MMT-ODTMA2 had less interaction with clay surface. In addition, the result suggested that MMT-ODTMA1 had less excess ODTMA-Br molecules than MMT-ODTMA2 since its weight loss at lower decomposition temperature was less than that of MMT-ODTMA2. In cases of ODA modified MMT, only MMT-ODA2 showed two decomposition steps while MMT-ODA0.5 and MMT-ODA1 showed one decomposition step. This implied that the excess ODA molecules were observed only on the surface of MMT-ODA2. Among three surfactant types, MMT-ODA had the highest weight loss at the second decomposition temperature. This was because ODA had the smallest molecular size and easily intercalated into MMT layer.

The TGA results revealed that there were two types of adsorbed surfactant molecules on the modified MMT surfaces. The first type had good interaction with MMT surface, so they decomposed at the higher temperature as compared with that of the pure surfactant. On the other hand, the second type was the excess surfactant molecules that had less interaction with the modified MMT surface so they decomposed at the temperature which was close to the decomposition temperature of the pure surfactant.

4.2 Effect of surfactant on properties of NR nanocomposites

4.2.1 Dispersion and structures of clay and organoclays

XRD and TEM are commonly complementary techniques in investigating structures and morphologies of polymer nanocomposites (Alexandre and Dubois, 2000). Figure 4.5 shows XRD spectra of NR nanocomposites based on MMT-ODA, MMT-ODTMA and MMT-TDMA at 5 phr of the organoclays. XRD spectrum of NR/MMT composite showed a diffraction peak around $2\theta = 6.0^\circ$ which was in the same position as that of MMT. In addition, TEM micrograph of NR/MMT composite in Figure 4.6 (a) illustrated the agglomeration of clay platelets in the NR matrix. These results suggested that NR molecules could not intercalate into the layers of unmodified MMT. This was due to the polarity difference between MMT and NR. So, the addition of unmodified MMT into NR matrix resulted in a conventional composite rather than a nanocomposite.

When MMT was treated with ODA, ODTMA-Br or TDMA-Br at 0.5 times clay CEC, XRD spectra of the obtained NR nanocomposites showed diffraction peaks at $2\theta = 6.0^\circ$ which corresponded to the diffraction peak of MMT. This XRD result was supported by TEM micrographs in Figure 4.6 (b), 4.7 (a) and 4.7 (d). These TEM micrographs indicated the agglomerated structures of organoclay in NR nanocomposites when MMT was treated with a surfactant at the content of 0.5 times clay CEC. These phenomena were observed in all types of surfactants. The XRD and TEM results suggested that there was still no insertion of NR molecules into MMT layers at the surfactant content of 0.5 times clay CEC.

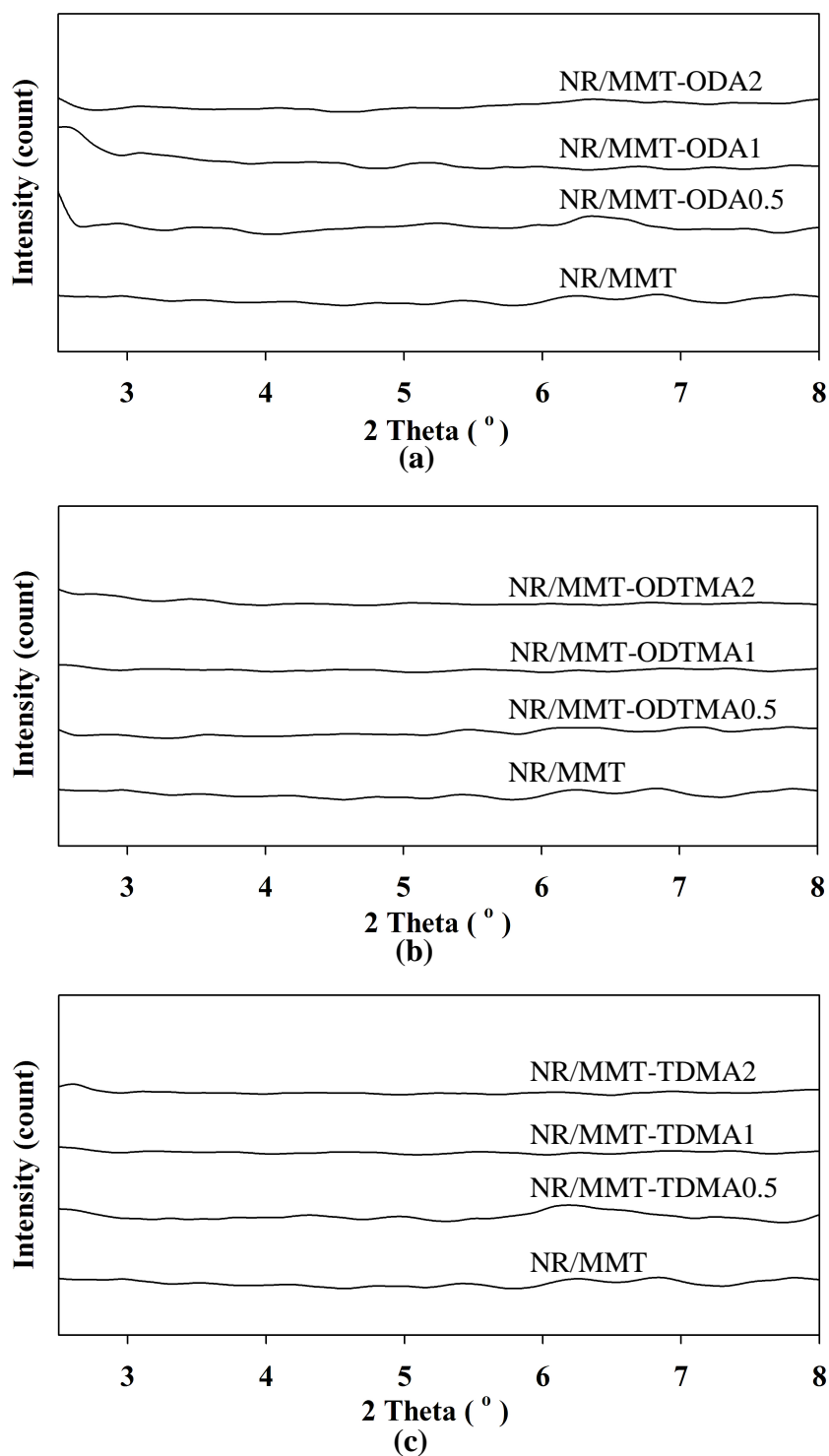


Figure 4.5 XRD spectra of NR nanocomposites containing 5 phr of (a) MMT-ODA, (b) MMT-ODTMA and (c) MMT-TDMA at 0.5, 1 and 2 times clay CEC.

With increasing the surfactant content to 1 times clay CEC, the diffraction peak of NR/MMT-ODA1 nanocomposite was observed at $2\theta = 5.0^\circ$ while those of NR/MMT-ODTMA1 and NR/MMT-TDMA1 nanocomposites were not observed. This indicated that NR molecules had intercalated into MMT layers. In addition, TEM micrograph in Figure 4.6 (c), revealed intercalated structure of MMT-ODA1 in NR nanocomposites and those in Figure 4.7 (b) and 4.7 (e) revealed the exfoliated structures of MMT-ODTMA1 and MMT-TDMA1 in NR nanocomposites.

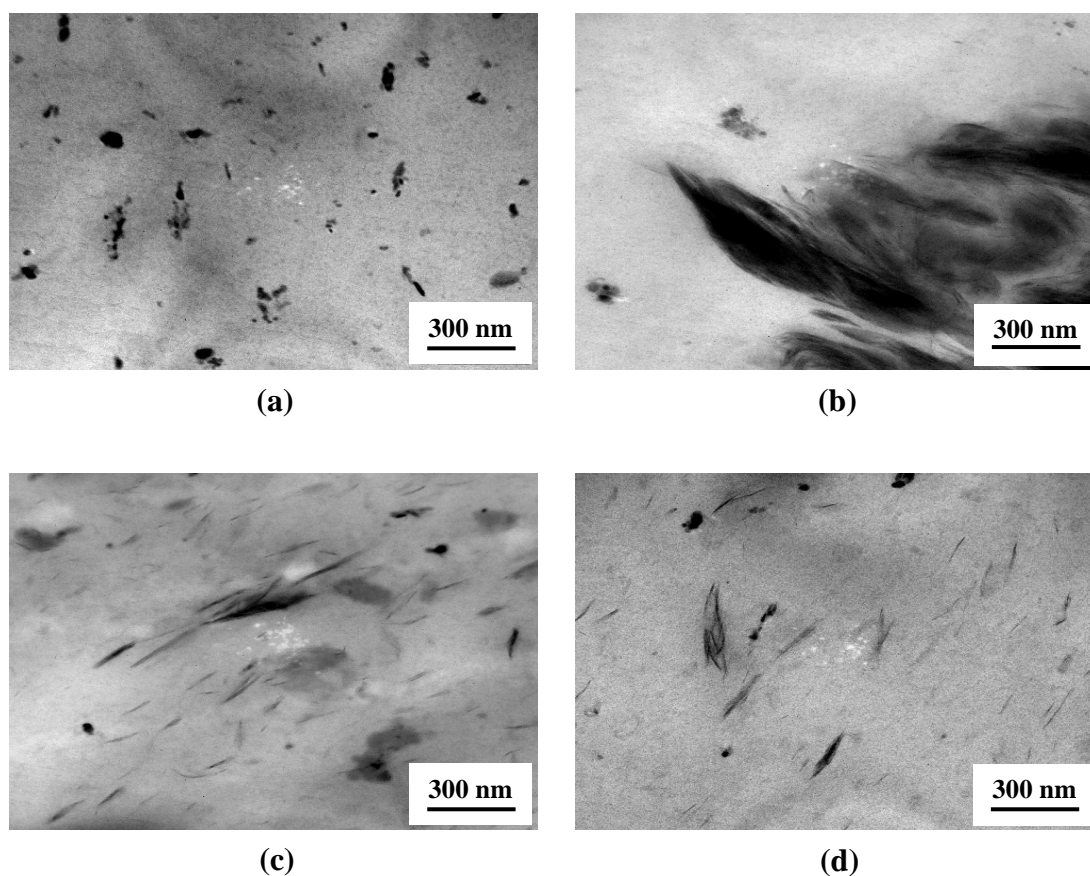


Figure 4.6 TEM micrographs of NR nanocomposites containing 5 phr of (a) MMT, (b) MMT-ODA0.5, (c) MMT-ODA1 and (d) MMT-ODA2.

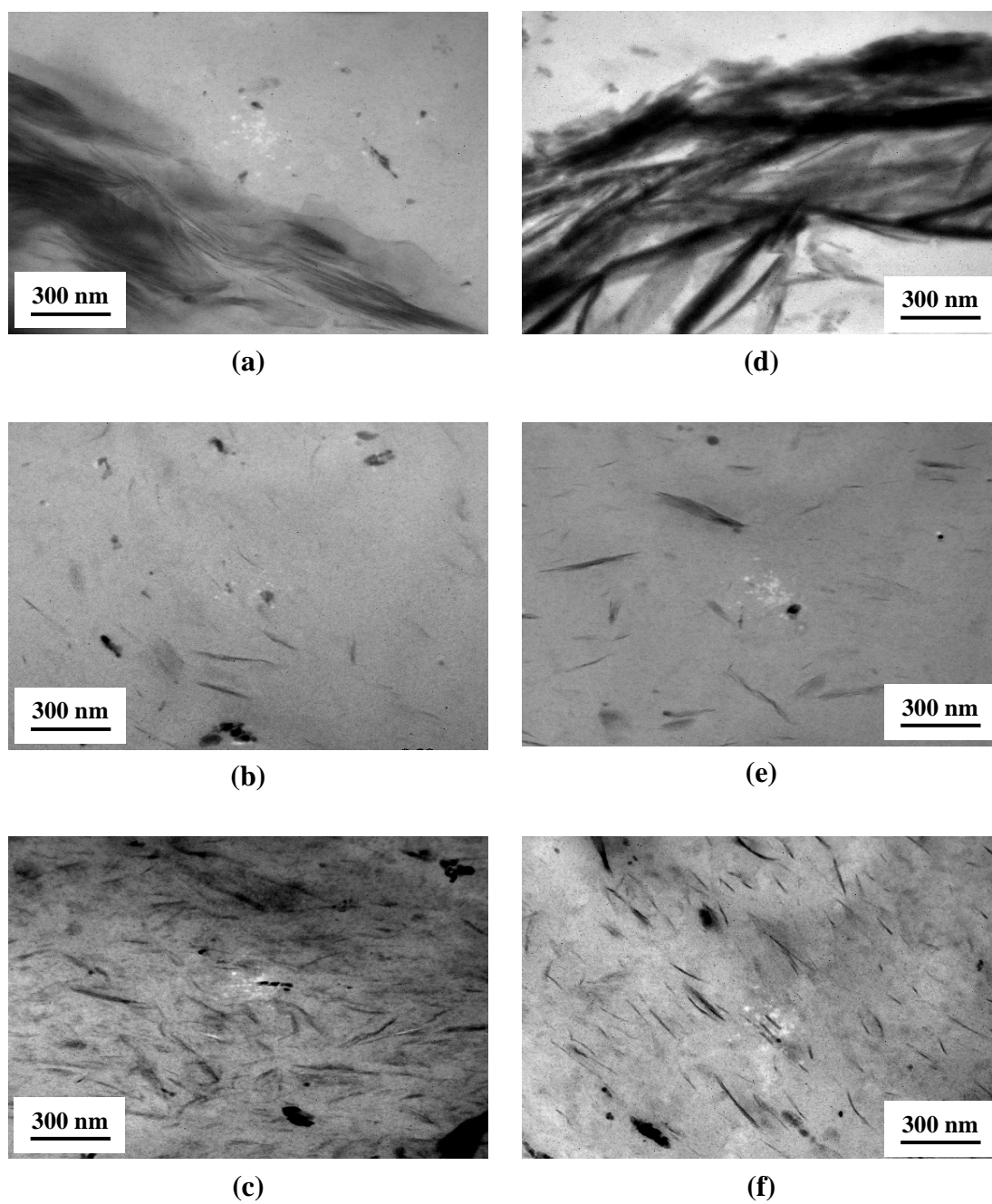


Figure 4.7 TEM micrographs of NR nanocomposites containing 5 phr of (a) MMT-ODTMA0.5, (b) MMT-OTMDA1, (c) MMT-OTMDA2, (d) MMT-TDMA0.5, (e) MMT-TDMA1 and (f) MMT-TDMA2.

At the surfactant content of 2 times clay CEC, the diffraction peak of all organoclays in NR nanocomposites disappeared suggesting the presence of exfoliated structures of the organoclays. In addition, the existence of the exfoliated structures of MMT-ODA₂, MMT-ODTMA₂ and MMT-TDMA₂ were clearly observed in TEM micrographs in Figure 4.6 (d), 4.7 (c) and 4.7 (f), respectively. This indicated that the higher interlayer spacing and the exfoliated structures of the organoclays in the NR nanocomposites could be achieved with increasing surfactant content.

In comparison between primary amine (ODA) and quaternary amine (ODTMA-Br) surfactants, which have 18 carbon atoms in their alkyl chains, the structures of the organoclays in NR nanocomposites were varied with increasing the surfactant content. At the surfactants content of 0.5 times clay CEC, NR nanocomposite with MMT-ODA_{0.5} and MMT-ODTMA_{0.5} showed the agglomerated structures of organoclays. With increasing the surfactant content to 1 times clay CEC, NR nanocomposite with MMT-ODA₁ showed intercalated structures of the organoclay while that with MMT-ODTMA₁ showed exfoliated structure of the organoclay. This was because ODTMA-Br, due to its bigger head group, expanded the interlayer spacing of the organoclay much more effectively than ODA. However, with increasing the surfactant content up to 2 times clay CEC, the exfoliated structures of both MMT-ODA₂ and MMT-ODTMA₂ in NR nanocomposites were observed. This suggested that the excess content of both primary amine and quaternary amine surfactants expanded the interlayer spacing of the organoclays and eased exfoliation of both organoclays in NR matrix.

For quaternary amine surfactants of different alkyl chain length, *i.e.* TDMA-Br (14 carbon atoms) and ODTMA-Br (18 carbon atoms), agglomerated structures of both organoclays were observed in NR nanocomposites when MMT was treated with a surfactant at the content of 0.5 times clay CEC. On the other hand, when MMT was modified with either TDMA-Br or ODTMA-Br at the content of 1 and 2 times clay CEC, the exfoliated structures of the organoclays in NR nanocomposite were observed although the interlayer spacing of MMT-TDMA was lower than that of MMT-ODTMA. According to the FTIR results of MMT-TDMA and MMT-ODTMA in Figure 4.2 and Table 4.2, the mobility of alkyl chains in MMT-TDMA was greater than that in MMT-ODTMA. Therefore, the intercalation of NR molecules into the layers of MMT-TDMA was easier than their intercalation into the layer of MMT-ODTMA. Although, the low mobility of alkyl chains in MMT-ODTMA may hinder penetration of NR molecules into the MMT-ODTMA layers, the exfoliated structures of MMT-ODTMA in NR nanocomposite were still observed when MMT was treated with ODTMA-Br at content of 1 or 2 times clay CEC. This may be due to a combination of the partial intercalation of NR molecules into clay layers and the shear force generated during mixing process.

4.2.2 Cure characteristics

Cure characteristics of NR nanocomposites, expressed in term of scorch time, cure time, maximum torque (S_{max}), minimum torque (S_{min}) and torque difference ($S_{max}-S_{min}$) are illustrated in Figure 4.8-4.12 and summarized in Table 4.3.

As shown in Figure 4.8 and 4.9, scorch time and cure time of NR/organoclay nanocomposites were shorter than that of NR/MMT. This implied that alkyl amine surfactants may react with Zn compounds and sulfur to form

Zn–sulfur–ammonium complexes which act as accelerators for NR vulcanization (Kim *et al.*, 2006). Moreover, scorch time and cure time of the NR nanocomposites decreased with increasing surfactant content from 0.5 to 2 times clay CEC. These results indicated that the content of surfactant affected cure characteristics of NR vulcanizates. The increase in deposited surfactant content on organoclay surface led to the increase in Zn complex contents and resulted in acceleration of NR vulcanization.

Table 4.4 Cure characteristics of of NR nanocomposites at various surfactant types and surfactant contents.

Designation	Scorch time (min)	Cure time (min)	S _{max} (dNm)	S _{min} (dNm)	S _{max} -S _{min} (dNm)
gum NR	5.19	8.44	20.74	3.70	17.04
NR-MMT	5.49	9.19	21.13	3.62	17.51
NR/MMT-ODA0.5	4.48	8.35	29.32	5.70	23.62
NR/MMT-ODA1	4.04	6.49	32.49	5.55	26.94
NR/MMT-ODA2	2.49	5.20	35.34	4.85	30.50
NR/MMT-TDMA0.5	2.24	6.30	32.31	4.30	28.01
NR/MMT-TDMA1	1.20	4.23	35.29	4.95	30.34
NR/MMT-TDMA2	1.06	4.19	36.09	5.20	30.89
NR/MMT-ODTMA0.5	3.18	7.41	30.26	4.96	25.30
NR/MMT-ODTMA1	1.20	4.33	36.29	6.07	30.21
NR/MMT-ODTMA2	0.46	3.35	44.21	5.04	39.16

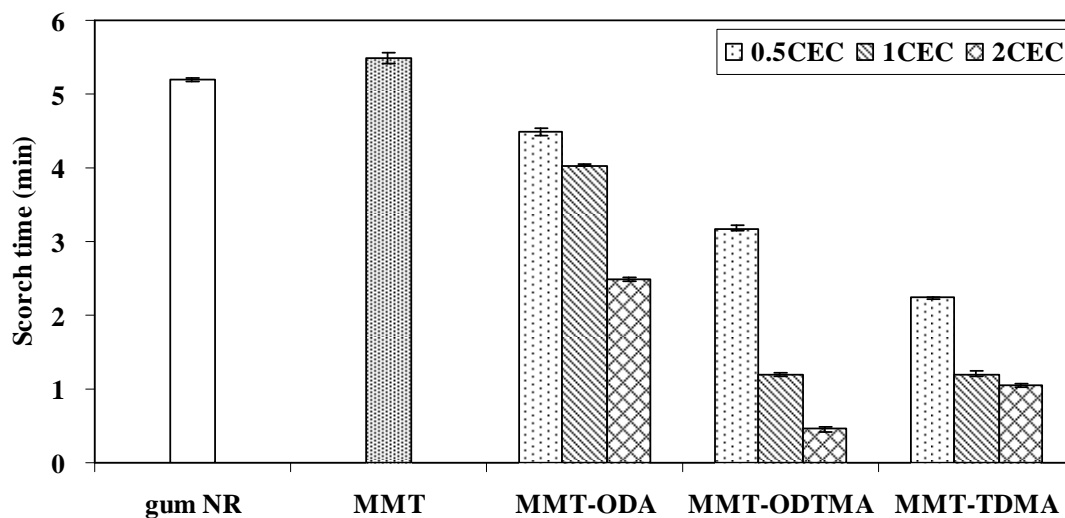


Figure 4.8 Scorch time of NR nanocomposites at various surfactant types and surfactant contents.

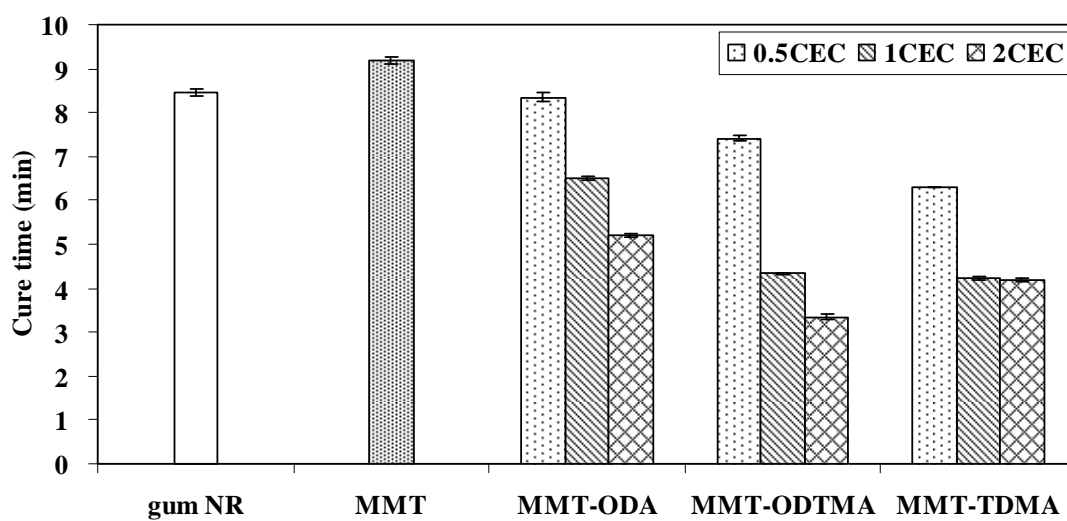


Figure 4.9 Cure time of NR nanocomposites at various surfactant types and surfactant contents.

Maximum torques (S_{\max}) of NR nanocomposites are shown in Figure 4.10. Maximum torque can be considered as a measure of storage modulus which was increased due to rubber/clay interactions including intercalation and exfoliation of clay in the matrix (Teh *et al.*, 2004). The maximum torques of NR/organoclay nanocomposites were higher than that of NR/MMT composite. This result was due to a poor compatibility between unmodified MMT and hydrophobic NR. The increase in the maximum torque of NR/organoclay nanocomposite was more pronounced with increasing surfactant content to 2 times clay CEC. This suggested that the increase in surfactant content enhanced hydrophobicity of organoclay resulting in a good compatibility between NR and organoclay. Nonetheless, NR/MMT-ODTMA2 nanocomposite had the highest maximum torque values as compared with NR/MMT-TDMA2 and NR/MMT-ODA2 nanocomposites.

The difference between maximum torque and minimum torque ($S_{\max} - S_{\min}$), or torque difference, is indirectly related to crosslink density of a rubber vulcanizates (Teh *et al.*, 2004). As shown in Figure 4.11, NR/organoclay nanocomposites had higher torque difference than NR/MMT composite. In addition, NR/MMT-ODTMA2 showed the highest torque difference value among the nanocomposites. Arroyo *et al.* (2003); Teh *et al.* (2004); and Arroyo *et al.* (2007) reported that the increase in torque difference of the rubber/organoclay nanocomposites was due to the increase in crosslink density of the vulcanizate. On the other hand, in this study the crosslink density of all nanocomposites showed insignificant difference. Therefore, the increase in torque difference of NR/organoclay nanocomposites as compared with that of NR/MMT composite may be due to the interaction between organoclay and matrix. Furthermore, the torque difference of the

NR nanocomposites increased with increasing surfactant content. This suggested that high content of surfactant improved the interaction between NR and organoclay by the separation of clay layers at high content of surfactant. This was confirmed by TEM micrographs of NR nanocomposites in Figure 4.6-4.7.

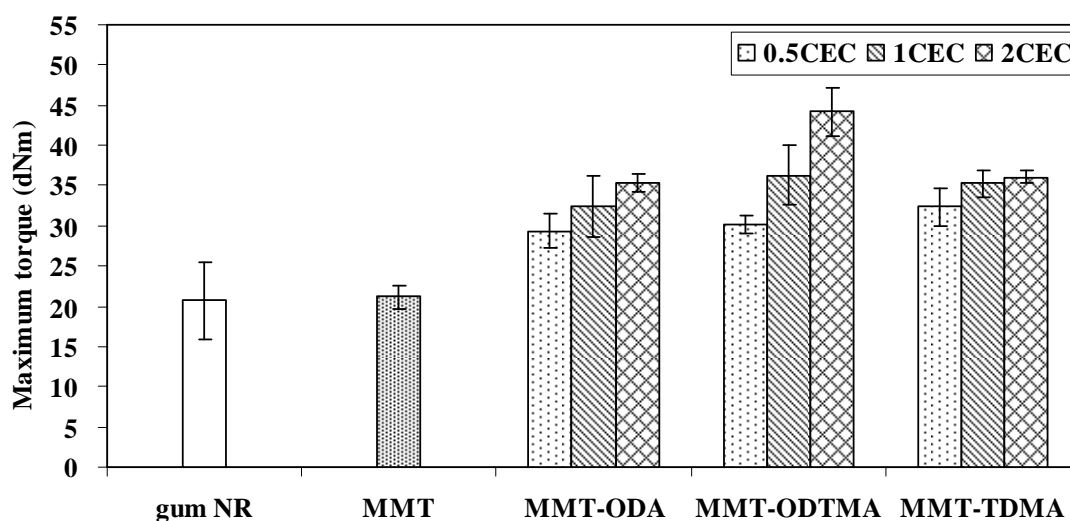


Figure 4.10 Maximum torque of NR nanocomposites at various surfactant types and surfactant contents.

The minimum torques (S_{\min}) of NR nanocomposites are shown in Figure 4.12. Minimum torque is related to the viscosity of the NR nanocomposites before vulcanization (Teh *et al.*, 2004). The minimum torques of NR/organoclay nanocomposites were higher than those of NR and NR/MMT composite. This implied the good compatibility between hydrophobic NR and hydrophobic organoclay.

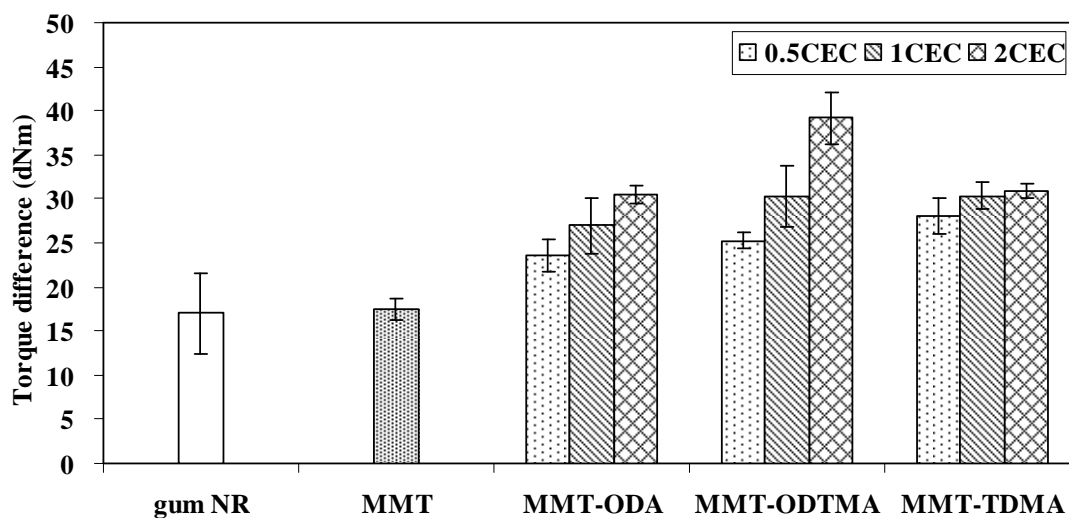


Figure 4.11 Torque difference of NR nanocomposites at various surfactant types and surfactant contents.

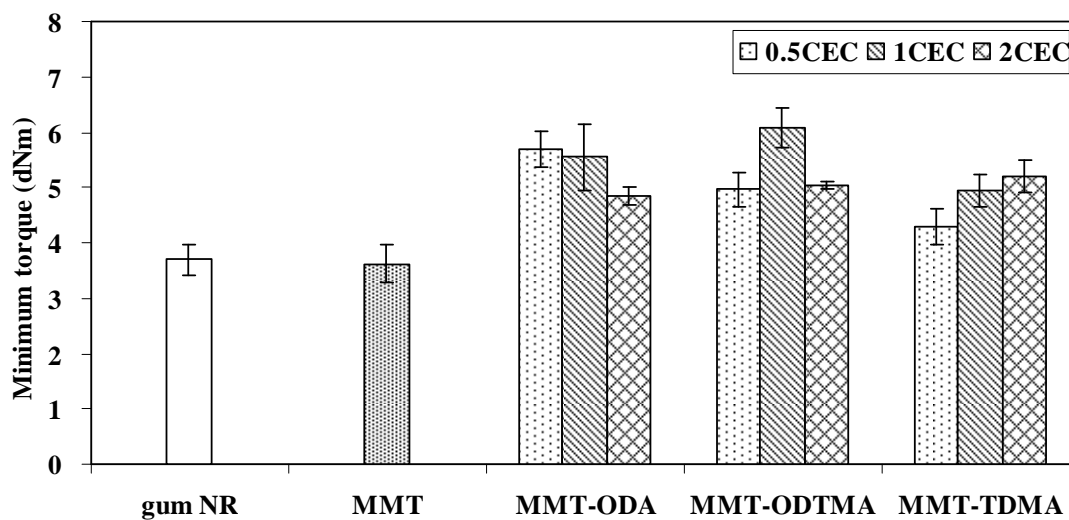


Figure 4.12 Minimum torque of NR nanocomposites at various surfactant types and surfactant contents.

Treating MMT with ODA ($R-NH_3^+$) or ODTMA ($R-NMe_3^+$), which have 18 carbon atoms in their alkyl chains, affected the cure characteristics of NR/organoclay nanocomposites. NR/MMT-ODTMA gave shorter scorch time and cure time than NR/MMT-ODA nanocomposite. This was because the excess ODTMA-Br molecules had less interaction with clay surface. So they can react and form complex with zinc and sulfur faster than the ODA molecules. This can be supported by TGA thermograms (Figure 4.3). The weight loss (wt%) of ODTMA-Br in MMT-ODTMA was higher than that of ODA in MMT-ODA. Additionally, another possibility why NR/MMT-ODTMA nanocomposites had shorter scorch time and cure time than NR/MMT-ODA nanocomposites may be because methylene groups of quaternary ammonium compound accelerated the vulcanizing reaction in NR vulcanizate better than hydrogen atoms of primary amine compound. Moreover, NR nanocomposites with quaternary ammonium surfactant treated MMT gave higher torque difference than that of NR nanocomposites with primary amine surfactant treated MMT. This indicated that NR/MMT-ODTMA had stronger interaction between the organoclay and NR matrix than NR/MMT-ODA.

In comparison between quaternary ammonium surfactants of different alkyl chain length, *i.e.* TDMA-Br (14 carbon atoms) and ODTMA-Br (18 carbon atoms), NR/MMT-ODTMA nanocomposite gave shorter scorch time and cure time than NR/MMT-TDMA nanocomposite. This was because the excess ODTMA-Br molecules had less interaction with clay surface. So they can react and form complex with zinc and sulfur faster than TDMA-Br molecules. This was confirmed by TGA thermograms (Figure 4.3). The weight loss (wt%) of ODTMA-Br was higher than TDMA-Br. Moreover, NR/MMT-ODTMA nanocomposites showed higher torque

difference than that of NR/MMT-TDMA nanocomposites. This indicated that a stronger interaction between NR matrix and organoclay occurred in the presence of long alkyl chain.

4.2.3 Mechanical properties

Tensile strength, modulus at 100% elongation (M100), modulus at 300% elongation (M300), elongation at break, hardness and crosslink density of NR nanocomposites at various surfactant types and surfactant contents are illustrated in Figure 4.13–4.18. As shown in Figure 4.13, tensile strength of NR/organoclay nanocomposites was higher than that of gum NR. This indicated that the organoclays acted as reinforcing fillers in NR matrix. In comparison, at the same clay content, NR/organoclay nanocomposites had higher tensile strength than NR/MMT composite. This result suggested that the organoclay was more compatible with NR matrix than unmodified MMT leading to better dispersion of organoclay in the matrix and better interaction between matrix and filler. In addition, the tensile strength of the nanocomposites increased with increasing surfactant content. This may be because the excess content of surfactant can expand the interlayer spacing of the organoclays and facilitate penetration of NR molecules into the layers. Then, the separation of organoclay layers was obtained. This led to intercalated/exfoliated structures of organoclay in the nanocomposites. This was supported by XRD spectra (Figure 4.5) and TEM micrographs (Figure 4.6-4.7) of NR nanocomposites, indicating the existence of intercalated/exfoliated structures in the nanocomposites. These results suggested that the increase of surfactant content significantly enhanced tensile strength of NR nanocomposites.

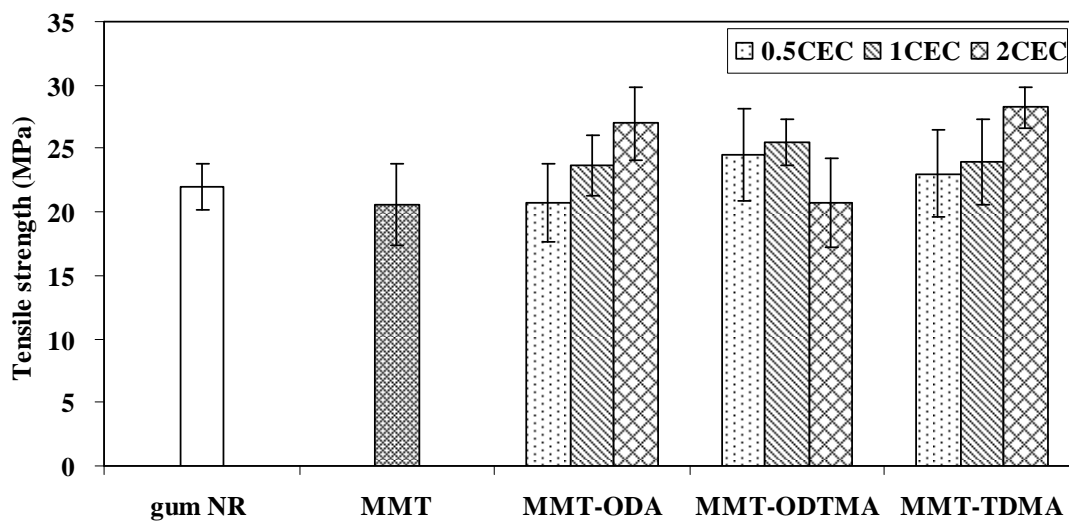


Figure 4.13 Tensile strength of NR nanocomposites at various surfactant types and surfactant contents.

Elongation at break of NR/organoclay nanocomposites was slightly higher than that of gum NR and NR/MMT composite, as shown in Figure 4.14. This was because the large amount of long alkyl amine ions within the organoclay layers may act as plasticizers in NR nanocomposites and facilitate the movement of NR molecules (Kim, Kang, Cho, Ha, and Bae, 2007). This suggested that the incorporation of organoclay in NR nanocomposites increased elasticity of NR chains.

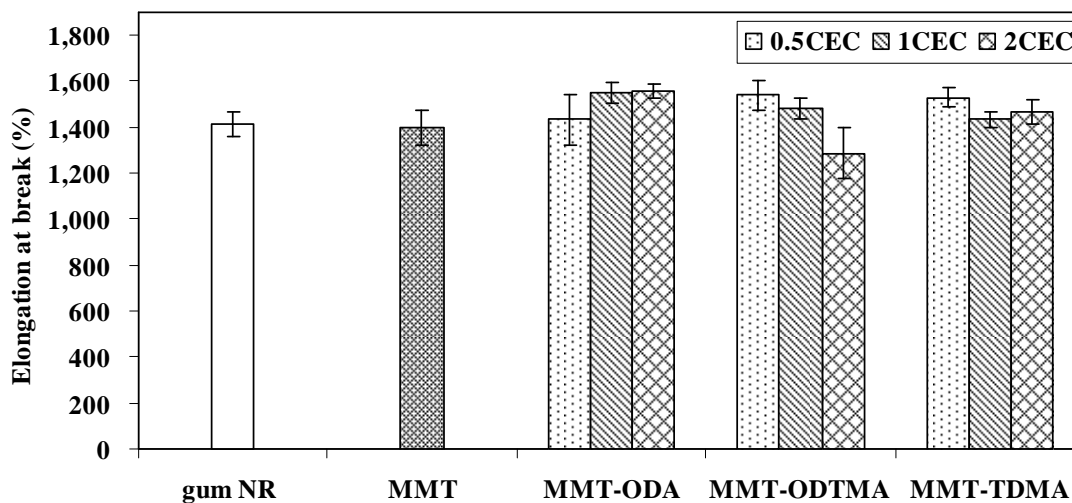


Figure 4.14 Elongation at break of NR nanocomposites at various surfactant types and surfactant contents.

As shown in Figure 4.15-4.16, the modulus at 100% elongation and 300% elongation of NR/MMT composites were lower than those of gum NR. The low compatibility between hydrophilic MMT and hydrophobic NR led to the poor MMT dispersion in NR matrix. On the other hand, the modulus at 100% elongation and 300% elongation of NR/organoclay nanocomposites were higher than those of gum NR and NR/MMT composite. This was due to the high aspect ratio and a large surface area of organoclay which tended to improve interfacial interaction between organoclay and NR. In addition, the improvement in the modulus was due to the good dispersion and the compatibility of organoclay in the NR matrix (Zhang and Loo, 2008).

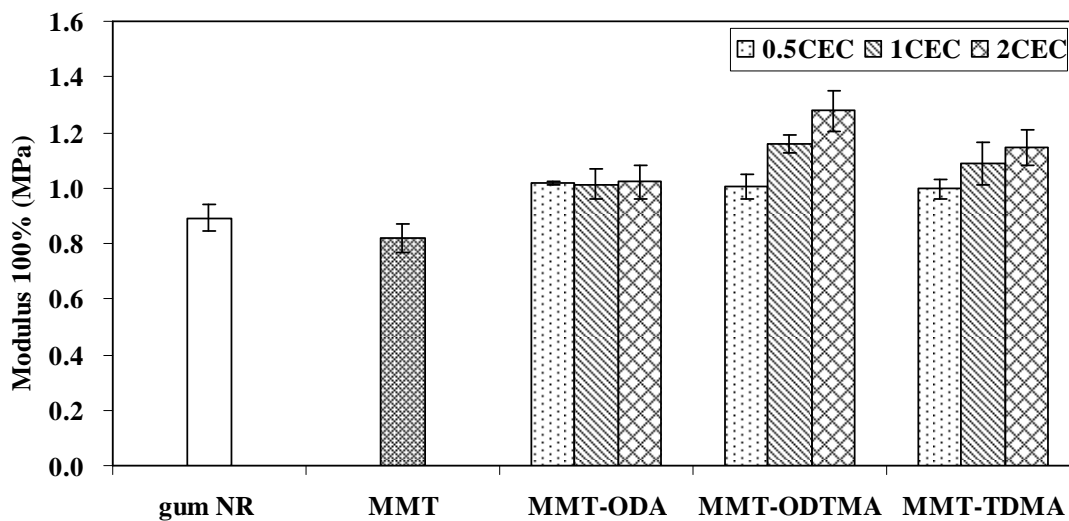


Figure 4.15 Modulus at 100% elongation of NR nanocomposites at various surfactant types and surfactant contents.

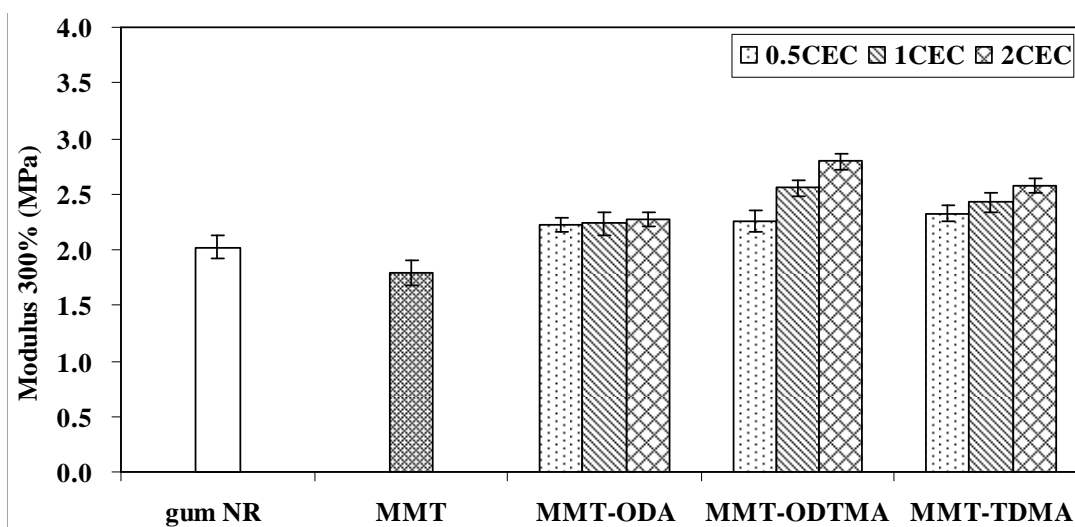


Figure 4.16 Modulus at 300% elongation of NR nanocomposites at various surfactant types and surfactant contents.

The hardness of NR/organoclay nanocomposites was higher than that of gum NR and NR/MMT composite, as shown in Figure 4.17. This was because the organoclay acted as a reinforcing filler in NR matrix. The increase in hardness was related to high modulus of NR matrix (Brown and Soulagnet, 2001). In addition, the hardness of the nanocomposites slightly increased with increasing surfactant content.

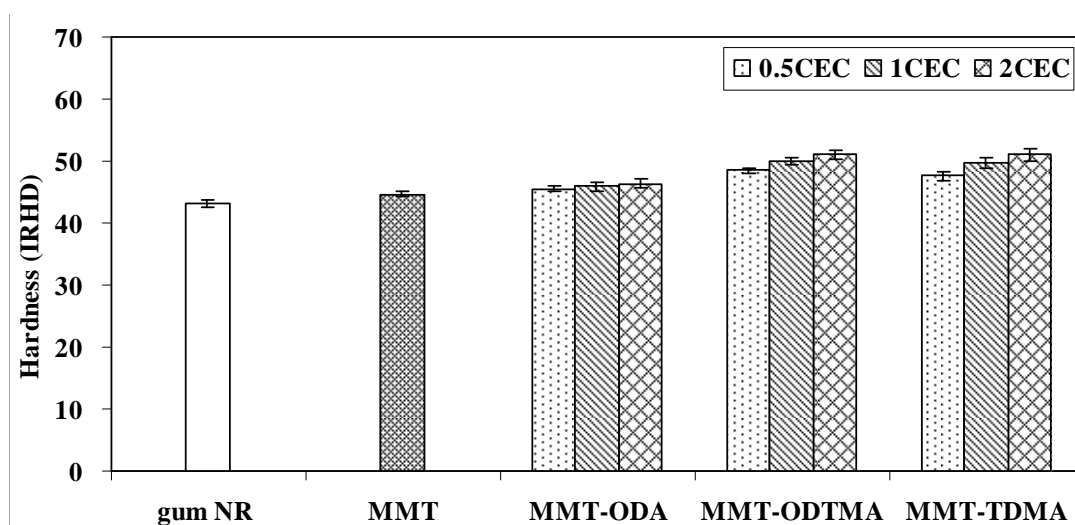


Figure 4.17 Hardness of NR nanocomposites at various surfactant type and surfactant contents.

The crosslink density of NR/organoclay nanocomposites was calculated on the basis of the nanocomposites swelling in toluene. There was no significant difference in the crosslink density of NR/organoclay nanocomposites, NR/MMT composite and gum NR (Figure 4.18). This indicated that the crosslinking of rubber had no effect on the properties of NR nanocomposites. Therefore, the increase of torque difference and mechanical properties of the nanocomposites was due to the improved interaction between organoclay and NR matrix.

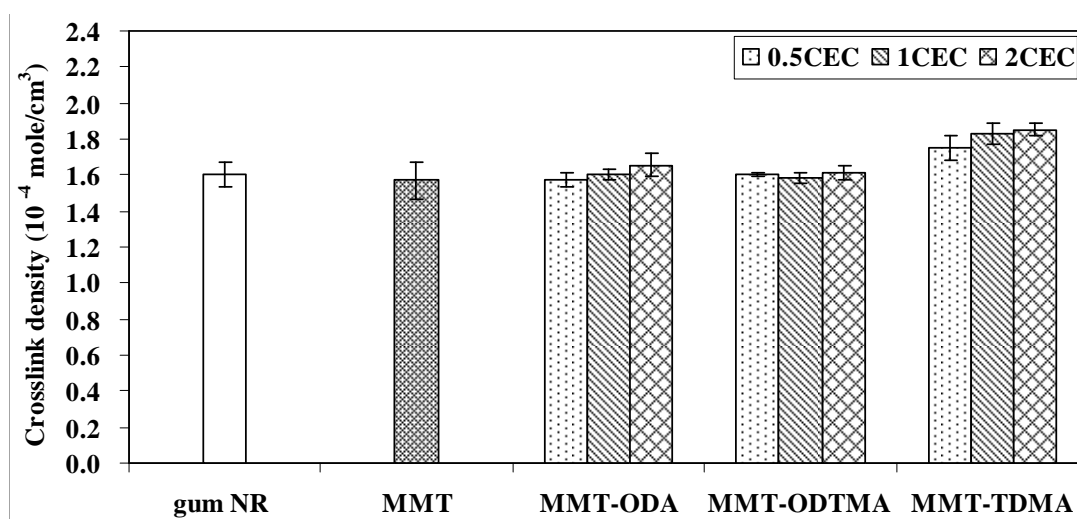


Figure 4.18 Crosslink density of NR nanocomposites at various surfactant types and surfactant contents.

Table 4.5 Mechanical properties and crosslink density of NR nanocomposites at various surfactant types and surfactant contents.

Designation	Tensile strength (MPa)	Modulus 100% (MPa)	Modulus 300% (MPa)	Elongation at break (%)	Hardness (IRHD)	Crosslink density (10^{-4} mole/cm³)
gum NR	22.01	0.89	2.02	1384.58	43.16	1.6045
NR/MMT	20.55	0.82	1.79	1418.72	44.70	1.5703
NR/MMT-ODA0.5	20.66	1.04	2.28	1357.14	45.50	1.5742
NR/MMT-ODA1	23.63	0.98	2.16	1550.57	45.94	1.6027
NR/MMT-ODA2	26.95	0.98	2.18	1559.91	46.42	1.6571
NR/MMT-TDMA0.5	23.46	1.00	2.33	1502.02	47.64	1.7500
NR/MMT-TDMA1	23.99	1.09	2.48	1433.01	49.76	1.8295
NR/MMT-TDMA2	28.22	1.14	2.58	1466.42	51.08	1.8526
NR/MMT-ODTMA0.5	24.55	0.93	2.07	1541.62	48.46	1.6029
NR/MMT-ODTMA1	25.47	1.16	2.55	1483.42	49.88	1.5842
NR/MMT-ODTMA2	23.10	1.28	2.79	1285.73	51.12	1.6159

As compared between ODA and ODTMA-Br which have 18 carbon atoms in the alkyl chain, NR/MMT-ODA0.5 nanocomposite gave lower tensile strength than NR/MMT-ODTMA0.5 nanocomposite. In addition, the tensile strength of NR/MMT-ODA1 nanocomposite was also lower than that of NR/MMT-ODTMA1 nanocomposite. This was because the ODA surfactant with primary ammonium ions, $R-NH_3^+$, can form hydrogen bond with the clay surface. Thereby, the numbers of available surface areas for interacting with the NR molecules were decreased (Zhang and Loo, 2008). Then, the interaction between NR and MMT-ODA was lower than that between NR and MMT-ODTMA. On the other hand, the tensile strength of NR/MMT-ODA2 nanocomposite was higher than that of NR/MMT-ODTMA2 nanocomposite. This was because the excess quaternary amine ($R-N(Me)_3^+$) molecules had no orientation in the layers and formed aggregates on the surfaces of MMT. This tended to be the weak points that promoted failure initiation, resulting in the decrease in the tensile strength of the nanocomposites. With increasing the surfactant content from 0.5 to 2 times clay CEC, the results, as shown in Figure 4.15–4.16, revealed that NR/MMT-ODTMA nanocomposites had higher modulus at 100% elongation and modulus at 300% elongation than NR/MMT-ODA nanocomposites. This was because of good dispersion of MMT-ODTMA platelets in the matrix, as confirmed by TEM micrographs of the nanocomposites in Figure 4.5. On the other hand, with increasing surfactant content from 0.5 to 2 times clay CEC, the elongation at break of NR/MMT-ODA nanocomposites slightly increased while the elongation at break of NR/MMT-ODTMA nanocomposites slightly decreased.

In comparison between quaternary ammonium surfactants of different alkyl chain length, *i.e.* TDMA-Br (14 carbon atoms) and ODTMA-Br (18 carbon atoms), the results showed that the tensile strength of NR/MMT-ODTMA nanocomposite increased with increasing surfactant content up to 1 times clay CEC. Then, the tensile strength of NR/MMT-ODTMA nanocomposites decreased when the surfactant content increased to 2 times clay CEC. This indicated that the modification of MMT with ODTMA-Br at 1 times clay CEC was sufficient to obtain NR nanocomposites with high tensile strength. On the other hand, the tensile strength of NR/MMT-TDMA nanocomposites increased with increasing surfactant content up to 2 times clay CEC. At surfactant content of 0.5 and 1 times clay CEC, the tensile strength of NR/MMT-ODTMA nanocomposites was slightly higher than those of NR/MMT-TDMA nanocomposites. This may be because exfoliated structures of MMT-ODTMA, due to the long alkyl chain of ODTMA-Br, in NR nanocomposites tended to give good interaction between NR and organoclay platelets. However, it is interesting to note that the tensile strength of NR/MMT-ODTMA₂ nanocomposite was lower than NR/MMT-TDMA₂ nanocomposite. This may be because the excess of ODTMA-Br surfactant promoted failure initiation and, thus, decreased the tensile strength of the nanocomposites. Modulus at 100% elongation and modulus at 300% elongation of NR/MMT-ODTMA and those of NR/MMT-TDMA nanocomposites showed insignificant difference.

By varying types (*i.e.* ODA, ODTMA-Br, TDMA-Br) and contents of surfactant (*i.e.* 0.5, 1, 2 times clay CEC), it was found that the NR nanocomposites with MMT-TDMA₂ had the highest tensile strength. In addition, the NR nanocomposites with MMT-TDMA₂ gave optimum scorch time and cure time, which

decreased processing time for fabricating the nanocomposites. In order to obtain NR nanocomposite with good mechanical properties and cure characteristics, MMT-TDMA2 was selected for preparation of NR nanocomposites at various contents of the organoclay.

4.3 Effect of organoclay content on properties of NR nanocomposites

4.3.1 Dispersion and structures of organoclay

From the previous topic, NR nanocomposite with MMT-TDMA2 gave good mechanical properties and optimum processing time. Therefore, MMT-TDMA2 was selected to further investigate effect of organoclay content on properties of NR/organoclay nanocomposites.

Figure 4.19 shows XRD spectra of MMT-TDMA2 and NR nanocomposites at various contents of MMT-TDMA2. As shown in Figure 4.19, MMT-TDMA2 showed a diffraction peak at $2\theta = 4.66^\circ$ with an interlayer spacing of 1.90 nm. This peak was not observed in NR nanocomposites at low MMT-TDMA2 contents (1, 3 and 5 phr). This suggested the presence of exfoliated structure of MMT-TDMA2 platelets in the NR nanocomposites. On the other hand, the NR nanocomposite with the MMT-TDMA2 content of 10 phr showed the diffraction peak at $2\theta = 2.20^\circ$ which was in a lower angle compared with that of MMT-TDMA2 indicating an intercalated structure of the organoclay in the NR/MMT-TDMA2 nanocomposite.

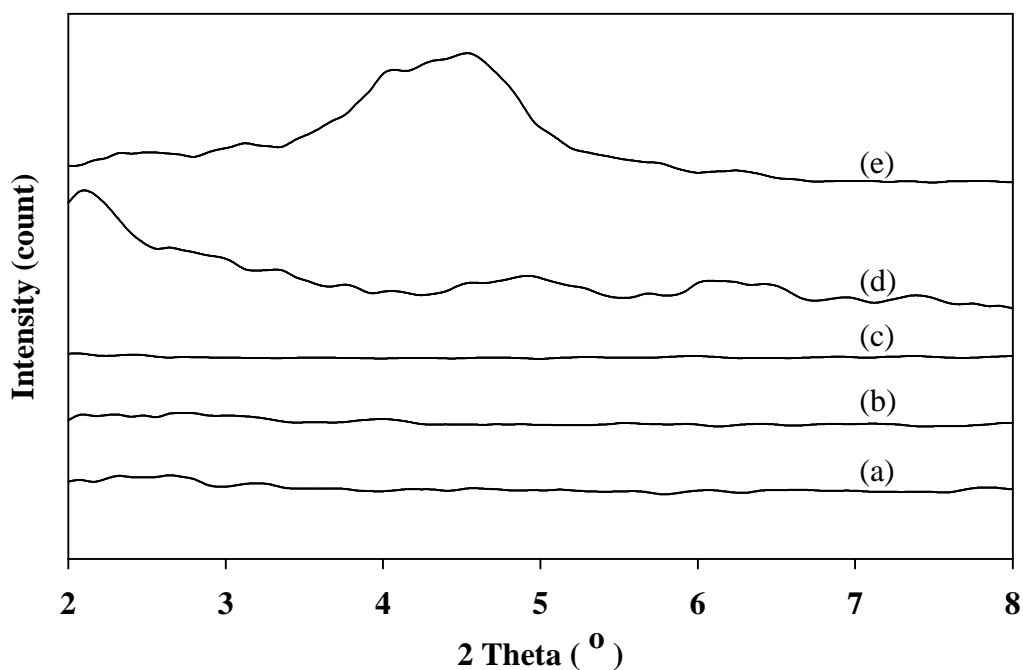


Figure 4.19 XRD spectra of NR nanocomposites at various contents of MMT-TDMA2:

(a) 1 phr, (b) 3 phr, (c) 5 phr, (d) 10 phr, and (e) MMT-TDMA2.

4.3.2 Cure characteristics

Scorch time, cure time, maximum torque, minimum torque and torque difference of gum NR and NR nanocomposites at various contents of MMT-TDMA2 are illustrated in Figure 4.20–4.22, and summarized in Table 4.6. Scorch time of NR nanocomposites decreased with increasing organoclay content, as shown Figure 4.20. Similarly, cure time also gradually decreased when the organoclay content in NR nanocomposites was increased. This effect was attributed to the acceleration of NR vulcanization induced by ammonium groups in TDMA-Br (Arroyo *et al.*, 2003).

Table 4.6 Cure characteristics of NR nanocomposites at various contents of MMT-TDMA2

Designation	Scorch time (min)	Cure time (min)	S_{max} (dNm)	S_{min} (dNm)	$S_{max}-S_{min}$ (dNm)
gum NR	5.19	8.44	20.74	3.70	17.04
NR/MMT-TDMA2-1phr	2.11	4.22	26.31	5.82	20.49
NR/MMT-TDMA2-3phr	1.17	4.20	28.49	5.82	22.68
NR/MMT-TDMA2-5phr	1.06	4.19	36.09	5.20	30.89
NR/MMT-TDMA2-10phr	0.55	2.56	36.52	5.89	30.63

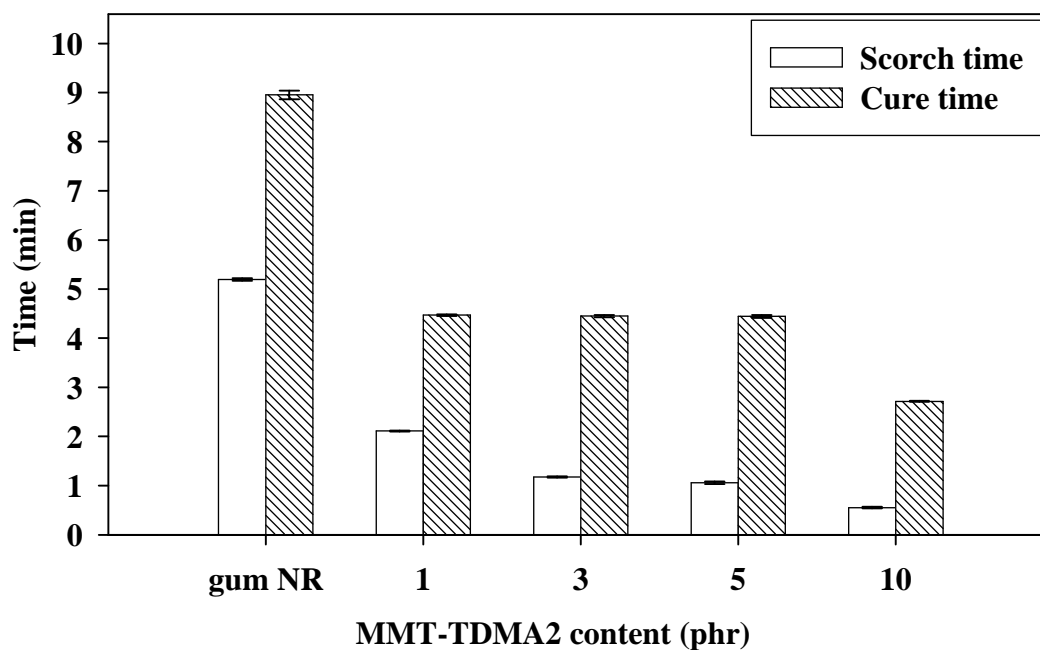


Figure 4.20 Scorch time and cure time of NR nanocomposites at various contents of MMT-TDMA2.

Figure 4.21 shows maximum torque of gum NR and NR/MMT-TDMA2 nanocomposites at various contents of organoclay. The maximum torque increased with increasing MMT-TDMA2 content up to 5 phr. This suggested good dispersion of organoclay platelets in matrix and good compatibility between organoclay and NR. However, the maximum torque of NR nanocomposite with MMT-TDMA2 of 10 phr was level with that of the NR nanocomposite with MMT-TDMA2 of 5 phr. When the organoclay content in the nanocomposites was beyond 5 phr, the organoclay structure changed from exfoliation to intercalation (Figure 4.19) leading to the less interfacial interaction between the organoclay and the NR matrix. A similar trend was observed in torque difference (Figure 4.21). The torque difference increased with increasing MMT-TDMA2 content up to 5 phr. This suggested that the NR nanocomposite with 5 phr of TDMA2 had the good compatibility between organoclay and NR. As shown in Figure 4.21, the organoclay content had no effect on the minimum torque of the nanocomposites.

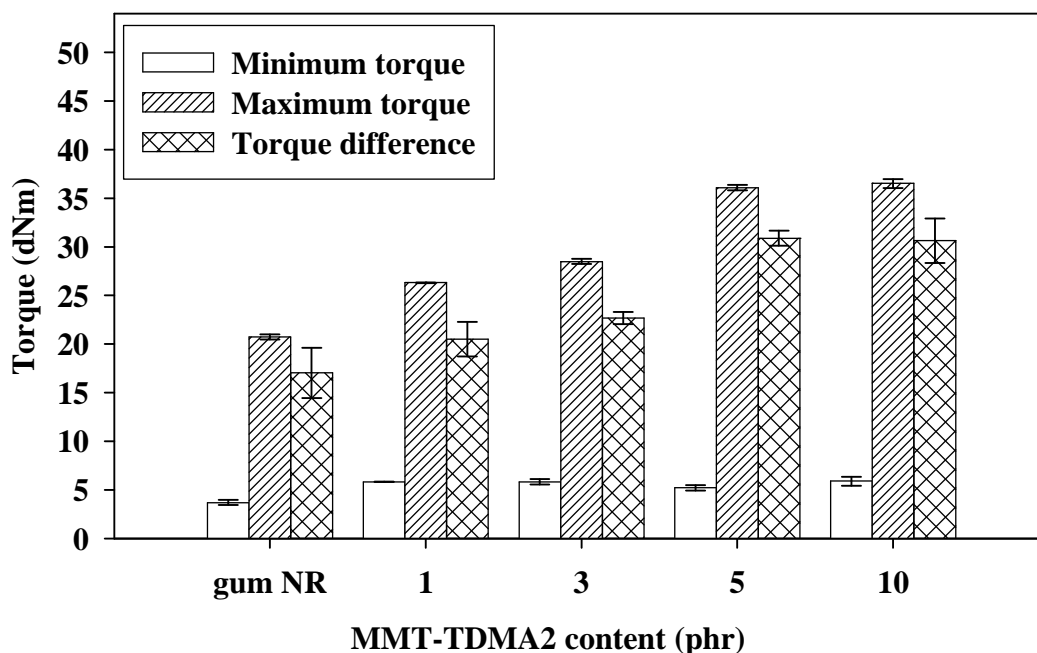


Figure 4.21 Minimum torque, maximum torque and torque difference of NR nanocomposites at various contents of MMT-TDMA2.

4.3.3 Mechanical properties

Tensile strength, modulus at 100% elongation (M100), modulus at 300% elongation (M300), elongation at break, hardness and crosslink density of NR/MMT-TDMA2 nanocomposites at various MMT-TDMA2 contents are illustrated in Figure 4.22–4.24, and summarized in Table 4.7. It can be seen, in Figure 4.23, that the tensile strength of NR nanocomposites with 1 phr of MMT-TDMA2 was lower than that of gum NR. This was because, at low content of organoclay, the organoclay acted as a foreign inclusion and disturbed orientation of the NR chain. However, the addition of MMT-TDMA2 between 3-5 phr increased the tensile strength of the NR nanocomposites. This indicated that good interaction between NR and organoclay and exfoliated structure of organoclay improved the compatibility between the organoclay

and NR. However, at the organoclay content of 10 phr, the tensile strength of NR nanocomposites decreased. This may be due to the change of organoclay structure from exfoliation to intercalation as observed from XRD spectra of NR nanocomposites (Figure 4.19) and the agglomeration of the organoclay. These may lead to less interfacial interaction between organoclay and NR matrix resulting in a reduction in tensile strength of NR nanocomposite containing 10 phr of MMT-TDMA2.

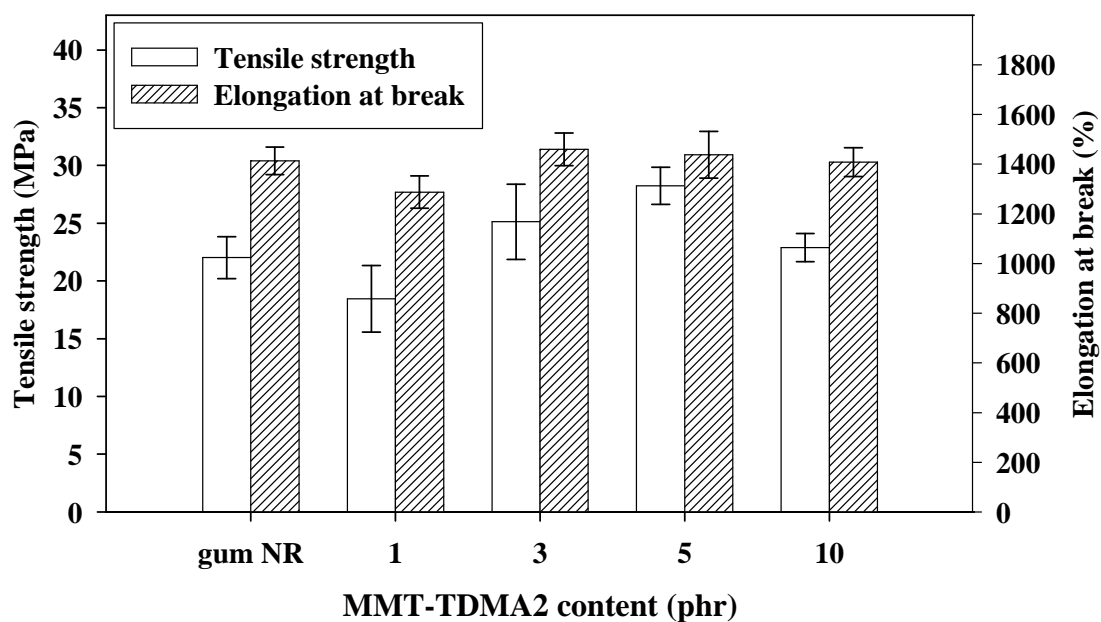


Figure 4.22 Tensile strength and elongation of NR nanocomposites at various contents of MMT-TDMA2.

Elongation at break of NR/MMT-TDMA2 nanocomposites slightly increased with increasing MMT-TDMA2 content up to 3 phr, as shown in Figure 4.22. Then, its value was insignificant changed at higher content of the organoclay. This suggested that the addition of MMT-TDMA2 up to 10 phr did not deteriorate elasticity of NR nanocomposites.

M100 and M300 of NR/MMT-TDMA2 increased as a function of MMT-TDMA2 content, as shown in Figure 4.23. This was due to high stiffness of the organoclay. In addition, the hardness of NR nanocomposites (Figure 4.24) increased in the same trend as the modulus of the NR nanocomposites.

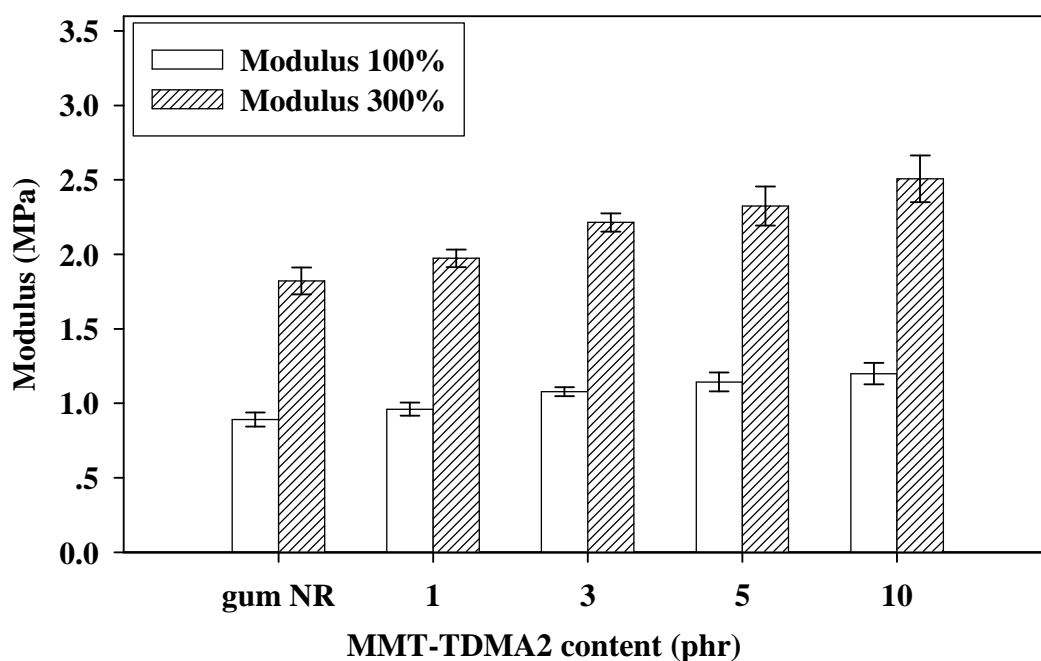


Figure 4.23 Modulus at 100% elongation and modulus at 300% elongation of NR nanocomposites at various contents of MMT-TDMA2.

Figure 4.24 shows crosslink density of NR/MMT-TDMA2 nanocomposites at various MMT-TDMA2 contents. The crosslink density of the NR/MMT-TDMA2 nanocomposites had no significant difference. This indicated that the crosslinking density of NR had no effect on properties of NR nanocomposites. This can be concluded that the change in properties of the nanocomposites was due to the organoclay content as well as the interaction between organoclay and NR matrix.

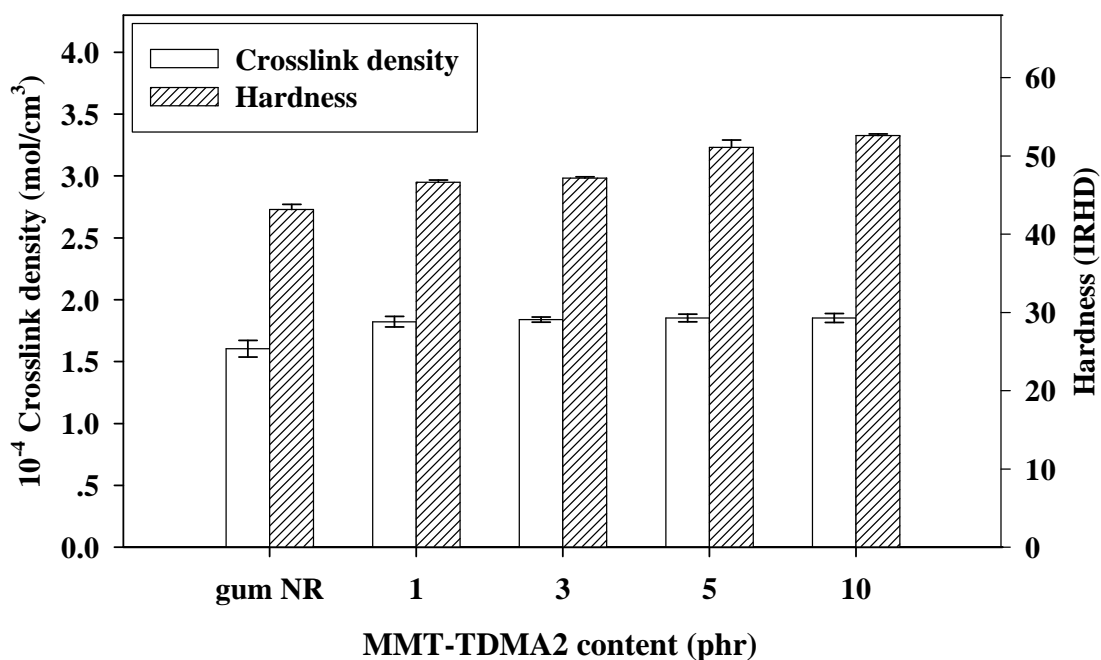


Figure 4.24 Hardness and crosslink density of NR nanocomposites at various contents of MMT-TDMA2.

Table 4.7 Mechanical properties and crosslink density of NR nanocomposites at various contents of MMT-TDMA2

Designation	Tensile strength (MPa)	Modulus 100% (MPa)	Modulus 300% (MPa)	Elongation at break (%)	Hardness (IRHD)	Crosslink density (10^{-4} mole/cm³)
gum NR	22.01	0.89	2.02	1384.58	43.16	1.6045
NR/MMT-TDMA2-1phr	18.46	0.96	2.19	1287.39	46.63	1.8229
NR/MMT-TDMA2-3phr	25.13	1.08	2.46	1459.08	47.17	1.8390
NR/MMT-TDMA2-5phr	28.22	1.14	2.58	1437.79	51.08	1.8526
NR/MMT-TDMA2-10phr	22.89	1.13	2.79	1408.00	52.63	1.8530

According to the results, the content of organoclay affected the mechanical properties of NR/organoclay nanocomposites. With increasing MMT-TDMA2 content in the NR nanocomposites, the scorch time and cure time decreased while tensile strength increased up to 5 phr of MMT-TDMA2. Therefore, the addition of 5 phr of MMT-TDMA2 was enough to improve mechanical properties of the NR nanocomposites. Based on the XRD spectra of NR nanocomposites, an exfoliation of organoclay was observed with the addition of organoclay content up to 5 phr. In addition, torque difference increased with increasing MMT-TDMA2 content up to 5 phr. According to the mechanical properties and cure characteristics of NR nanocomposites in this study, the optimum content of MMT-TDMA2 in the nanocomposites was 5 phr. Therefore, 5 phr of MMT-TDMA2 was selected to further investigate effect of matrix polarity on properties of NR/organoclay nanocomposites.

4.4 Effect of matrix polarity on properties of NR nanocomposites

An approach to improve interaction between organoclay and NR is to adjust matrix polarity since organoclay would be more easily dispersed in polar matrix phase than in non-polar matrix phase. Therefore, ENR was selected to blend with NR since it has higher polarity compared with NR. The NR/ENR blend ratios were varied *i.e.*, 100/0, 60/40, 40/60 and 0/100 by weight. From the previous topics, the selected surfactant was TDMA-Br at the content of 2 times clay CEC and the optimum organoclay content was 5 phr.

4.4.1 Dispersion and structures of organoclay

Figure 4.25 shows the XRD spectra of NR, ENR and NR/ENR nanocomposites at 5 phr of MMT-TDMA2. As shown in this figure, the diffraction peak of NR/MMT-TDMA2 disappeared indicating the presence of exfoliated structures of the organoclay in the nanocomposite. This can be further confirmed by TEM micrograph as shown in Figure 4.26 (a). On the other hand, XRD spectrum of ENR/MMT-TDMA2 nanocomposite showed two diffraction peaks appeared at around $2\theta = 2.5^\circ$ and $2\theta = 5.0^\circ$ indicating the existence of both intercalated and agglomerated structures of the MMT-TDMA2 in the ENR nanocomposite as confirmed by TEM micrograph in Figure 4.26 (d). This suggested the poor interaction between ENR and organoclay due to the polarity difference.

It should be noted that the organoclay structures in the NR/ENR nanocomposites were varied depending on the added ENR content. When NR was blended with 40 wt% of ENR, the diffraction peak of NR/ENR(60/40)/MMT-TDMA2 nanocomposite appeared at lower 2θ compared with that of MMT-TDMA2. This suggested that both NR and ENR chains intercalated into the organoclay layers. The intercalated structure of organoclay platelets in this nanocomposite was also observed by TEM micrograph in Figure 4.26 (b). Also, this figure revealed that NR and ENR phases were separated and the organoclay platelets were partially dispersed in ENR phase and partially presented at the interphase between NR and ENR. Moreover, with increasing ENR content in the nanocomposite to 60 wt%, the diffraction peak of NR/ENR(40/60)/MMT-TDMA2 nanocomposite disappeared suggesting the appearance of exfoliated structure of the MMT-TDMA2. The exfoliated structures of organoclay platelets in nanocomposites were also observed from TEM micrograph as shown in

Figure 4.26 (c). In addition, this figure revealed that NR and ENR phases were separated and the organoclay were thoroughly dispersed in the matrix.

From the results it can be concluded that when NR was blended with 60 wt% of ENR, the organoclay platelets were exfoliated and well dispersed in both phases which implied a good interaction between the organoclay and the matrix.

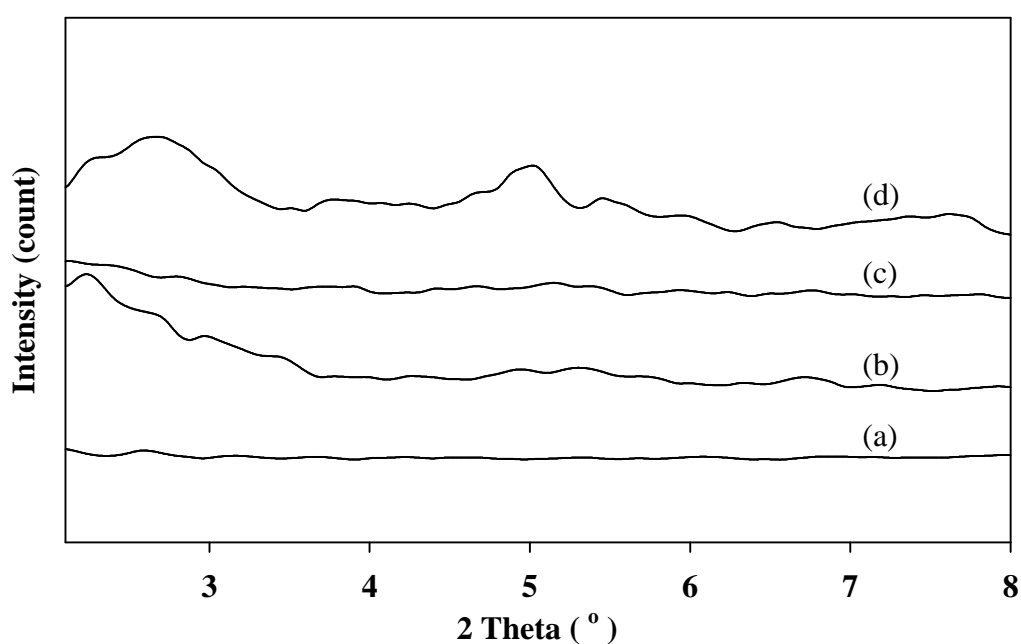


Figure 4.25 XRD spectra of (a) NR, (b) NR/ENR (60/40), (c) NR/ENR (40/60), and (d) ENR nanocomposites with 5 phr of MMT-TDMA2.

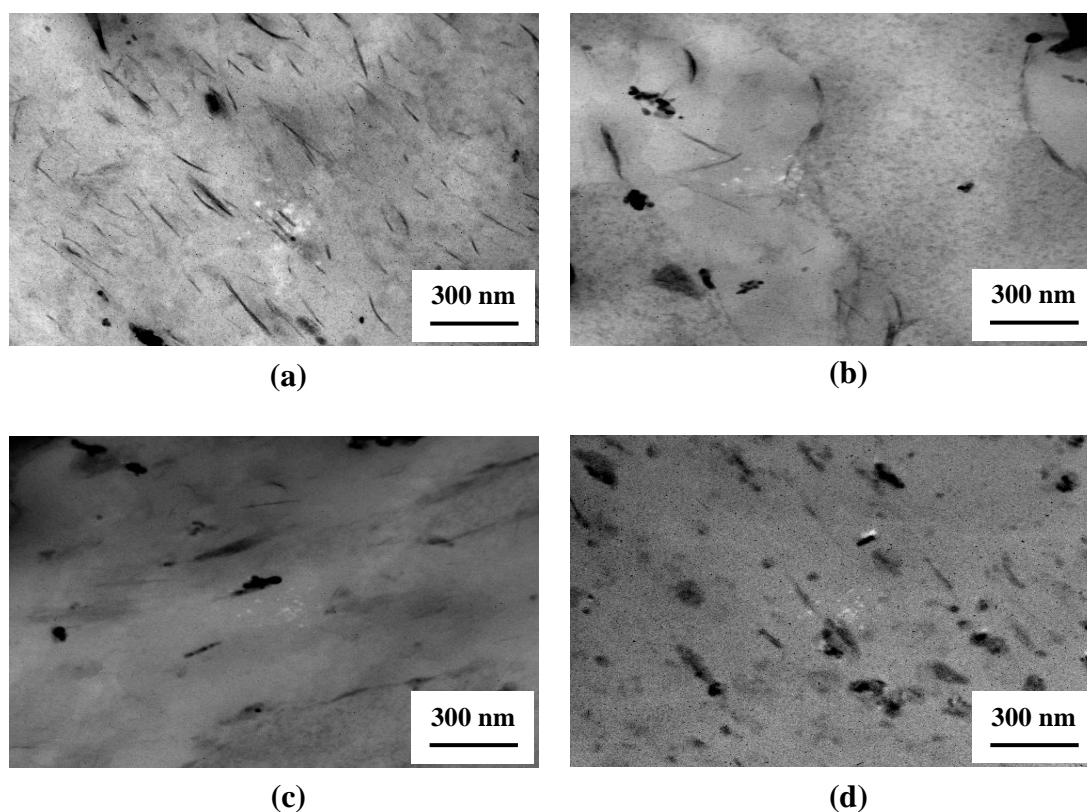


Figure 4.26 TEM micrographs of (a) NR, (b) NR/ENR (60/40), (c) NR/ENR (40/60), and (d) ENR nanocomposites with 5 phr of MMT-TDMA2.

4.4.2 Cure characteristics

Scorch time, cure time, minimum torque, maximum torque and torque difference of NR, ENR and NR/ENR nanocomposites are illustrated in Figure 4.27–4.28, and summarized in Table 4.8. With increasing ENR content in the matrix, scorch times of the nanocomposites had no significant difference, as shown in Figure 4.27. However, the cure time of the nanocomposites increased with increasing ENR content (Figure 4.27). In addition, the minimum torque, maximum torque and torque difference of the nanocomposites showed insignificant difference with increasing ENR content, as shown in Figure 4.28.

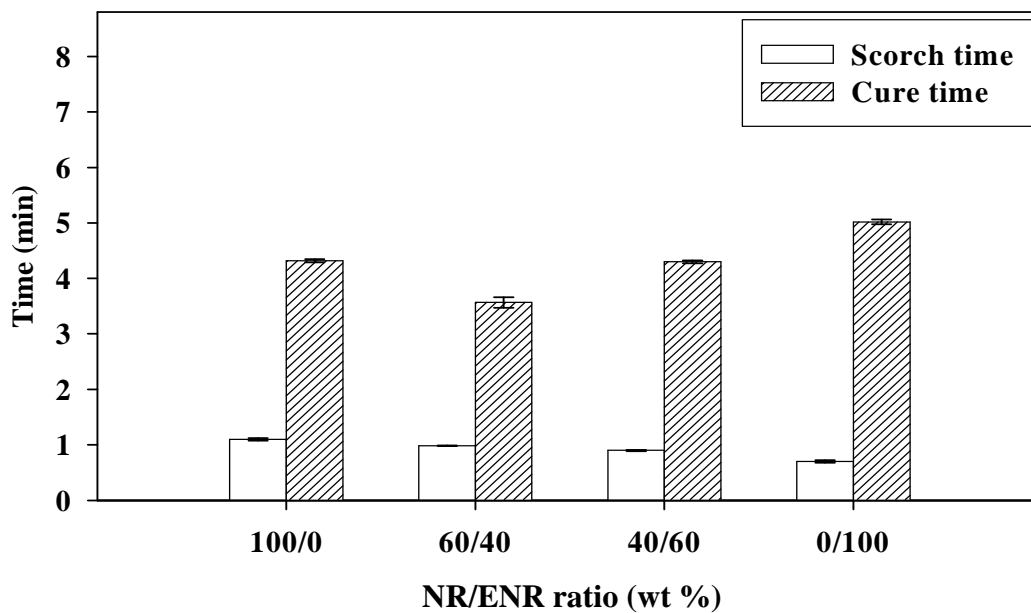


Figure 4.27 Scorch time and cure time of nanocomposites containing 5 phr of MMT-TDMA2.

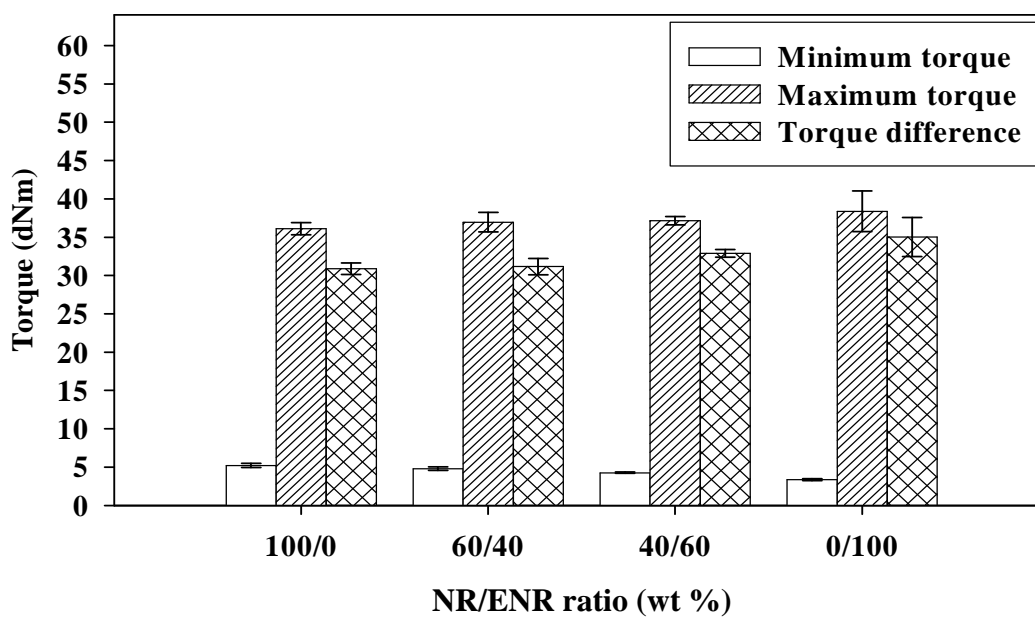


Figure 4.28 Minimum torque, maximum torque and torque difference of nanocomposites containing 5 phr of MMT-TDMA2.

Table 4.8 Cure characteristics of nanocomposites containing 5 phr of MMT-TDMA2

Designation	Scorch time (min)	Cure time (min)	S_{max} (dNm)	S_{min} (dNm)	S_{max}-S_{min} (dNm)
NR/MMT-TDMA2	1.06	4.19	36.09	5.20	30.89
NR/ENR(60/40)/MMT-TDMA2	0.59	3.34	36.94	4.78	31.16
NR/ENR(40/60)/MMT-TDMA2	0.54	4.18	37.14	4.26	32.88
ENR/MMT-TDMA2	0.42	5.01	38.37	3.36	35.02

4.4.3 Mechanical properties

Tensile strength, modulus at 100% elongation, modulus at 300% elongation, elongation at break, hardness and crosslink density of NR, ENR and NR/ENR nanocomposites with 5 phr of MMT-TDMA2 are illustrated in Figure 4.29–4.31, and summarized in Table 4.9.

In comparison between NR/MMT-TDMA2 and ENR/MMT-TDMA2 nanocomposites, tensile strength and elongation at break of the NR nanocomposite was higher than those of the ENR nanocomposite, as shown in Figure 4.29. This may be due to the agglomeration of organoclay particles in the ENR matrix, as confirmed by TEM micrograph in Figure 4.26 (d). These agglomerates restricted ENR chain orientation leading to the decrease in elongation at break of the ENR nanocomposite. When NR was blended with ENR, the tensile strength of NR/ENR(40/60)/MMT-TDMA2 nanocomposite was slightly higher than that of NR/ENR(60/40)/MMT-TDMA2 nanocomposite while the elongation at break of NR/ENR(40/60)/MMT-TDMA2 nanocomposite was slightly lower than that of NR/ENR(60/40)/MMT-TDMA2 nanocomposite. This was due to the exfoliated structures of the organoclay in NR/ENR(40/60)/MMT-TDMA2 nanocomposite, which organoclay platelets were thoroughly dispersed in the matrix. As shown in Figure 4.30, modulus at 100% elongation and modulus at 300% elongation of the nanocomposites showed insignificant change with increasing amount of ENR in the matrix. In addition, the hardness of the nanocomposites, as shown in Figure 4.31, also had no significant difference.

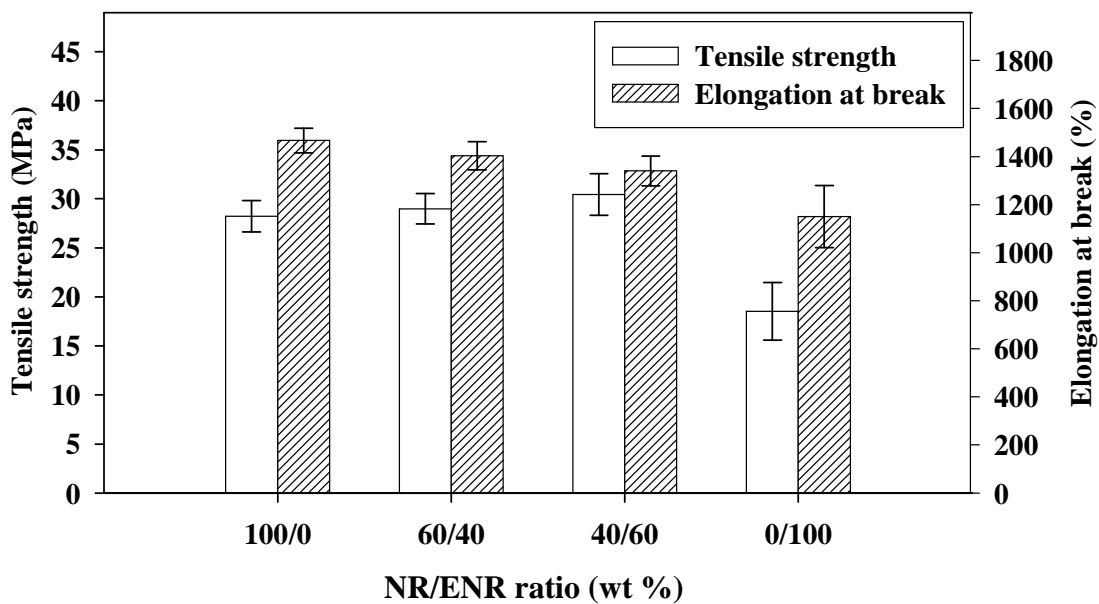


Figure 4.29 Tensile strength and elongation at break of nanocomposites containing 5 phr of MMT-TDMA2.

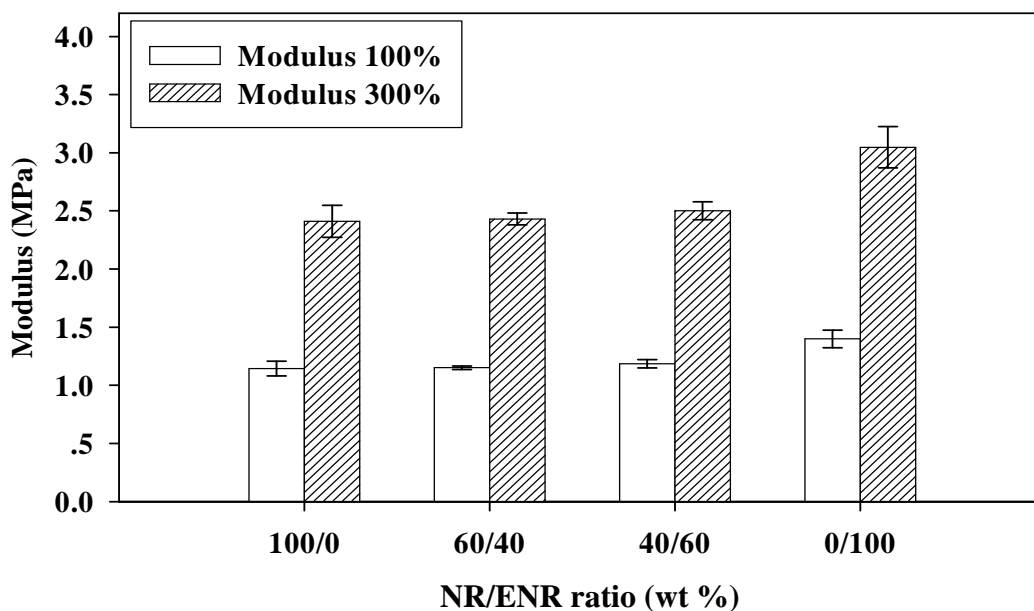


Figure 4.30 Modulus at 100% elongation and modulus at 300% elongation of nanocomposites containing 5 phr of MMT-TDMA2.

Figure 4.31 shows the crosslink density of NR, ENR and NR/ENR nanocomposite with 5 phr of MMT-TDMA2. The crosslink density of NR, ENR and NR/ENR nanocomposites showed insignificant difference. This indicated that the crosslinking of rubber had no effect on the properties of the nanocomposites. Therefore, the increase in tensile strength of the NR/ENR nanocomposites with increasing ENR content was due to the improved interaction between rubber matrix and organoclay.

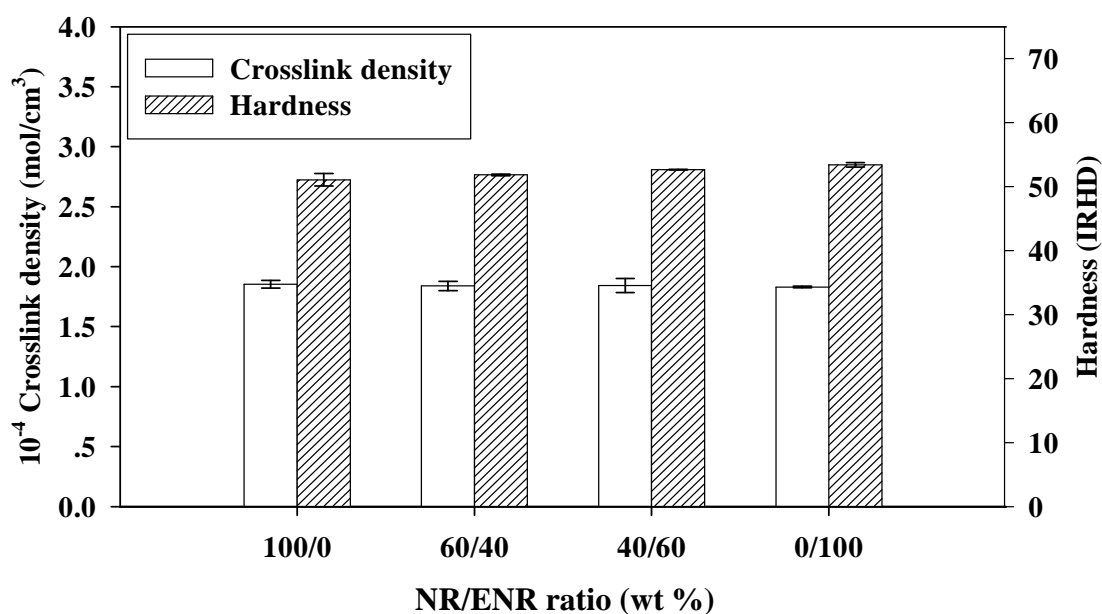


Figure 4.31 Hardness and crosslink density of nanocomposites containing 5 phr of MMT-TDMA2.

According to the results, blending ENR with NR slightly improved mechanical properties of the nanocomposites. This was due to the exfoliated or intercalated structures of the organoclay in the matrix and the good interaction between the rubber matrix and the organoclay.

Table 4.9 Mechanical properties and crosslink density of nanocomposites containing 5 phr of MMT-TDMA2

Designation	Tensile strength (MPa)	Modulus 100% (MPa)	Modulus 300% (MPa)	Elongation at break (%)	Hardness (IRHD)	Crosslink density (10^{-4} mole/cm³)
NR/MMT-TDMA2	28.22	1.14	2.58	1466.42	51.08	1.8526
NR/ENR(60/40)/MMT-TDMA2	28.98	1.15	2.60	1403.40	51.83	1.8398
NR/ENR(40/60)/MMT-TDMA2	30.44	1.18	2.68	1340.29	52.67	1.8419
ENR/MMT-TDMA2	18.53	1.40	3.26	1150.81	53.40	1.8299

CHAPTER V

CONCLUSIONS

MMT surface was modified by three different types of surfactants, *i.e.* ODA, ODTMA-Br or TDMA-Br at various contents of the surfactants, *i.e.* 0.5, 1, 2 times clay CEC. The intercalation of surfactant molecules into MMT layers was confirmed by the increase of interlayer spacing of organoclays, the appearance of C-H stretching band of alkyl ammonium surfactants and the increase in decomposition temperatures of the intercalated surfactant.

Effect of surfactant on physical properties of NR nanocomposites was studied. NR nanocomposites containing 5 phr of the organoclays were prepared by a two-roll mill. Among all the NR/organoclay nanocomposites, NR nanocomposites with MMT-TDMA2 had the highest tensile strength and optimum scorch time and cure time. Also, XRD and TEM results revealed the exfoliated structure of MMT-TDMA2 in NR nanocomposites. This exfoliated MMT-TDMA2 led to good dispersion of MMT-TDMA platelets in NR matrix and good interaction between NR and MMT-TDMA2.

Effect of organoclay content on physical properties of NR nanocomposites was studied. MMT-TDMA2 contents in the NR nanocomposites were varied, *i.e.* 1, 3, 5 and 10 phr. With increasing MMT-TDMA2 content up to 5 phr, scorch time and cure time of the NR nanocomposites decreased while tensile strength of the nanocomposites increased. In addition, XRD spectra of NR nanocomposites revealed the exfoliated structures of MMT-TDMA2 in the NR nanocomposites containing 1-5 phr of the organoclay and the intercalated structure of MMT-TDMA2

in the NR nanocomposites containing 10 phr of the organoclay. Therefore, the increase in tensile strength of NR nanocomposites with the addition of MMT-TDMA2 up to 5 phr may be due to the good interfacial interaction between MMT-TDMA2 and NR matrix.

Effect of matrix polarity on properties of NR nanocomposites was studied. Epoxidized natural rubber (ENR) was blended with NR to improve matrix polarity. NR/ENR blend ratios were 60/40 and 40/60 wt%. MMT-TDMA2 was fixed at 5 phr. Blending ENR with NR slightly improved mechanical properties of the nanocomposites.

REFERENCES

- Alexandre, M., and Dubois, P. (2000). Polymer-layered silicate nanocomposites: preparation, properties and uses of a new class of material. **Mater. Sci. Eng.** 28: 1-63.
- Arroyo, M., Lopez-Manchado, M. A., and Herrero, B. (2003). Organomontmorillonite as substitute of carbon black in natural rubber compounds. **Polymer.** 44: 2447–2453.
- Arroyo, M., Lopez-Manchado, M. A., Valentin, J. L., and Carretero, J. (2007). Morphology/behaviour relationship of nanocomposites based on natural rubber/epoxidized natural rubber blends. **Compos. Sci. Tech.** 67: 1330–1339.
- Avalos, F., Ortiz, J. C., Zitzumbo, R., Lopez-Manchado, M. A., Verdejo, R., Arroyo M. (2008). Effect of montmorillonite intercalant structure on the cure parameters of natural rubber. **Eur. Polym. J.** 44: 3108–3115.
- Brown, R. P., Soulagnet, G. (2001). Microhardness profiles on aged rubber compounds. **Polym. Test.** 20: 295-303.
- Flory., P. J. (1953). **Principles of polymer chemistry.** Ithaca, New York: Cornell University Press. p. 576.
- Gatos, K. G., and Karger-Kocsis, J. (2005). Effects of primary and quaternary amine intercalants on the organoclaydispersion in a sulfur-cured EPDM rubber. **Polymer.** 46: 3069–3076.

- Heinz, H., Vaia, R. A., Krishnamoorti, R., Farmer, B. L. (2007). Self-assembly of alkylammonium chains on montmorillonite: Effect of chain length, head group structure, and cation exchange capacity. **Chem. Mater.** 19: 59-68.
- Kim, M-S., Kim, D-W., Chowdhury, S. R., and Kim, G-H. (2006). Melt-compounded butadiene rubber nanocomposites with improved mechanical properties and abrasion resistance. **J. Appl. Polym. Sci.** 102: 2062–2066.
- Kim, W., Kang, B-S, Cho, S-G., Ha, C-S., Bae, J-W. (2007). Styrene butadiene rubber-clay nanocomposites using a latex method: morphology and mechanical properties. **Compos. Interface.** 14: 409–425.
- Lagaly, G. (1981). Characterization of clays by organic compounds. **Clay. Minerals.** 16: 1-21.
- Lagaly, G., Gonzalez, M. F., Weiss A. (1976). Problems in layer-charge determination of montmorillonites. **Clay. Minerals.** 11: 173-187.
- Liang, Y., Wang, Y., Wu, Y., Lu, Y., Zhang, H., and Zhang, L. (2005). Preparation and properties of isobutylene–isoprene rubber (IIR)/clay nanocomposites. **Polym. Test.** 24: 12–17.
- Magaraphan, R., Thaijaroen, W., and Lim-ochakun, R. (2003). Structure and properties of natural rubber and modified montmorillonite nanocomposites. **Rubber. Chem. Tech.** 76: 406-418.
- Marras, S. I., Tsimpliaraki, A., Zuburtikudis, I., Panayiotou, C. (2007). Thermal and colloidal behavior of amine-treated clays: The role of amphiphilic organic cation concentration. **J. Colloid. Interface. Sci.** 315: 520–527.

- Marras, S. I., Tsimpliaraki, A., Zuburtikudis, I., Panayiotou, C. (2009). Morphological, thermal, and mechanical characteristics of polymer/layered silicate nanocomposites: The role of filler modification level. **Polym. Eng. Sci.** 49: 1206-1217.
- Rajasekar, R., Pal, K., Heinrich, G., Das, A., Das, C.K. (2009). Development of NBR-nanoclay composites with epoxidized natural rubber as compatibilizer. **Mater. Design.** 30: 3839-3845.
- Ray, S. S., Okamoto, M. (2003). Polymer/layered silicate nanocomposites: a review from preparation to processing. **Prog. Polym. Sci.** 28: 1539–1641.
- Sadhu, S., and Bhowmick, A. K. (2003). Effect of chain length of amine and nature and loading of clay on styrene-butadiene rubber-clay nanocomposites. **Rubber. Chem. Tech.** 76: 860-875.
- Teh, P.L., Mohd-Ishak, Z. A., Hashim, A.S., Karger-Kocsis, J., and Ishiaku, U. S. (2004). Effects of epoxidized natural rubber as a compatibilizer in melt compounded natural rubber–organoclay nanocomposites. **Eur. Polym. J.** 40: 2513–2521.
- Tjong, S. C. (2006). Structural and mechanical properties of polymer nanocomposites. **Mater. Sci. Eng.** 53: 73–197.
- Umpush, J., and Wibulsawat, R. (2006). Kinetic of commercial dyes removal from dyeing process wastewater of household-scale industries by montmorillonite clay in mixing tank system. **Research & Development Journal of the Engineering Institute of Thailand.** 17: 40–47.
- Vansant, E. F., and Peeters, G. (1978). The exchange of alkylammonium ions on Na-laponite. **Clays. Clay. Miner.** 26: 279-284.

- Varghese, S., and Karger-Kocsis, J. (2004). Melt-compounded natural rubber nanocomposites with pristine and organophilic layered silicates of natural and synthetic origin. **J. Appl. Polym. Sci.** 91: 813–819.
- Varghese, S., Karger-Kocsis, J., and Gatos, K. G. (2003). Melt compounded epoxidized natural rubber/layered silicate nanocomposites: structure-properties relationships. **Polymer.** 44: 3977–3983.
- Vaia, R., Teukolsky, R. K., and Giannelis, E. P. (1994). Interlayer structure and molecular environment of alkylammonium layered silicates. **Chem. Mater.** 6: 1017-1022.
- Wan, C., Dong, W., Zhang, Y., and Zhang, Y. (2008). Intercalation process and rubber–filler interactions of polybutadiene rubber/organoclay nanocomposites. **J. Appl. Polym. Sci.** 107: 650–657.
- Wang, S., Zhang, Y., Peng, Z., and Zhang, Y. (2005). New method for preparing polybutadiene rubber/clay composites. **J. Appl. Polym. Sci.** 98: 227–237.
- Wang, Y., Zhang, L., Tang, C., and Yu, D. (2000). Preparation and characterization of rubber–clay nanocomposites. **J. Appl. Polym. Sci.** 78: 1879–1883.
- Wibulswas, R. (2004). Batch and fixed bed sorption of methylene blue on precursor and QACs modified montmorillonite. **Separ. Purif. Tech.** 39: 3–12.
- Xi, Y., Ding, Z., He, H., and Frost, R. L. (2004). Structure of organoclays-an X-ray diffraction and thermogravimetric analysis study. **J. Colloid. Interface. Sci.** 277: 116–120.
- Zhang, X., Loo, L. S. (2008). Morphology and mechanical properties of a novel amorphous polyamide/nanoclay nanocomposite. **J. Polym. Sci. Part B: Polym. Phys.** 46: 2605–2617.

- Zeng, Q. H., Yu, A. B., Lu, G. Q. (Max), and Paul, D. R. (2005). Clay-based polymer nanocomposites: research and commercial development. **J. Nanosci. Nanotech.** 5: 1574–1592.
- Zhang, L., Wang, Y., Wang, Y., Sui, Y., and Yu, D. (2000). Morphology and mechanical properties of clay/styrene-butadiene rubber nanocomposites. **J. Appl. Polym. Sci.** 78: 1873–1878.
- Zhu, J., He, H., Zhu L., Wen, X., Deng, F. (2005). Characterization of organic phases in the interlayer of montmorillonite using FTIR and ^{13}C NMR. **J. Colloid. Interface. Sci.** 286: 239–244.

APPENDIX A

PUBLICATIONS

EFFECT OF SURFACTANTS ON CURE CHARACTERISTICS OF NR/ORGANOCLAY NANOCOMPOSITES

C. Keawkumay^{1,2} K. Jarukumjorn^{1,2} N. Suppakarn^{1,2*}

¹School of Polymer Engineering, Suranaree University of Technology, Nakhon Ratchasima 30000, Thailand.

²Center of Excellent for Petroleum, Petrochemicals, and Advanced Materials, Chulalongkorn University, Bangkok 10330, Thailand.

*E-mail:nitinat@sut.ac.th, Tel: +66-44-224439

Abstract: In this work, NR/organoclay nanocomposites were prepared. Modification of clay surface was done by two different types of surfactants, *i.e.* octadecylamine (ODA) and tetradecyltrimethyl ammonium bromide (TDMA-Br). Effect of surfactant content corresponding to the CEC of clay on cure characteristics of NR nanocomposites were investigated using a moving die rheometer (MDR). The characteristics of the organoclays were also examined by an X-ray diffraction spectrometer (XRD) and a thermogravimetric analyzer (TGA).

Introduction

Natural Rubber (NR) is considered one of the most widely used rubbers throughout the world. NR has many attractive properties including low cost, low hysteresis, high resilience, excellent dynamic properties, etc [1]. Typical fillers for rubber composites are carbon black, silica, kaolin, talc, etc. However, high filler loading must be added in order to achieve rubber composite with desirable mechanical properties.

Recently, layer silicate clays, *e.g.* bentonite, montmorillonite, have become one of interesting candidates for reinforcing NR [2]. The layer thickness of a silicate clay is around 1 nm. The lateral dimension of these layers can vary up to several microns [2]. The most commonly used layered silicates for preparation of polymer-clay nanocomposites is montmorillonite (MMT) [3]. One of drawbacks of using clay as a filler for a polymer is the incompatibility between hydrophilic clay and hydrophobic polymer, which often causes agglomeration of clay in the polymer matrix. Therefore, modification of clay surface is an important parameter to achieve polymer nanocomposite. Such modified clays are commonly referred to organoclays [4].

Normally, the modification of clay surface can be done via ion exchange of the interlayer cations of clay with those of organic surfactants. Ion exchange reactions depend on types of organic surfactant and the cation exchange capacity (CEC) of the clay. The CEC of a clay is very important factor for producing nanocomposite because it relates to the amounts of a surfactant, which intercalate between the silicate layers [3]. Organic surfactants normally used to modify clay are alkylamine surfactants. The length and the numbers of alkyl chains on the surfactant molecules directly affect the ion exchange reaction.

In this work, sodium montmorillonite clay (MMT) was modified using either ODA or TDMA-Br. The content of added surfactant as compared to CEC of the clay was varied. The characteristics of organoclay were examined. Also, effect of surfactant types and surfactant content added to clay on cure characteristics of NR nanocomposites were investigated.

Materials and Methods

Materials: Natural rubber (STR 5L) was purchased from Thai Hoa Rubber Public Co., Ltd. Sodium montmorillonite clay (MMT) with cation exchange capacity (CEC) value of 80 meq/100g was supplied by Thai Nippon Co., Ltd. Octadecylamine (ODA) and tetradecyltrimethyl ammonium bromide (TDMA-Br) were purchased from Acros and Fluka, respectively.

Clay surface modification with octadecylamine (ODA): 100 g of MMT was dispersed into 2000 ml of hot water (70°C) with continuous stirring. ODA and conc. hydrochloric acid were dissolved into 1000 ml of hot deionized water, with vigorous stirring. Then the ODA solution was poured into the hot clay-water dispersion and vigorously stirred for 2 hours. After that the suspension was washed several times with hot deionized water (70°C) until water conductivity was below 10 μ S. The modified clay, called organoclay, was vacuum-filtrated, dried at 60 °C in an oven and ground for further uses. The contents ODA added were equivalent to 1.0 and 2.0 CEC of the MMT. So, the ODA modified clays were called ODA1 and ODA2, respectively.

Clay surface modification with tetradecyltrimethyl ammonium bromide (TDMA-Br): TDMA-Br were dissolved into 3000 ml of water with continuous stirring. Then, 100 g of MMT was added to the TDMA-Br solution. The suspension was stirred vigorously for 24 hours. After that the suspension was washed several times with deionized water until water conductivity was below 10 μ S. The modified clay was vacuum-filtrated, dried at 60°C in an oven and ground for further uses. The contents of TDMA-Br added were equivalent to 1.0 and 2.0 CEC of the MMT. So, the TDMA-Br modified clays were called TDMA1 and TDMA2, respectively.

NR nanocomposite preparation: All rubber compounds were mixed on a two-roll mill (Chaicharoen) at room temperature. Mixing time was

15 min. The rotors were operated at a speed ratio of 1:1.4. The vulcanization ingredients were added to the compound after the incorporation of clay and, lastly, sulfur was added. The formulations of the rubber compounds are given in Table 1.

Table 1: Formulations of rubber compounds

Material	Content (phr)					
NR	100	100	100	100	100	100
Zinc oxide	5	5	5	5	5	5
Stearic acid	2	2	2	2	2	2
CBS ^a	1	1	1	1	1	1
Sulfur	2.5	2.5	2.5	2.5	2.5	2.5
MMT	-	5	-	-	-	-
ODA1	-	-	5 ^b	-	-	-
ODA2	-	-	-	5 ^c	-	-
TDMA1	-	-	-	-	5 ^d	-
TDMA2	-	-	-	-	-	5 ^e

^a N-Cyclohexyl-2-benzothiazolesulfenamide

^b ODA/CEC = 1, ^c ODA/CEC = 2

^d TDMA/CEC = 1, ^e TDMA/CEC = 2

Characterization: X-ray diffraction spectrometer (XRD) (OXFORD/ED2000) with a Cu-K α as a radiation source was used to characterize clay, organoclay and NR/organoclay nanocomposites.

Thermal stability of clay and organoclays was analyzed by a thermogravimetric analyzer (TGA) (STD 2690, TA instrument). The sample was heated from room temperature to 500 °C at a rate of 20 °C/min under a nitrogen atmosphere.

Cure characteristics of rubber compounds were determined on a moving die rheometer (MDR) (GT-M200F) at a temperature of 150 °C.

Results and Discussion

Characterization of clay and organoclays: Figure 1 and Table 2 show XRD spectra and interlayer spacing of clay and organoclay, respectively.

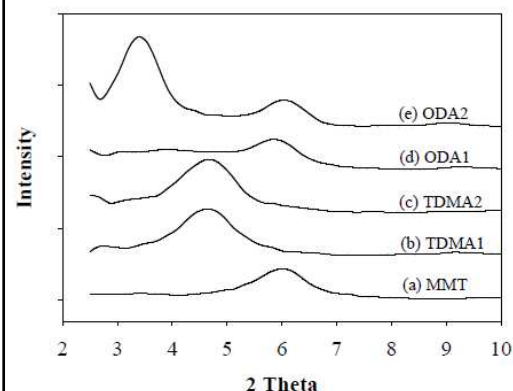


Figure 1. XRD spectra of clay and organoclays

The interlayer spacing of organoclays was larger than that of unmodified clay (MMT). The interlayer spacing

of ODA1 was slightly larger than that of MMT while two different interlayer spacing at 1.55 nm and 3.02 nm were observed in ODA2. The results indicated the heterogeneous interlayer expansion of clay with increasing ODA content. On the other hand, TDMA1 and TDMA2 showed the same interlayer spacing. This implied that the content of TDMA at 1 CEC was sufficiently for exchanging with interlayer ions (Na⁺, Ca²⁺) of clay. Therefore, cation exchange mechanism might be dominant for the intercalation of quaternary ammonium cation between the interlayer of the clay [5]. In comparison between two types of surfactants, ODA modified MMT give larger interlayer spacing than TDMA modified MMT.

Table 2: 2 Theta (2θ) and interlayer spacing of clay and organoclays

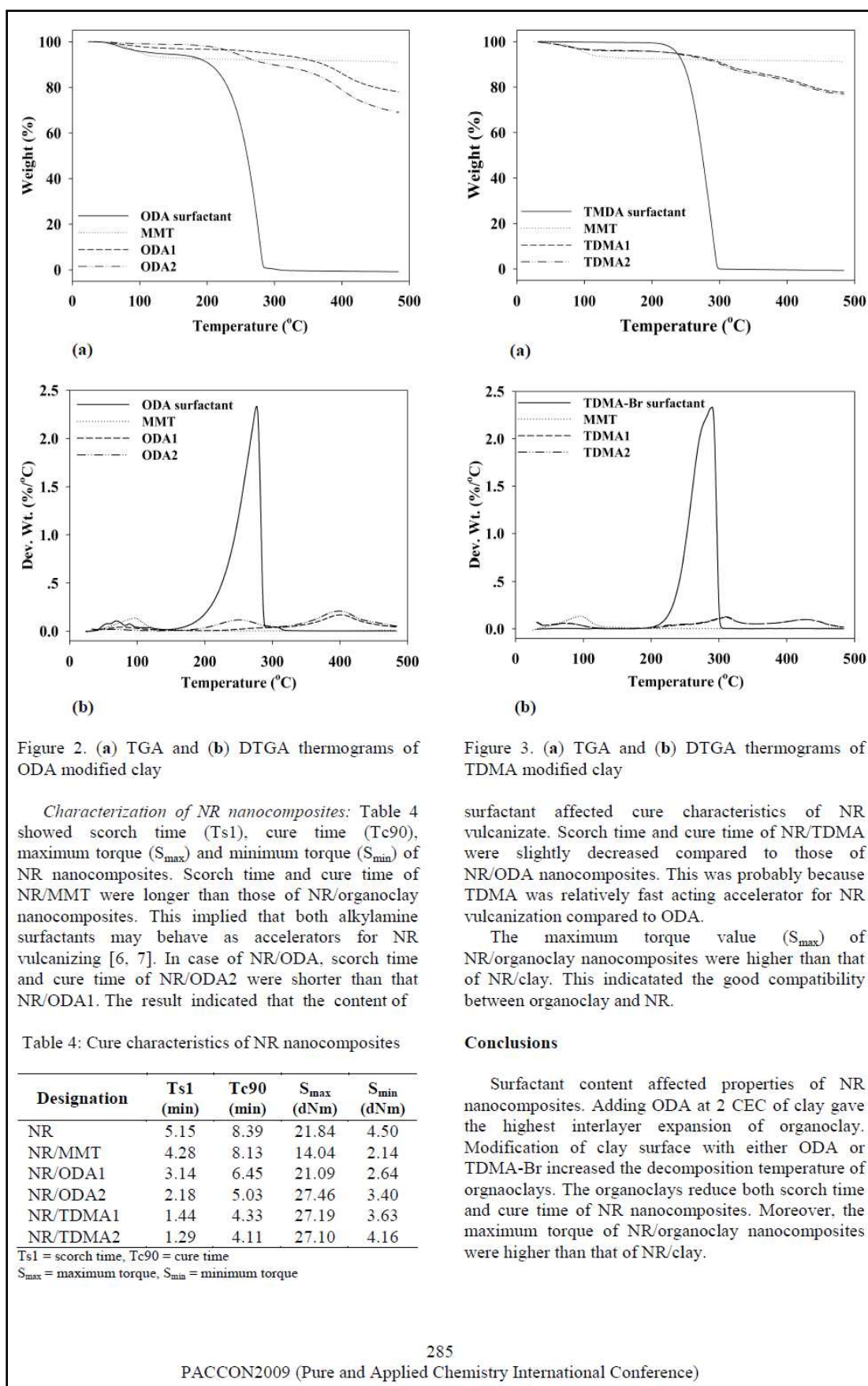
Clay/Organoclay	2 Theta ($^{\circ}$)	Interlayer spacing (nm)
MMT	6.08	1.45
ODA1	5.68	1.55
ODA2	2.92, 5.68	3.02, 1.55
TDMA1	4.68	1.89
TDMA2	4.66	1.90

Figure 2 and Figure 3 showed TGA and DTG thermograms of ODA modified clay and TDMA-Br modified clay, respectively. The thermal decomposition temperature of the clay and the organoclays were then summarized in Table 3.

Table 3: Decomposition temperature (T_d) of clay and organoclays

Designation	T_d ($^{\circ}$ C)		
	Step1	Step2	Step3
MMT	96.2	-	-
ODA surfactant	71.2	276.9	-
ODA1	76.9	-	401.9
ODA2	56.0	250.0	398.1
TDMA surfactant	-	292.3	-
TDMA1	75.0	311.5	432.7
TDMA2	75.0	311.5	432.7

The weight loss observed at the temperature range 56.0 °C- 96.2 °C was attributed to the dehydration of adsorbed water. In ODA1, the ODA molecules had strong interaction with MMT via interlayer cation exchanged reaction and had high thermal stability. As a result, ODA1 decomposed at the higher temperature compared to the pure ODA. Modifying clay with high content of ODA, the extra ODA molecules interacted with each other and decomposed in similar temperature range to the pure ODA as seen in the TGA and DTG thermogram of ODA2. In cases of TDMA modified clays, both TDMA1 and TDMA2 showed two decomposition steps. The results can be explained by the similar reasons as mentioned in the case of ODA modified clays.



Acknowledgements

The authors would like to thank Suranaree University of Technology and Center of Excellent for Petroleum, Petrochemicals, and Advanced Materials, Chulalongkorn University, Thailand for financial support and Thai Nippon Co., Ltd. for providing Montmorillonite.

References

- [1] P.L. Teh, Z.I. Mohd Ishak, A.S. Hashim, J. Karger and U.S. Ishiaku, *Eur. Polym. J.* **40**, (2004), pp. 2513-2521.
- [2] M. Arroyo, M.A. Lopez-Manchado and B. Herrero, *Polymer*, **44**, (2003), pp. 2447-2453.
- [3] S.S. Ray and M. Okamoto, *Prog. Polym. Sci.* **28**, (2003), pp. 1539-1641.
- [4] Q.H. Zeng, A.B. Yu, G.Q. Lu (Max) and D.R. Paul, *J. Nanosci. Nanotech.* **5**, (2005), pp. 1574-1592.
- [5] R. Wibulswas, *Separ. Purif. Tech.* **39**, (2004), pp. 3-12.
- [6] S. Varghese and J. Karger-Kocsis, *J. Appl. Polym. Sci.* **91**, (2004), pp. 3069-3076.
- [7] M.A. Lopez-Manchado, M. Arroyo, B. Herrero, and J. Biagiotti, *J. Appl. Polym. Sci.* **89**, (2003), pp. 1-15.



Cure Characteristics and Tensile Properties of NR/MMT Nanocomposites

C. Keawkumay^{1,2} K. Jarukumjorn^{1,2} N. Suppakarn^{1,2*}

1. School of Polymer Engineering, Suranaree University of Technology, Nakhon Ratchasima 30000, Thailand.

2. Center of Excellent for Petroleum, Petrochemicals, and Advanced Material, Chulalongkorn University, Bangkok 10330, Thailand.

*nitinat@sut.ac.th

Introduction

Natural rubber (NR) based nanocomposites have attracted much attention since NR products fulfil important functions in almost all areas of daily life. Arroyo *et. al.*¹ have found that mechanical properties of NR with 10 phr of organomodified montmorillonite (MMT) were comparable with those of NR with 40 phr of carbon black. Magaraphan *et. al.*² and Wibulswas³ have shown that chemical structure of surfactants was an important parameter that needs to be considered in order to use a modified clay as a filler for NR. In addition, using epoxidized natural rubber (ENR) as a compatibilizer for NR/MMT nanocomposite would enhance properties of the NR nanocomposites. So, this work aimed to improve cure characteristics and tensile properties of NR/MMT nanocomposites by modifying clay surface and adding ENR as a compatibilizer.

Experimental

MMT was surface modified by tetradecyltrimethyl ammonium bromide (TDMA) and was called organoclay. XRD and FTIR were used to investigate the characteristic of MMT and organoclay. 5 phr of either MMT or organoclay was incorporated into NR compounds. The vulcanization ingredients were sulphur, ZnO, CBS and stearic acid. Moreover, the NR/organoclay compound with the addition of 10 phr of ENR was also prepared. A moving die rheometer (MDR) was used to investigate cure characteristics of NR compounds. All NR compounds were cured and cut into dumbbell shape before performing tensile test.

Results and Discussion

XRD spectra of MMT and organoclay in Fig. 1 revealed that treating MMT surface with TDMA expanded the interlayer spacing of MMT since organoclay showed a lower angle of the diffraction peak than MMT. In Fig. 2, FTIR spectrum of organoclay showed additional peaks, *i.e.* 2925, 2853, 1478 and 1380 cm^{-1} , compared to that of clay indicating the appearance of TDMA on MMT surface. XRD spectrum of NR/MMT nanocomposite (Fig. 3 (b)) showed the diffraction peak of the same position as that of MMT indicating no insertion of NR molecule into clay layer. This was due to the polarity difference between MMT and NR. Nonetheless, XRD spectrum of NR/organoclay nanocomposite in Fig. 3 (c) showed no indication of organoclay diffraction peak. This suggested that the NR molecules preferred inserting into the organoclay layers leading to an exfoliated structure of organoclay in NR/organoclay nanocomposite. However, a rather small peak around $2\theta = 5.0^\circ$ was observed in the XRD spectrum of NR/organoclay nanocomposite. This was probably due to some reaggregation of organoclay layers. In the case of ENR compatibilized NR/organoclay nanocomposites (NR/ENR/organoclay), this diffraction peak disappeared. This suggested that the interlayer spacing of the organoclay layers in the compatibilized NR nanocomposite was higher than that of the organoclay layers in the uncompatibilized system. This was because the incorporation of ENR as a compatibilizer in NR matrix eased penetration of NR and ENR molecules in between the organoclay layers leading to an exfoliated structure of NR/ENR/organoclay nanocomposite.



From Table 1, the NR/ENR/organoclay nanocomposite showed the shortest scorch time and cure time among the NR nanocomposites. This suggested that epoxy groups in ENR may affect the activation/crosslinking processes via reactions with the amine groups of organoclay and activator.⁴ In comparison to NR, the addition of MMT into NR decreased both S_{max} and S_{min} of the NR/MMT nanocomposites. This suggested that NR was incompatible with clay which led to weak interaction between NR and clay. However, the S_{max} of ENR compatibilized and uncompatibilized NR/organoclay nanocomposites were higher than that of NR. This was because the surface modification of MMT or the addition of ENR improved compatibility between NR and MMT. Tensile strength of NR/ENR/organoclay nanocomposite showed the highest value among the NR nanocomposites. Moreover, M100 and M300 of NR/ENR/organoclay nanocomposite were slightly increased compared to that of uncompatibilized NR/organoclay nanocomposite. This evidence confirmed that adding ENR enhanced compatibility between NR and organoclay.

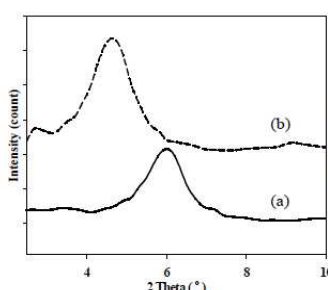


Fig. 1: XRD spectra of (a) MMT and (b) organoclay.

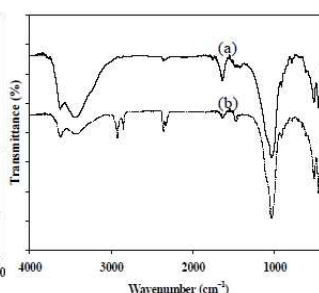


Fig. 2: FTIR spectra of (a) MMT and (b) organoclay.

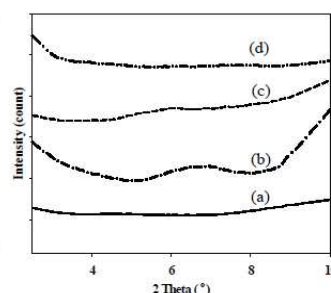


Fig. 3: XRD spectra of (a) NR, (b) NR/MMT, (c) NR/organoclay, and (d) NR/ENR/organoclay nanocomposites

Table 1: Cure characteristics and tensile properties of NR nanocomposites.

Designation	Scorch time, min	Cure time, min	S_{max} , dNm	S_{min} , dNm	Tensile strength, MPa	M100, MPa	M300, MPa
NR	5.51	8.84	26.52	5.08	15.54	0.88	1.97
NR/MMT	5.06	8.29	20.39	3.53	19.96	0.78	1.70
NR/organoclay	1.08	3.33	30.78	3.88	23.69	1.04	2.38
NR/ENR/organoclay	1.05	3.26	32.79	4.80	25.65	1.07	2.44

S_{max} = maximum torque, S_{min} = minimum torque, M100 = modulus at 100% of elongation and M300 = modulus at 300% of elongation

Conclusions

TDMA modified MMT gave a higher interlayer spacing than unmodified MMT. The organoclay reduced both scorch time and cure time of NR nanocomposites. In addition, ENR enhanced the compatibility between NR and organoclay leading to the improvement of tensile properties and cure characteristics of NR/MMT nanocomposites.

Acknowledgements

The authors thank Suranaree University of Technology and Center of Excellent for Petroleum, Petrochemicals and Advanced Materials, Thailand for the financial support and Thai Nippon Co., Ltd. for providing MMT.

References

- Arroyo M., Lopez-Manchado A., Herrero B. *Polymer* **2003**, *44*, 2447-2453.
- Magaraphan R., Thajjaroen W., Lim-ochakum, R. *Rubber Chem. Tech.* **2003**, *76*, 406-418.
- Wibulswas R. *Separ. Purif. Tech.* **2004**, *39*, 3-12.
- Teh P.L., Mohd Ishak Z.A., Hashim A.S., Karger-Kocsis J., Ishiaku U.S. *Eur. Polym J.* **2004**, *40*, 2513-2521.

BIOGRAPHY

Mr. Chalermpan Keawkumay was born on August 12, 1983 in Nan Province, Thailand. He graduated from Uttaradit Rajabhat University in 2005 with the Bachelor of Science in Chemistry (2nd class honors). During his undergraduate study, he has taken a position of leader of chemistry club and vice president of science and technology student union of Uttaradit Rajabhat University. After graduation, he has been employed as a technician at MAXXIS International (Thailand) Co., Ltd., for 2 years. He then pursued his Master's degree in Polymer Engineering at school of Polymer Engineering, Institute of Engineering, Suranaree University of Technology. During his master's degree study, he presented two papers. One entitled **“Effect of surfactants on cure characteristics of NR/organoclay nanocomposites”** in Pure and Applied Chemistry International Conference 2009 (PACCON2009) in Phitsanulok, Thailand. Two entitled **“Cure characteristics and tensile properties of NR/MMT nanocomposites”** in 11th Pacific Polymer Conference 2009 (PPC11) in Cairns, Australia.